Generation of FN3 Monobodies That Selectively Bind to the Src Family of Protein Kinases

BY

RENHUA HUANG
B.S., Guangxi University, China, 2002

THESIS

Submitted as partial fulfillment of the requirements
for the degree of Doctor of Philosophy in Biological Sciences
in the Graduate College of the
University of Illinois at Chicago, 2012

Chicago, Illinois

Defense Committee:

David Stone, Chair
Brian Kay, Advisor
Ronald Dubreuil
Constance Jeffery
Scott Brady, Anatomy and Cell Biology

To my parents.

ACKNOWLEDGEMENTS

It would be impossible to reach this step without the help from my thesis advisor, Dr. Brian Kay, a wonderful person and PI, to whom I am grateful for giving me the opportunity to be his student, and for guiding me throughout these years with so many ideas and great patience. Brian always has a lot of ideas for me but at the same time gives me freedom to design my experiments. He understands my need to learn and always gives me the opportunities to do that, no matter it is a conference, a workshop, or a trip to learn a new technique. He is also a role model for me in many aspects, a very organized person, always want to learn more, and a nice and humble person while being an accomplished scientist. Last but not least, I am grateful for his help with writing the thesis. Without his help, writing up the thesis in six weeks would almost impossible.

I also want to extend my gratitude to my committee members, Dr. David Stone, Dr. Scott Brady, Dr. Ron Dubreuil and Dr. Connie Jeffery. It is their critical comments and feedbacks that make me aware of so many aspects of biology when I try to generate tools for basic biological research. Their input and suggestions have brought a lot of value to this thesis research. I also want to thank Dr. Jennifer Schmidt for using her cell culture hood.

ACKNOWLEDGEMENTS (continued)

Kay lab is a wonderful place to work, with so many nice lab co-workers and a self-learning team of so much intellectual exchanges. My friends in the lab, Kritika, Gosia, Mike and Sujatha, have spent so much great time with me and offer me help when I need it. I also want to thank my fellow graduate students Liming, Yangzi and David, for giving me help and all the good time we spent together. I want to thank Erin and Oliver for teaching me how to do cell culture.

I want to express my special gratitude to all the undergraduates that have worked with me, Peter Jang, Raman, Amulya, Pete Fang, and Reem for their help with my thesis research. Here I especially want to thank Pete Fang, for being a great co-worker, a collaborator, for contributing to my thesis research and for being a friend that has helped me personally.

I also want to thank all the other undergraduates in the lab that have helped maintain the lab in a good shape.

I also want to thank two of my best friends here in Chicago, Duan Sha and Xiaoyu, who are like part of my family. It is them who have carried me through the most difficult and challenging time here in the US and their being here make me feel the warmth of a family.

I also want to thank all my other friends here in Chicago for their help and giving me so much good time here in town or in beautiful Florida or Wisconsin in those unforgettable trips.

ACKNOWLEDGEMENTS (continued)

Lastly I want to thank Beth, Margaret, Corinna, and Omar for answering all my questions, for organizing all the events and it is their great work that keeps this program running smoothly.

TABLE OF CONTENTS

TABLE OF CONTENTS

TABLE OF CONTENTS

LIST OF TABLES

LIST OF FIGURES

LIST OF FIGURES

LIST OF ABBREVIATIONS

nM	Nanomolar
µM	Micromolar
pM	Picomolar
CB	Carbenicillin
CFP	Cyan fluorescent protein
DTT	Dithiothreitol
EGF	Epidermal growth factor
ELISA	Enzyme-linked immunosorbent assay
Fab	Antigen binding Fragment
FN3	Fibronectin type III domain
FRET	Fluorescence resonance energy transfer
GST	Glutathione S-transferase
GFP	Green fluorescent protein
HRP	Horse radish peroxidase
IMAC	Immobilized metal affinity chromatography
IC_{50}	The half maximal inhibitory concentration
ITC	Isothermal titration calorimetry
Kan	Kanamycin
K_D	Dissociation constant
LS-MS	Liquid chromatographyï mass spectrometry
MBP	Maltose binding protein
NAPPA	Nucleic acid programmable protein array
Pak1	P21 activating kinase 1
PxxP	Proline-rich motif

LIST OF ABBREVIATIONS

PCR	Polymerase chain reaction
PEG	Polyethylene glycol
PBS	Phosphate buffered saline
PBST	PBS with Tween 20
PVDF	Polyvinylidene difluoride
PTPŬ	Protein tyrosine phosphatase-Ŭ
PTP1B	Protein tyrosine phosphatase 1B
scFv	Single-chain fragments of variable region
SFKs	Src family kinases
SH2	Src Homology 2
SH3	Src Homology 3
ssDNA	Single-stranded DNA
SPR	Surface plasmon resonance
SUMO	Small ubiquitin-like modifier
Tip	Tyrosine kinase Interacting protein
TNF-Ŭ	Tumor necrosis factor-Ŭ
T_m	Melting temperature
VEGFR2	Vascular endothelial growth factor receptor 2
WT	Wild type
YFP	Yellow fluorescent protein
Y416	Tyrosine residue 416
Y527	Tyrosine residue 527

SUMMARY

Protein kinases, known for phosphorylating their protein substrates to relay signaling events in cells, contain 518 members and encompass ~2% of human genes. One subgroup of the kinase family, Src family kinases (SFKs), including Blk, Fgr, Fyn, Hck, Lck, Lyn, Src, and Yes, have been studied for their roles in cell proliferation, migration, differentiation and survival. Because SFKs members have a similar overall structure with highly conserved sequences, currently available antibodies fail to distinguish the active form of one kinase from other SFKs. As SFKs often phosphorylate substrates with similar amino acid sequence, current biosensors fail to discriminate activation of one kinase from other SFKs.

To generate affinity reagents that can be used to study the activation of individual member of SFKs, I used phage display technology for directed evolution of FN3 monobodies. To increase the efficiency of constructing a phage library of FN3 monobodies with Kunkel mutagenesis, I made three modifications to the previously published protocol. First, I incubated bacterial cells at 25°C instead of 37°C to achieve a 2- to 7-fold increase in the yield of the single-stranded DNA template. Second, with the introduction of restriction endonuclease sites into the diversified loops of the FN3 coding region, phage libraries with diversity up to 10^{10} and 99-100% recombinant were constructed. Finally, I designed a digestion- and ligation-free method for constructing secondary libraries, using DNA fragments amplified by error-prone and asymetric PCR as primer for conducting Kunkel mutagenesis. To demonstrate the

efficiency of this improved method, I constructed two secondary libraries based on a FN3 monobody that bound to the active form of Pak1 kinase. Screening one of the mutagenic libraries isolated three variants that bound 2- to 4-fold tighter than the original clone.

For generating affinity reagents to one member of the SFKs, Fyn tyrosine kinase, a phage-display library was screened for monobodies binding to the Fyn SH3 domain. The affinity selection identified three monobodies that bound selectively to the Fyn SH3 domain. One of the isolates, G9, bound exclusively to the Fyn SH3 domain out of 150 SH3 domains that I tested and had a dissociation constant (K_D) of 166 ± 6 nM. Interestingly, while the G9 monobody lacks proline in its randomized loops, it bound at the same site on the SH3 domain as proline-rich ligands. The G9 monobody could be used to pull-down active recombinant Fyn kinase *in vitro*, demonstrating its potential as a highly selective probe for detecting active cellular Fyn kinase.

To generate affinity reagents for another SFKs member, Lyn tyrosine kinase, another phage library was screened. Two isolates, TA1 and TA8, selectively bound to the Lyn SH3 domain out of 150 SH3 domains. Both TA1 and TA8, in the absence of a canonical PxxP motif in their binding loops, competed with a PxxP proline-rich peptide, Tip, for binding to Lyn SH3 domain. Due to the weak affinity of TA8 for Lyn SH3 (K_D= ~5 μM), I used affinity maturation techniques to identify variants that bound > 8-fold tighter than the original TA8 clone. As a

proof-of-concept experiment, one monobody was fused to GFP and converted into a sensor that increased fluorescence upon binding to the Lyn SH3 domain in solution.

CHAPTER 1

INTRODUCTION

1.1 Src family kinases

Protein kinases are enzymes that catalyze the transfer of the gamma-phosphoryl group of ATP onto tyrosine, serine and threonine residues of their protein substrates. The human genome encodes 518 protein kinases (*1*) that regulate many signal transduction pathways, and approximately one third of the human proteins are the substrates of protein kinases (*2*). While the normal expression and activity of protein kinases are essential for life, their elevated expression is associated with various types of diseases in human, making them a valuable therapeutic target class (*3*).

Protein kinases carry a kinase domain, which is responsible for catalyzing the hydrolysis of ATP and transferring its gamma-phosphoryl group to the substrate. Based on the sequence similarity of the kinase domain, human protein kinases have been divided into nine groups (*1*), one of which is the non-receptor tyrosine kinase group. Non-receptor tyrosine kinases, of which there are 90 members in humans (*1*), reside in the cytosol and nucleus. One well-known non-receptor tyrosine kinase is Src, which is the first proto-oncogene (4) and protein tyrosine kinase (4) characterized in mammals.

The Src family kinases (SFKs), named after Src tyrosine kinase, consists of eight members, Blk, Fgr, Fyn, Hck, Lck, Lyn, Src, and Yes (Table 1.1). Each SFKs member has a unique expression pattern in tissues and cells: Src, Fyn, and Yes are ubiquitously expressed, whereas Blk, Fgr, Hck, Lyn, Lck are expressed primarily in hematopoietic cells (5) (Table 1.1). However, in several human tissues two or more SFKs are expressed simultaneously (6) and deleting

one member leads to little or no phenotype, suggesting that there is functional redundancy among the SFKs. Only when more than two SFKs are simultaneously deleted, substantial defects, such embryonic lethality, are observed (*7*).

SFKs members respond individually or simultaneously to external cellular stimuli (6). For example, they are activated in cells by epidermal growth factor (8, 9), platelet-derived growth factor (10, 11), nerve growth factor (12), fibroblast growth factor (12), insulin-like growth factor (13), and several immune-related growth factors (14). Consequently, they play important roles in many essential cell signaling pathways and have been implicated in the pathogenesis of many diseases, especially cancer (15-17) (Table I.). As a result, they are currently under intensive investigation as targets for drug therapy. Recently two drugs, Dasatinib (18), and Bosutinib (19), have been approved by the Federal Drug Administration (FDA) for treating chronic myelogenous leukemia. Crystal structures and docking analysis suggest that both of the drugs bind to the kinase site and are competitive inhibitors of SFKs (20-22).

Table I. Expression, physiological functions and disease involvement of SFKs

SFKs member	Expression tissues	Physiological roles	Related diseases	Reference
Src	Ubiquitously expressed	Cell migration, apoptosis; cell cycle progression, cell differentiation, gene synthesis	Various cancers; hepatitis C	(6, 23-27)
Yes	Ubiquitously expressed	Gene synthesis, cell differentiation	Colon cancer, pancreatic cancer	(23, 28-30)
Fyn	Ubiquitously; T-cell isoform	Gene synthesis, T cell differentiation, neural function	Alzheimer; various cancers	(16, 31-36)
Fgr	B-cells, myeloid cells	Immune response, cell differentiation, apoptosis	Airway inflammation, leukemia	(37-40)
Lyn	Brain, B-cells, myeloid cells	Activation of mast cells and B-cell, apoptosis, Immune response	Various cancers; autoimmunity	(*39, 41-46*)
Hck	myeloid cells	Cell differentiation, cell migration, HIV infection	HIV, acute leukemia, pulmonary disease	(37, 47-51)
Lck	Brain, T-cells, NK cells	T cell differentiation, immune response, HIV infection	Autoimmunity diseases; HIV	(52-54)
Blk	B-cells	B-cell activation, apoptosis	Chronic leukemia; autoimmunity diseases	(6, 55-57)

1.2 The structures of Src family kinases

SFK members share a highly conserved architecture (Figure 1.1). From the N- to C-terminus, SFKs have a unique domain, a Src Homology 3 (SH3) domain, a Src Homology 2 (SH2) domain, a proline-rich (PxxP) linker and a kinase domain, followed by a C-terminal regulatory segment, which contains a tyrosine residue, Y527 (In Src kinase), that can be phosphorylated/dephosphorylated. Each of these structural elements is described in more detail below.

The unique region, as its name suggests, varies significantly amongst the Src family kinases, and may contribute to the specific function of each SFK member. The unique region also includes amino acid sequences for myristoylation and palmitylation, both of which are involved in directing the proteins to cellular membranes (58-60).

The SH3 domain is about 60 amino acid residues in length and plays an important role in mediating protein-protein interactions. In human there are about 300 SH3 domains present in various kinds of proteins(61), representing one of the largest families of protein-interaction modules in eukaryotic proteins (62). SH3 domains are highly conserved, with sequence identity ranging from 20% to 95% (*63*). A typical structure of SH3 domain is a beta-barrel structure, consisting of 5 to 6 beta-stands (*64*).

SH3 domains preferentially interact with ligands containing consensus proline-rich (PxxP) motifs, such as RPLPPLP (*65*). SH3 domains, mostly via residues in n-Src and RT loops, form a relatively flat surface for interacting with proline-rich

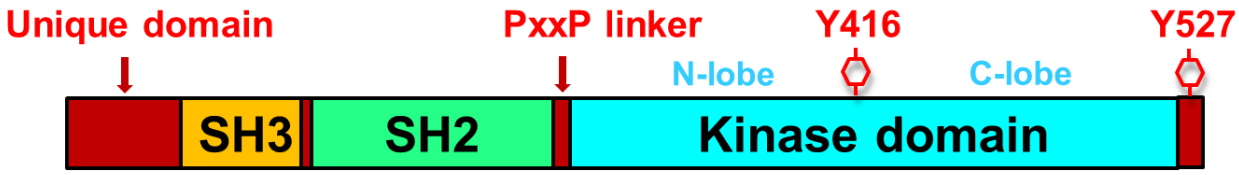

Figure 1.1. Primary structure of SFKs. SFKs members share a conserved architecture. From the N-terminus to the C-terminus, they all have a unique domain, which differs significantly among members, followed by a Src Homology 3 (SH3) domain and a Src Homology 2 (SH2) domain. Between the SH2 domain and the kinase domain, there is a proline-rich linker (PxxP). The kinase domain is divided into an N-lobe and a C-lobe by a catalytic cleft, where there is a conserved tyrosine residue, Y416. Upon activation, Y416 is autophosphorlated to fully activate the kinase. C-terminal to the kinase domain, there is short tail containing a tyrosine residue, Y527, which, upon phosphorylation, inhibits kinase activation by interacting with the SH2 domain.

motif (*64, 66*). The RPLPPLP peptide ligand adopts a left-handed helical structure, with 3 residues per turn, for binding (*67*). The two most conserved proline residues of the ligand (i.e. RPLPPLP) interact with the SH3 surface and contribute most of the binding energy, whereas the other proline residues promote the formation of the helical structure (*68*). Other non-proline residues, such as arginine and leucine, make additional contact outside the main binding groove and contribute to binding specificity (*68*).

There are two classes of proline-rich motifs that SH3 domains interact in two orientations (*67*). The class I has a consensus sequence of RPLPPLP (*65, 69*), whereas, the class II bear a motif of PxxPx(R/K), which interacts with the SH3 domain in the opposite direction (*67*). Besides the PxxP motif, SH3 domains also bind to several other motifs, such as R/KxxK (*70, 71*), RKxxYxxY (*72*), R(S/T)(S/T)SL (*73*), PxxDY (*74*) and Px(V/I)(D/N)RxxKP (*75*), in cellular proteins.

The SH3 domain plays two major roles in SFKs. First, it binds to the proline-rich linker between the SH2 domain and the kinase domain, to hold the SFKs in an inactive conformation (*76*). Second, it directs binding of SFKs to particular adaptor proteins, for translocation purposes within the cell (*77, 78*) or for orienting the substrate to perform subsequent phosphorylation (*79*). While SH3 domains contribute to numerous protein-protein interactions in cells (62), they generally bind to the PxxP ligands with weak specificity, as shown by studies with phage display (*80*). Consequently, one may wonder how the 300 SH3 domains in the human proteome mediate specific interactions in cells. Some studies suggest that additional contacts made outside the PxxP motif may enhance specificity to

an intact protein (*81*), and interactions with multiple SH3 domains simultaneously can lead to better specificity (*82, 83*). In contrast to the interactions mediated by proline-rich motifs, other rare motifs, such R/KxxK (*70*) and RKxxYxxY (*72*), interact with SH3 domains with high specificity, which may help explain some of our work, in which a monobody bearing a RxxK motif appears to achieve remarkable specificity in binding the Fyn SH3 domain (*84*).

At the C-terminal of the SH3 domain is the SH2 domain, which with a size of about 100 amino acid residues, binds to phosphotyrosine-containing motifs. In human there are 120 SH2 domains (*85*), representing the largest class of protein domains that recognize phosphotyrosine motifs (*86*). For interacting with a phosphorylated tyrosine, SH2 domains use a conserved arginine in its binding pocket to create electrostatic interactions (*87*). SH2 domains interact not only the phosphotyrosine residue but also several residues C-terminal of the conserved tyrosine (*85*); for example, the SH2 domain of the Src tyrosine kinase binds pYEEI (*88*), which was identified by screening peptide arrays.

Between the SH2 domain and the kinase domain, there is a proline-rich linker, which interacts with the SH3 domain in the inactive conformation of Src (*89*) and Hck (*90*). In the crystal structure of Hck (*90*), and in the primary structure of Blk, Lck and Lyn, there is a canonical PxxP consensus for interacting with SH3 domains, whereas in other SFKs members, the second proline of the consensus sequence is absent (*91*). Nonetheless, crystal structures reveal that SH3 domains from both subgroups use a similar mode for interacting with the proline-rich linkers (*89, 90*).

The kinase domain is composed of two lobes, the N-lobe and the C-lobe, with a catalytic cleft in between. In the cleft, there is a conserved tyrosine residue, Y416 (Src kinase), which can be autophosphorylated upon kinase activation; the autophosphorylation of Y416 is required for maximal kinase activity (*76*). The primary structure of the kinase domain is highly conserved across protein kinases (*1*), reflecting a shared mechanism for catalyzing phosphorylation. For example, the structure of the Lck kinase domain is strikingly similar to that of protein kinase A (*92, 93*), and both kinase domains share the conserved tyrosine 416 for autophosphorylation (*94*). The phosphoryl group at Y416 can be removed by several phosphatases, such as protein tyrosine phosphatase-Ŭ (PTPŬ) (*95*) and trans-membrane receptor-like tyrosine phosphatase (CD45) (*96*), leading to inactivation of the protein kinase.

C-terminal to the kinase domain, there is a short sequence in SFKs that contains a conserved tyrosine residue, Y527. When this tyrosine residue is phosphorylated, the C-terminal tail binds intramolecularly to the SH2 domain. Removal of the phosphoryl group by a phosphatase disrupts this interaction (*2*). While all SFKs members carry this conserved tyrosine residue, there are two consensus motifs among the two SFKs subfamilies, with QYxxQP in Lyn, Hck, Blk and Lck, and QYQPGxxx in Src, Yes, and Fyn and Fgr. Mutation of Y527 to phenylalanine disrupts the binding between the SH2 domain and the C-terminal segment, resulting in constitutive activation of SFKs (*97, 98*).

1.3 Inhibition and activation of Src family kinases

SFKs members share a common architecture, suggesting a possible shared mechanism governing inhibition and activation. As mentioned above, constitutive activation of SFKs leads to various forms of cancers (6, 15, 17). The ability to quickly shut down the kinase activity is crucial for the normal function of cells. In the presence of certain protein tyrosine phosphatases, such as protein tyrosine phosphatase-Ŭ (PTPŬ), SFKs become inactivated due to dephosphorylation of Y416 (*95*). Once the SFKs are inactivated, they fold into a ćlosedô configuration due to two intramolecular interactions (Figure 1.2) (*89*): the interaction between the SH3 domain and the proline-rich linker, and between the SH2 domain and the C-terminal tail containing Y527. The Y527 residue is phosphorylated by the C-terminal Src kinase (Csk) or the Csk homolog kinase (Chk) (*99, 100*).

There are several ways for SFKs to be activated. First, protein tyrosine phosphatases, such as PTP1B (*101*), dephosphorylate Y527 and relieve the inhibitory interaction between the C-terminal tail and the SH2 domain. Second, mutations in SH2 domain (*102*) or deletion of the regulatory C-terminus, in the case of Rous sarcoma virus (4), lead to constitutive activation of Src kinase (4). Third, cellular proteins, such as focal adhesion kinase (*103*), bind tightly to the SH2 domain of SFKs, displacing the bound C-terminus, and activating Src. Fourth, autophosphorylation of Y416, by other members of SFKs or other unrelated kinases, activates the kinase, even in the presence of the two inhibitory interactions (*104, 105*). Fifth, mutations in the SH3 domain (*106*) or inter-molecular interactions with proline-rich ligands (*107, 108*) can disengage the SH3

domain from its own proline-rich motif, thereby activating the SFKs (*107, 108*). In all of the activation mechanisms mentioned above, the folded SFKs molecules open up and expose the proline-rich binding interface of their SH3 domains (*109*). Thus, affinity reagents that target this surface of SH3 domain will only bind to the active SFKs.

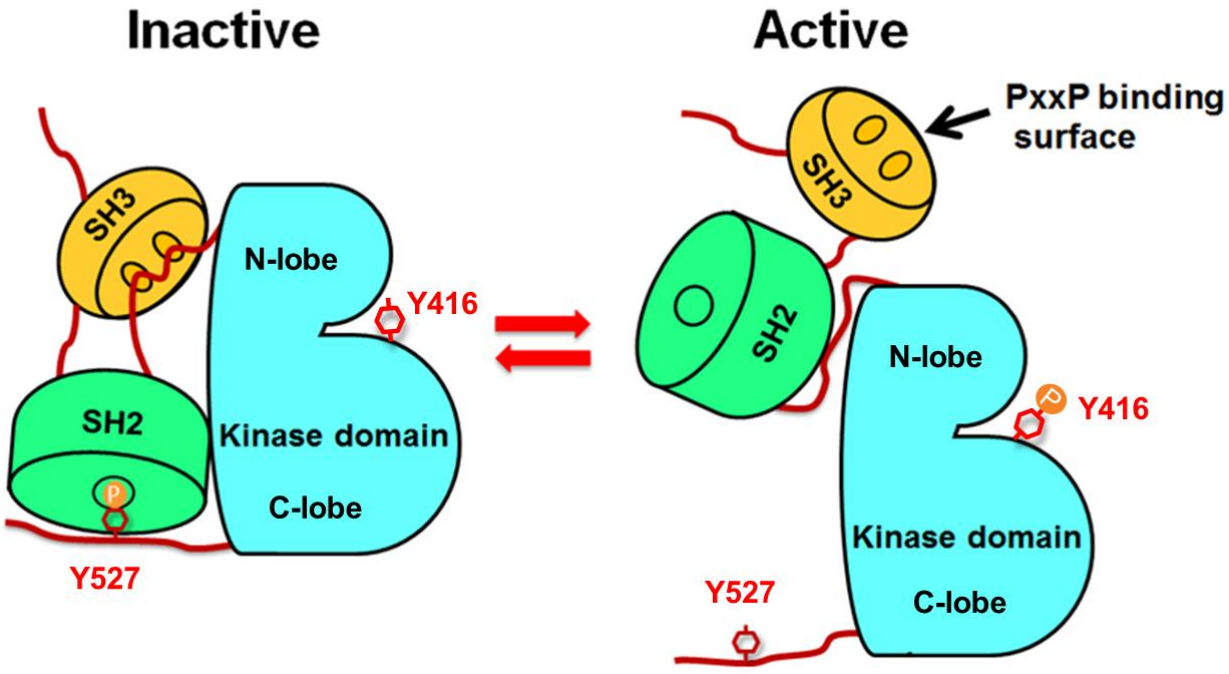

Figure 1.2. SFKs change configuration upon activation. When SFKs are catalytically inactive, they adopt a ócloseddconformation due to two intramolecular interactions: the one between the SH3 domain and the proline-rich linker, and that between the SH2 domain and the C-terminal tail containing phosphorylated Y527. When Y527 is dephosphorylated, the SH2 domain dissociates from the C-terminal tail, which promotes the detachment of the SH3 domain from the proline-rich linker. The abolishment of the two inhibitory interactions exposes the PxxP-binding interface of the SH3 domain to the cytoplasm. In the meantime, Y416 undergoes autophosphorylation, which leads to full activation and prepares the kinase for phosphorylating its substrate.

1.4 Affinity reagents for monitoring kinase activation

In response to different cellular stimuli, protein kinases switch between inactive and active states to fulfill their functions in a manner that is spatiotemporally precise (*110*). Consequently, reagents capable of discriminating between inactive and active kinases are invaluable for studying kinases. To detect the active form of the kinase molecules, antibodies have been developed for recognizing the autophosphorylation site in the kinase domain. However, due to the highly conserved sequences flanking the autophosphorylation site (e.g., > 90% identity in SFKs), these antibodies generally fail to discriminate one kinase from its closely-related kinases (*111*).

The ability to monitor activation of protein kinases in living cells will provide valuable information for a variety of reasons. First, in response to a changing environment, protein kinases in living cells constantly switch on and off (*110*), and tracking such dynamics permits studies of how kinases instantly respond to outside stimuli, such as to mechanical force (*112*) or drugs (*112-114*). Second, in living cells, different signaling pathways interact with one another momentarily to generate combinatorial responses to stimuli (*115*), studying of which requires sensors that can record the responses in real-time. Third, studies suggest that treating cells with the same reagent for different lengths of time has distinct effects on cells behavior (*116*), and a living-cell sensor will allow convenient monitoring over time.

Unfortunately it is challenging to express functional antibodies inside cells, as their disulfide bonds, which are required for proper antibody folding and antigen recognition, will not form in the reducing environment of the cell cytoplasm. Thus, most of the available biosensors utilize endogenous proteins, coupled with the technique of fluorescence resonance energy transfer (FRET), which requires fusion with GFP variants (Figure 1.3A). An example of FRET biosensors for Src activation (*117*) consists of a substrate site for Src kinase, an SH2 domain, and yellow (YFP) and cyan (CFP) fluorescent proteins at the termini. Upon phosphorylation of the tyrosine residue in the substrate sequence by Src kinase, the phosphopeptide binds to the SH2 domain, bringing CFP and YFP close to each other, leading to energy transfer between them and change of fluorescence emission (Figure 1.3A). There are several disadvantages with this type of biosensor. First, there are a huge number of protein kinases, for which there are currently no known substrates, synthetic or naturally occurring, available in the literature for engineering into sensors. Second, short substrate motifs are recognized and phosphorylated by multiple kinases. Third, the biosensor signal is weak due to the inefficient energy transfer of FRET. Finally, this sensor does not correct the change of fluorescence intensity caused by the irregular shape of the cells, in which a FRET signal may be lower in a thick region of the cell compared to a thin region.

Due to the above limitations with the current FRET-based sensors, scaffold-based affinity reagents provide an attractive alternative for generating living-cell biosensors. In a recent study by Hahn and his co-workers (*114*), a FN3

monobody is converted into a biosensor that monitors the activation of Src in cells (Figure 1.3B). The FN3 monobody for building the sensor was previously isolated by the Kay group for binding to the Src SH3 domain (*118*). The Hahn group engineers the monobody into the sensor by conjugating a solvatochromatic dye, merocyanine, to a free cysteine inserted into the FN3 scaffold. To conduct the ratio-imaging, the Hahn Group fuses the alkylated monobody to a GFP variant, which is positioned far away from the binding interface of the monobody. As a result, the fluorescence emission of the GFP is independent of the binding event of the sensor and its intensity can be used to divide the emission of merocyanine dye to obtain the ratiometric fluorescence response (dye emission/GFP emission). This ratiometric imaging corrects the fluorescence change caused by the uneven shape of the cells.

The biosensor built by the Hahn group offers several advantages over FRET-based biosensors. First, unlike the FRET-based Src sensor, which tracks the location of the Src kinase substrates (*112, 117*), the reporter-dye sensor locates the Src kinase itself for its activation events (as defined by the exposure of the SH3 domain). Thus, with this sensor they are able to quantitatively correlate the protrusion velocity of the leading cell edge with the distribution of endogenous Src activity (*114*). Second, the reporter-dye sensor is much more sensitive (e.g., >2.4-fold brighter) than FRET-based biosensors (*114*), due to the brightness of the merocyanine dye. However, it does have the disadvantage that the dye-labeled sensor must be microinjected into cells.

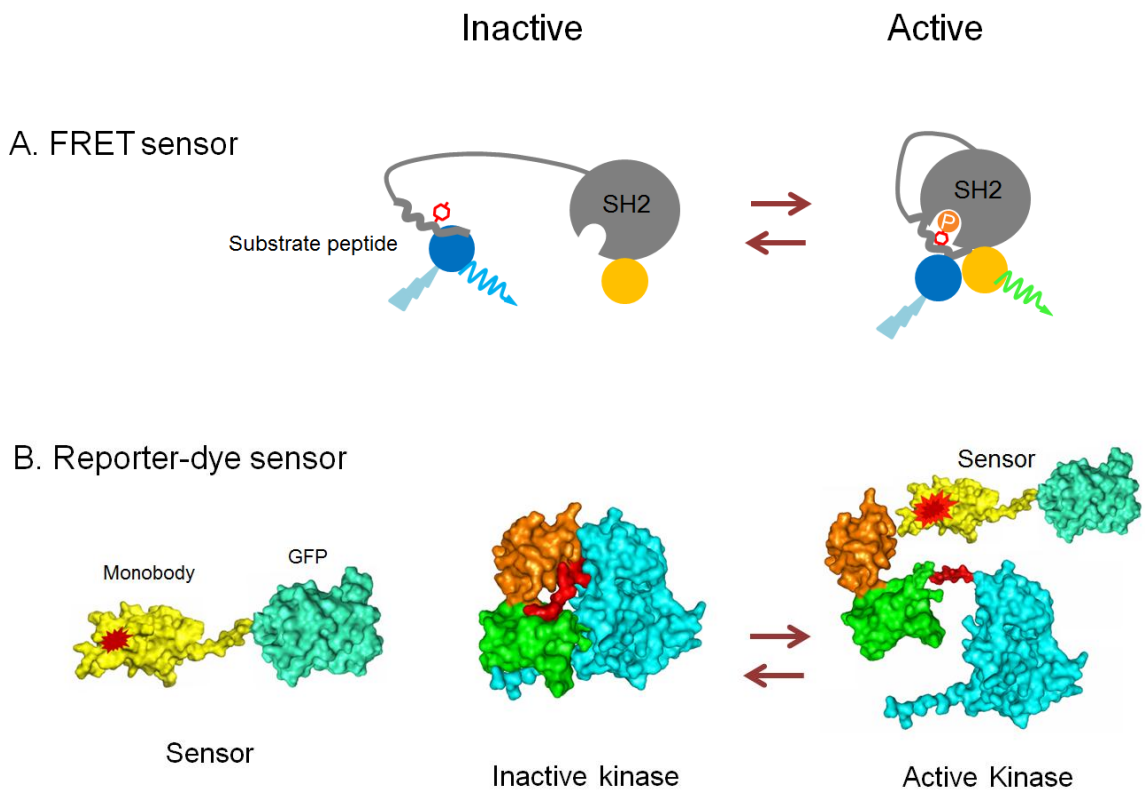

Figure 1.3. Comparison of a FRET sensor with a reporter-dye sensor. A. In a FRET sensor, cyan (CFP) and yellow (YFP) fluorescent proteins are fused to two different protein domains. One is a substrate peptide containing a tyrosine that can be phosphorylated. The other one is a SH2 domain (Grey circle) that contains a pocket for binding to phosphotyrosine. A polypeptide linker connects the two domains. Upon phosphorylation of the substrate tyrosine residue by a cellular kinase, substrate peptide binds to the SH2 domain. Their interaction brings CFP and YFP close to each other, leading to energy transfer between them and the change of fluorescence emission (*117, 119*). **B.** In a reporter-dye sensor, the sensor consists of a FN3 monobody, a solvatochromatic dye (Red ósturô within the depicted monobody) and a GFP variant, which is used to normalize the thickness of the cell. When a cellular regulator activates the kinase, it changes its conformation and exposes its SH3 domain, which is recognized by the FN3 monobody. The binding of the sensor to the SH3 domain changes the environment of the reporter dye, leading to an increase in fluorescence intensity (*114*). Figures were generated with PyMol (*120*), using the following PDB files: 1TTG (monobody), 2WSO (GFP), and 1FMK (Src).

1.5 Isolation of affinity reagents with phage-display

To generate reagents for monitoring the activation of SFKs members, I used a molecular evolution method involving filamentous phage display. In óphage displayô a foreign polypeptide, whose sequence is encoded by the genome of the bacteriophage, is displayed on the surface of the bacteriophage as a fusion protein to the phage capsid protein, thereby establishing a linkage of genotype and phenotype. A pool of phage particles, displaying polypeptides with different sequences, yields a mutant library, screening of which leads to discovery of protein variants with desired characteristics.

Since the invention of phage display by George Smith in 1985 (*121*), tremendous progress has been made through many molecular evolution experiments, ranging from generating tools for basic science research to the development of therapeutic reagents. Phage display has been used to map protein-protein interactions (*122, 123*), improve protein stability (*124, 125*) and solubility (*126*), identify protease substrates (*127, 128*), design enzymatically active antibodies (*129, 130*), and develop cell-penetrating reagents (*131, 132*). One of the most popular applications of phage display is for isolating affinity reagents binding to various targets, such as inert materials (*133*), metabolites (*134*), lipids (*135, 136*), cell surfaces (*137, 138*), and cytosolic proteins (*139-141*). For this purpose, polypeptide sequences, such as linear or cyclic peptides (*142, 143*), stable protein scaffolds (*144, 145*), and antibody fragments (*146, 147*), have been displayed on the virion surface.

Due to their short sequences and the limited number of side-chain residues involved in molecular interactions, the majority of the peptide ligands isolated from phage libraries have relatively weak affinity to protein targets (*148*). Conversely, antibody fragments, in the form of single-chain variable fragments (scFv) (*147*) or the fragments antigen-binding (Fab) (*149, 150*), can be routinely isolated to a wide range forms of targets. While these isolated antibody fragments exhibit remarkable binding affinity and specificity, their expression levels in E. coli hosts varies significantly among different isolates (*151*), making it very challenging to obtain enough samples of such recombinant antibodies for various applications. Similar to full-length antibodies, these fragments of antibodies also require disulfide bond for folding and thus restrict their application in live-cell studies. To circumvent such limitations, diverse types of protein scaffolds have been engineered into affinity reagents as antibody alternatives. These scaffolds include affibodies (*152*), avimers (*153*), lipocalin (*154*), designed ankyrin repeat proteins (*155*), SH3 domains (*156*), SH2 domains (*139*), and fibronectin type III (FN3) monobodies (*144*). The FN3 monobody is the scaffold that I have used to generate affinity reagents in this thesis work.

1.6 FN3 monobody

The FN3 monobody is a cognate of the 10th subunit of human fibronectin type III repeat (FN3), which contains an Arg-Gly-Asp (RGD) tripeptide motif for binding to integrins on the cell surface (*157*). The FN3 scaffold, 94 amino acids in size, contains seven beta-strands, which fold into a structure that resembles the

variable domain of the immunoglobulin heavy chain, leading to the name ómonobodyô(Figure 1.4)(*144*). There are six flexible loops linking the beta-strands, and mutational studies show that two loops (BC and FG) tolerate insertions of amino acids sequences, without loss of thermostability (*158*).

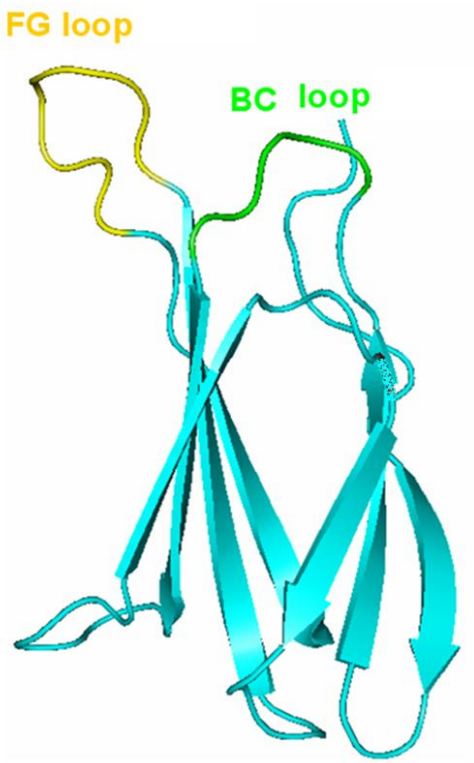

Figure 1.4. The crystal structure of FN3 scaffold. The scaffold consists of seven beta-strands that assemble into a sandwich-like structure. Of the six flexible loops connecting the beta-stands, the FG and BC loops are frequently used for engineering monobodies with novel binding properties. The cartoon representation of FN3 was created with PyMol (*120*) (PDB code: 1ttg).

Molecular evolution experiments, including phage display (*118, 144*), mRNA display (*159, 160*), and yeast display (*161, 162*), have been used to engineer the FN3 scaffold for binding to a wide variety of targets, such as ubiquitin (*144*), maltose binding protein (*163*), lysozyme (*162*), streptavidin (*118*), hSUMO (*164*), Phosphor-IəBŬ peptide (*160*) and GFP (*150*). For a list of the selected FN3 monodies that have been isolated since the development of FN3 monobodies, please refer to the Table II.

There are several advantages of FN3 monobodies that make them suitable for monitoring the activation of proteins kinases *in vitro* and *in vivo*. First, the monobody lacks disulfide bond and thus functional monobodies can be expressed in mammalian cells. Second, FN3 monobodies with high specificity (*84, 140, 165*) and affinity (*162, 166*) have been engineered. Third, a number of monobodies have also been engineered into sensors for monitoring a conformation-specific kinase (*160*) in cell lysate, and sensors for detecting the estrogen receptor (*167*) and Src tyrosine kinase in living cells (*114*). Fourth, residues in the FN3 scaffold have been mutated to accept a bright solvatochromatic dye, merocyanine, which increases fluorescence when the FN3 monobody binds to its target *in vitro* and *in vivo* (*114*).

Table II. Characteristics of FN3 monobodies discovered by various display methods.

Display method	Library size	Target	Highest affinity Measured (nM)	Reference
Phage display (pIII)	1×10^{8}	Ubiquitin	Not determined	(*144*)
Phage display (pIII)	2×10^{9}	Src SH3	250	(*118*)
Phage display (pIII)	1×10^{10}	MBP, hSUMO ySUMO	5	(*164*)
Phage display (pIII)	1×10^{9}	ARVCF peptide	<4	(*168*)
Phage display (pIII)	5×10^{9}	Abl SH2	7	(*140*)
Phage display (pIII)/Yeast	2×10^{10} 1.5×10^{10}	SUMO, Abl SH2, GFP	9	(*169*)
Phage display (pVIII)	1.5×10^{6}	Integrin	0.8	(*170*)
Yeast two-hybrid	2×10^{6}	Estrogen receptor	Not determined	(*167*)
Yeast display	3×10^{7} ï 6×10^{8}	Lysozyme	0.35	(*161*)
Yeast display	6.5×10^{7}	Lysozyme	0.001	(*162*)
mRNA display	1×10^{12}	TNF-Ŭ	0.02	(*159*)
mRNA display	1×10^{13}	VEGFR2	0.06	(*166*)
mRNA display	3×10^{13}	Phosphoryated IəBŬ peptide	18	(*160*)
mRNA display	3×10^{13}	SARŝs N protein	1.7	(*171*)

1.7 Directed evolution of existing FN3 monobodies

For several reasons, directed evolution of existing FN3 monobodies is needed to achieve the desired characteristics for being useful as affinity reagents (*172, 173*). First, the intended targets (i.e., protein kinases), share conserved primary or three-dimensional structures with other similar proteins in the cell, making it challenging to isolate binders that selectively recognize a particular target. Consequently, isolated binders often need to be engineered for greater selectivity. Second, there is an optimal range of binding affinity for the sensors to interact with their targets. Weak affinity makes sensors insensitive or incapable of detecting their targets as the concentration of active molecules of a particular kinase in cells is extremely low. At the same time, extremely high affinity, such as a K_D with a low nM value, may interfere with the natural dynamics of kinase molecules (*174*). Third, some FN3 monobodies have poor solubility, and directed evolution can be implemented to increase their solubility (*126*).

There are several approaches to engineer existing FN3 monobodies. One method is to amplify the DNA sequence of a particular clone through a mutagenic polymerase chain reaction (PCR) and create a secondary mutant library (*172, 173*), which will be affinity selected under highly stringent conditions (etc., more washes, longer wash times, addition of competitor proteins). A second approach is to randomize certain residues in the diversified loops of an isolated monobody and create a mutagenic library for further evolution (*162, 175*). A third approach is to create a new mutagenic library by shuffling mutagenized loops of an enriched binder pool (*140, 162*).

1.8 Thesis goals and organization

Src family kinases (SFKs) are a group of protein tyrosine kinases that regulate many cellular pathways and have been implicated in the pathogenesis of many diseases. In response to the changing environment, SFKs constantly switch on and off to regulate signaling pathways. Due to the highly conserved sequences among SFKs, currently available antibodies fail to distinguish the active form of one kinase from other SFKs. Thus, one of the goals of my Ph.D. thesis is to generate affinity reagents that can not only recognize the active kinase molecules but also can distinguish one member from the rest of the SFKs.

To generate such affinity reagents, I constructed several primary and secondary phage-display libraries. To make Kunkel mutagenesis more efficient, I discovered that culturing bacterial cells at 25°C versus 37°C yielded two- to sevenfold more single-stranded DNA template, and that restriction endonuclease digestion could be used to remove non-recombinants from the library. With both modifications in hand, I could generate high-quality libraries, with diversity up to 10^{10} and 99-100% recombinant. Finally, I designed a digestion- and ligation-free method for constructing secondary libraries for affinity-maturing binders. To demonstrate the efficiency of this improved method, I constructed two secondary mutagenic libraries based on an FN3 monobody that bound to the active form of Pak1 kinase. By screening one of the mutagenic libraries, I discovered three variants that bound 2- to 4-fold tighter than the original clone.

For generating affinity reagents to one member of the SFKs, Fyn tyrosine kinase, a phage-display library was screened for monobodies binding to Fyn SH3

domain. The affinity selection identified three monobodies that bound selectively to the Fyn SH3 domain. One of the isolates, G9, bound exclusively to the Fyn SH3 domain out of 150 SH3 domains examined in an array and had a dissociation constant (K_D) of 166 ± 6 nM, as measured by isothermal titration calorimetry. Interestingly, while the G9 monobody lacks proline in its randomized loops, it bound at the same site on the SH3 domain as proline-rich ligands. The G9 monobody could be used to pull down active recombinant Fyn kinase *in vitro*, demonstrating its potential as a highly selective probe for detecting active cellular Fyn kinase. The above work of generating affinity reagents to Fyn kinase is described in Chapter 3. The Appendix describes affinity maturation of a FN3 monobody for improved binding affinity and specificity to the Fyn SH3 domain.

To generate affinity reagents for another SFK member, Lyn tyrosine kinase, I screened the same phage-displayed library of FN3 monobodies (Chapter 4). Two isolates, TA1 and TA8, selectively bound to the Lyn SH3 domain out of 150 SH3 domains. Both TA1 and TA8, in the absence of a canonical PxxP motif in their binding loops, competed with a PxxP proline-rich peptide, Tip, for binding to the Lyn SH3 domain. As the dissociation constant (K_D) of TA8 for Lyn SH3 was ~5 μM, which is relatively weak, I used affinity maturation techniques to identify variants that bound > 8-fold tighter than the original TA8 clone. As a proof-of-concept experiment, the monobody was fused to GFP and converted into a sensor that increased fluorescence upon binding to the Lyn SH3 domain in solution.

1.9 References

1. Manning, G., Whyte, D. B., Martinez, R., Hunter, T., and Sudarsanam, S. (2002) The protein kinase complement of the human genome, *Science 298*, 1912-1934.

2. Roskoski, R., Jr. (2005) Src kinase regulation by phosphorylation and dephosphorylation, *Biochem Biophys Res Commun 331*, 1-14.

3. Cohen, P. (2002) Protein kinases--the major drug targets of the twenty-first century?, *Nat Rev Drug Discov 1*, 309-315.

4. Smart, J. E., Oppermann, H., Czernilofsky, A. P., Purchio, A. F., Erikson, R. L., and Bishop, J. M. (1981) Characterization of sites for tyrosine phosphorylation in the transforming protein of Rous sarcoma virus (pp60v-src) and its normal cellular homologue (pp60c-src), *Proc Natl Acad Sci U S A 78*, 6013-6017.

5. Bolen, J. B., and Brugge, J. S. (1997) Leukocyte protein tyrosine kinases: potential targets for drug discovery, *Annu Rev Immunol 15*, 371-404.

6. Thomas, S. M., and Brugge, J. S. (1997) Cellular functions regulated by Src family kinases, *Annu Rev Cell Dev Biol 13*, 513-609.

7. Lowell, C. A., and Soriano, P. (1996) Knockouts of Src-family kinases: stiff bones, wimpy T cells, and bad memories, *Genes Dev 10*, 1845-1857.

8. Luttrell, D. K., Luttrell, L. M., and Parsons, S. J. (1988) Augmented mitogenic responsiveness to epidermal growth factor in murine fibroblasts that overexpress pp60c-src, *Mol Cell Biol 8*, 497-501.

9. Weernink, P. A., and Rijksen, G. (1995) Activation and translocation of c-Src to the cytoskeleton by both platelet-derived growth factor and epidermal growth factor, *J Biol Chem 270*, 2264-2267.

10. Twamley, G. M., Kypta, R. M., Hall, B., and Courtneidge, S. A. (1992) Association of Fyn with the activated platelet-derived growth factor receptor: requirements for binding and phosphorylation, *Oncogene 7*, 1893-1901.

11. Kypta, R. M., Goldberg, Y., Ulug, E. T., and Courtneidge, S. A. (1990) Association between the PDGF receptor and members of the src family of tyrosine kinases, *Cell 62*, 481-492.

12. Kremer, N. E., D'Arcangelo, G., Thomas, S. M., DeMarco, M., Brugge, J. S., and Halegoua, S. (1991) Signal transduction by nerve growth factor and fibroblast growth factor in PC12 cells requires a sequence of src and ras actions, *J Cell Biol 115*, 809-819.

13. Peterson, J. E., Kulik, G., Jelinek, T., Reuter, C. W., Shannon, J. A., and Weber, M. J. (1996) Src phosphorylates the insulin-like growth factor type I receptor on the autophosphorylation sites. Requirement for transformation by src, *J Biol Chem 271*, 31562-31571.

14. Rabinowich, H., Manciulea, M., Metes, D., Sulica, A., Herberman, R. B., Corey, S. J., and Whiteside, T. L. (1996) Physical and functional association of Fc mu receptor on human natural killer cells with the zeta- and Fc epsilon RI gamma-chains and with src family protein tyrosine kinases, *J Immunol 157*, 1485-1491.

15. Sen, B., and Johnson, F. M. (2011) Regulation of SRC family kinases in human cancers, *J Signal Transduct 2011*, 865819.

16. Saito, Y. D., Jensen, A. R., Salgia, R., and Posadas, E. M. (2010) Fyn: a novel molecular target in cancer, *Cancer 116*, 1629-1637.

17. Summy, J. M., and Gallick, G. E. (2003) Src family kinases in tumor progression and metastasis, *Cancer Metastasis Rev 22*, 337-358.

18. Jabbour, E., Cortes, J., and Kantarjian, H. (2007) Dasatinib for the treatment of Philadelphia chromosome-positive leukaemias, *Expert Opin Investig Drugs 16*, 679-687.

19. Cortes, J. E., Kim, D. W., Kantarjian, H. M., Brummendorf, T. H., Dyagil, I., Griskevicus, L., Malhotra, H., Powell, C., Gogat, K., Countouriotis, A. M., and Gambacorti-Passerini, C. (2012) Bosutinib Versus Imatinib in Newly Diagnosed Chronic-Phase Chronic Myeloid Leukemia: Results From the BELA Trial, *J Clin Oncol*.

20. Lombardo, L. J., Lee, F. Y., Chen, P., Norris, D., Barrish, J. C., Behnia, K., Castaneda, S., Cornelius, L. A., Das, J., Doweyko, A. M., Fairchild, C., Hunt, J. T., Inigo, I., Johnston, K., Kamath, A., Kan, D., Klei, H., Marathe, P., Pang, S., Peterson, R., Pitt, S., Schieven, G. L., Schmidt, R. J., Tokarski, J., Wen, M. L., Wityak, J., and Borzilleri, R. M. (2004) Discovery of N-(2-chloro-6-methyl- phenyl)-2-(6-(4-(2-hydroxyethyl)- piperazin-1-yl)-2-methylpyrimidin-4- ylamino)thiazole-5-carboxamide (BMS-354825), a dual Src/Abl kinase inhibitor with potent antitumor activity in preclinical assays, *J Med Chem 47*, 6658-6661.

21. Tokarski, J. S., Newitt, J. A., Chang, C. Y., Cheng, J. D., Wittekind, M., Kiefer, S. E., Kish, K., Lee, F. Y., Borzillerri, R., Lombardo, L. J., Xie, D., Zhang, Y., and Klei, H. E. (2006) The structure of Dasatinib (BMS-354825) bound to activated ABL kinase domain elucidates its inhibitory activity against imatinib-resistant ABL mutants, *Cancer Res 66*, 5790-5797.

22. Thaimattam, R., Daga, P. R., Banerjee, R., and Iqbal, J. (2005) 3D-QSAR studies on c-Src kinase inhibitors and docking analyses of a potent dual kinase inhibitor of c-Src and c-Abl kinases, *Bioorg Med Chem 13*, 4704-4712.

23. Broome, M. A., and Hunter, T. (1996) Requirement for c-Src catalytic activity and the SH3 domain in platelet-derived growth factor BB and epidermal growth factor mitogenic signaling, *J Biol Chem 271*, 16798-16806.

24. Bockholt, S. M., and Burridge, K. (1993) Cell spreading on extracellular matrix proteins induces tyrosine phosphorylation of tensin, *J Biol Chem 268*, 14565-14567.

25. Basu, A., and Cline, J. S. (1995) Oncogenic transformation alters cisplatin-induced apoptosis in rat embryo fibroblasts, *Int J Cancer 63*, 597-603.

26. Hecker, G., Lewis, D. L., Rausch, D. M., and Jelsema, C. L. (1991) Nerve-growth-factor-treated and v-src-expressing PC 12 cells: a model for neuronal differentiation, *Biochem Soc Trans 19*, 385-386.

27. Pfannkuche, A., Buther, K., Karthe, J., Poenisch, M., Bartenschlager, R., Trilling, M., Hengel, H., Willbold, D., Haussinger, D., and Bode, J. G. (2011) c-Src is required for complex formation between the hepatitis C

virus-encoded proteins NS5A and NS5B: a prerequisite for replication, *Hepatology 53*, 1127-1136.

28. Lord, K. A., Abdollahi, A., Thomas, S. M., DeMarco, M., Brugge, J. S., Hoffman-Liebermann, B., and Liebermann, D. A. (1991) Leukemia inhibitory factor and interleukin-6 trigger the same immediate early response, including tyrosine phosphorylation, upon induction of myeloid leukemia differentiation, *Mol Cell Biol 11*, 4371-4379.

29. Anderson, K., Sancier, F., Dumont, A., Sirvent, A., Paquay de Plater, L., Edmonds, T., David, G., Jan, M., de Montrion, C., Cogé, F., Léonce, S., Burbridge, M., Bruno, A., Boutin, J. A., Lockhart, B., Roche, S., and Cruzalegui, F. (2011) Specific Oncogenic Activity of the Src-Family Tyrosine Kinase c-Yes in Colon Carcinoma Cells, *PLoS One 6*, e17237.

30. Kubo, T., Kuroda, Y., Kokubu, A., Hosoda, F., Arai, Y., Hiraoka, N., Hirohashi, S., and Shibata, T. (2009) Resequencing analysis of the human tyrosine kinase gene family in pancreatic cancer, *Pancreas 38*, e200-206.

31. Cooke, M. P., Abraham, K. M., Forbush, K. A., and Perlmutter, R. M. (1991) Regulation of T cell receptor signaling by a src family protein-tyrosine kinase (p59fyn), *Cell 65*, 281-291.

32. Twamley-Stein, G. M., Pepperkok, R., Ansorge, W., and Courtneidge, S. A. (1993) The Src family tyrosine kinases are required for platelet-derived growth factor-mediated signal transduction in NIH 3T3 cells, *Proc Natl Acad Sci U S A 90*, 7696-7700.

33. Beggs, H. E., Soriano, P., and Maness, P. F. (1994) NCAM-dependent neurite outgrowth is inhibited in neurons from Fyn-minus mice, *J Cell Biol 127*, 825-833.

34. Kanaan, N. M., Morfini, G., Pigino, G., LaPointe, N. E., Andreadis, A., Song, Y., Leitman, E., Binder, L. I., and Brady, S. T. (2012) Phosphorylation in the amino terminus of tau prevents inhibition of anterograde axonal transport, *Neurobiol Aging 33*, 826 e815-830.

35. Um, J. W., and Strittmatter, S. M. (2012) Amyloid-ss induced signaling by cellular prion protein and Fyn kinase in Alzheimer disease, *Prion 6*.

36. Schenone, S., Brullo, C., Musumeci, F., Biava, M., Falchi, F., and Botta, M. (2011) Fyn kinase in brain diseases and cancer: the search for inhibitors, *Curr Med Chem 18*, 2921-2942.

37. Lowell, C. A., Fumagalli, L., and Berton, G. (1996) Deficiency of Src family kinases p59/61hck and p58c-fgr results in defective adhesion-dependent neutrophil functions, *J Cell Biol 133*, 895-910.

38. Vicentini, L., Mazzi, P., Caveggion, E., Continolo, S., Fumagalli, L., Lapinet-Vera, J. A., Lowell, C. A., and Berton, G. (2002) Fgr deficiency results in defective eosinophil recruitment to the lung during allergic airway inflammation, *J Immunol 168*, 6446-6454.

39. Katagiri, K., Yokoyama, K. K., Yamamoto, T., Omura, S., Irie, S., and Katagiri, T. (1996) Lyn and Fgr protein-tyrosine kinases prevent apoptosis during retinoic acid-induced granulocytic differentiation of HL-60 cells, *J Biol Chem 271*, 11557-11562.

40. Link, D. C., and Zutter, M. (1995) The proto-oncogene c-fgr is expressed in normal mantle zone B lymphocytes and is developmentally regulated during myelomonocytic differentiation in vivo, *Blood 85*, 472-479.

41. Satterthwaite, A. B., Lowell, C. A., Khan, W. N., Sideras, P., Alt, F. W., and Witte, O. N. (1998) Independent and opposing roles for Btk and lyn in B and myeloid signaling pathways, *J Exp Med 188*, 833-844.

42. Stauffer, T. P., Martenson, C. H., Rider, J. E., Kay, B. K., and Meyer, T. (1997) Inhibition of Lyn function in mast cell activation by SH3 domain binding peptides, *Biochemistry 36*, 9388-9394.

43. Xiao, W., Nishimoto, H., Hong, H., Kitaura, J., Nunomura, S., Maeda-Yamamoto, M., Kawakami, Y., Lowell, C. A., Ra, C., and Kawakami, T. (2005) Positive and negative regulation of mast cell activation by Lyn via the FcepsilonRI, *J Immunol 175*, 6885-6892.

44. Kawakami, Y., Kitaura, J., Satterthwaite, A. B., Kato, R. M., Asai, K., Hartman, S. E., Maeda-Yamamoto, M., Lowell, C. A., Rawlings, D. J., Witte, O. N., and Kawakami, T. (2000) Redundant and opposing functions of two tyrosine kinases, Btk and Lyn, in mast cell activation, *J Immunol 165*, 1210-1219.

45. Zimmerman, E. I., Dollins, C. M., Crawford, M., Grant, S., Nana-Sinkam, S. P., Richards, K. L., Hammond, S. M., and Graves, L. M. (2010) Lyn kinase-dependent regulation of miR181 and myeloid cell leukemia-1 expression: implications for drug resistance in myelogenous leukemia, *Mol Pharmacol 78*, 811-817.

46. Trevino, J. G., Summy, J. M., Lesslie, D. P., Parikh, N. U., Hong, D. S., Lee, F. Y., Donato, N. J., Abbruzzese, J. L., Baker, C. H., and Gallick, G. E. (2006) Inhibition of SRC expression and activity inhibits tumor progression and metastasis of human pancreatic adenocarcinoma cells in an orthotopic nude mouse model, *Am J Pathol 168*, 962-972.

47. Lowell, C. A., Niwa, M., Soriano, P., and Varmus, H. E. (1996) Deficiency of the Hck and Src tyrosine kinases results in extreme levels of extramedullary hematopoiesis, *Blood 87*, 1780-1792.

48. Lake, J. A., Carr, J., Feng, F., Mundy, L., Burrell, C., and Li, P. (2003) The role of Vif during HIV-1 infection: interaction with novel host cellular factors, *J Clin Virol 26*, 143-152.

49. Guiet, R., Poincloux, R., Castandet, J., Marois, L., Labrousse, A., Le Cabec, V., and Maridonneau-Parini, I. (2008) Hematopoietic cell kinase (Hck) isoforms and phagocyte duties - from signaling and actin reorganization to migration and phagocytosis, *Eur J Cell Biol 87*, 527-542.

50. Zou, D., Yang, X., Tan, Y., Wang, P., Zhu, X., Yang, W., Jia, X., Zhang, J., and Wang, K. (2012) Regulation of the hematopoietic cell kinase (HCK) by PML/RARalpha and PU.1 in acute promyelocytic leukemia, *Leuk Res 36*, 219-223.

51. Yanagisawa, S., Sugiura, H., Yokoyama, T., Yamagata, T., Ichikawa, T., Akamatsu, K., Koarai, A., Hirano, T., Nakanishi, M., Matsunaga, K., Minakata, Y., and Ichinose, M. (2009) The possible role of hematopoietic cell kinase in the pathophysiology of COPD, *Chest 135*, 94-101.

52. Lewin, I., Nechushtan, H., Ke, Q., and Razin, E. (1993) Regulation of AP-1 expression and activity in antigen-stimulated mast cells: the role played by protein kinase C and the possible involvement of Fos interacting protein, *Blood 82*, 3745-3751.

53. Collette, Y., Dutartre, H., Benziane, A., Ramos, M., Benarous, R., Harris, M., and Olive, D. (1996) Physical and functional interaction of Nef with Lck. HIV-1 Nef-induced T-cell signaling defects, *J Biol Chem 271*, 6333-6341.

54. Tai, X., Van Laethem, F., Sharpe, A. H., and Singer, A. (2007) Induction of autoimmune disease in CTLA-4-/- mice depends on a specific CD28 motif that is required for in vivo costimulation, *Proc Natl Acad Sci U S A 104*, 13756-13761.

55. Simpfendorfer, K. R., Olsson, L. M., Manjarrez Orduno, N., Khalili, H., Simeone, A. M., Katz, M. S., Lee, A. T., Diamond, B., and Gregersen, P. K. (2012) The autoimmunity-associated BLK haplotype exhibits cis-regulatory effects on mRNA and protein expression that are prominently observed in B cells early in development, *Hum Mol Genet 21*, 3918-3925.

56. Zhang, H., Peng, C., Hu, Y., Li, H., Sheng, Z., Chen, Y., Sullivan, C., Cerny, J., Hutchinson, L., Higgins, A., Miron, P., Zhang, X., Brehm, M. A., Li, D., Green, M. R., and Li, S. (2012) The Blk pathway functions as a tumor suppressor in chronic myeloid leukemia stem cells, *Nat Genet 44*, 861-871.

57. Yao, X. R., and Scott, D. W. (1993) Antisense oligodeoxynucleotides to the blk tyrosine kinase prevent anti-mu-chain-mediated growth inhibition and apoptosis in a B-cell lymphoma, *Proc Natl Acad Sci U S A 90*, 7946-7950.

58. Saouaf, S. J., Wolven, A., Resh, M. D., and Bolen, J. B. (1997) Palmitylation of Src family tyrosine kinases regulates functional interaction with a B cell substrate, *Biochem Biophys Res Commun 234*, 325-329.

59. Alland, L., Peseckis, S. M., Atherton, R. E., Berthiaume, L., and Resh, M. D. (1994) Dual myristylation and palmitylation of Src family member p59fyn affects subcellular localization, *J Biol Chem 269*, 16701-16705.

60. Resh, M. D. (1994) Myristylation and palmitylation of Src family members: the fats of the matter, *Cell 76*, 411-413.

61. Karkkainen, S., Hiipakka, M., Wang, J. H., Kleino, I., Vaha-Jaakkola, M., Renkema, G. H., Liss, M., Wagner, R., and Saksela, K. (2006) Identification of preferred protein interactions by phage-display of the human Src homology-3 proteome, *EMBO Rep 7*, 186-191.

62. Mayer, B. J. (2001) SH3 domains: complexity in moderation, *J Cell Sci 114*, 1253-1263.

63. Sparks, A. B. (1996) Analysis of SH3 domain-ligand interactions using combinatorial peptide libraries, *Ph.D dissertation, University of North Carolina, Chapel Hill*.

64. Borchert, T. V., Mathieu, M., Zeelen, J. P., Courtneidge, S. A., and Wierenga, R. K. (1994) The crystal structure of human CskSH3: structural diversity near the RT-Src and n-Src loop, *FEBS Lett 341*, 79-85.

65. Sparks, A. B., Quilliam, L. A., Thorn, J. M., Der, C. J., and Kay, B. K. (1994) Identification and characterization of Src SH3 ligands from phage-displayed random peptide libraries, *J Biol Chem 269*, 23853-23856.

66. Yu, H., Rosen, M. K., Shin, T. B., Seidel-Dugan, C., Brugge, J. S., and Schreiber, S. L. (1992) Solution structure of the SH3 domain of Src and identification of its ligand-binding site, *Science 258*, 1665-1668.

67. Feng, S., Chen, J. K., Yu, H., Simon, J. A., and Schreiber, S. L. (1994) Two binding orientations for peptides to the Src SH3 domain: development of a general model for SH3-ligand interactions, *Science 266*, 1241-1247.

68. Yu, H., Chen, J. K., Feng, S., Dalgarno, D. C., Brauer, A. W., and Schreiber, S. L. (1994) Structural basis for the binding of proline-rich peptides to SH3 domains, *Cell 76*, 933-945.

69. Cohen, G. B., Ren, R., and Baltimore, D. (1995) Modular binding domains in signal transduction proteins, *Cell 80*, 237-248.

70. Berry, D. M., Nash, P., Liu, S. K., Pawson, T., and McGlade, C. J. (2002) A high-affinity Arg-X-X-Lys SH3 binding motif confers specificity for the interaction between Gads and SLP-76 in T cell signaling, *Curr Biol 12*, 1336-1341.

71. Lewitzky, M., Harkiolaki, M., Domart, M. C., Jones, E. Y., and Feller, S. M. (2004) Mona/Gads SH3C binding to hematopoietic progenitor kinase 1 (HPK1) combines an atypical SH3 binding motif, R/KXXK, with a classical PXXP motif embedded in a polyproline type II (PPII) helix, *J Biol Chem 279*, 28724-28732.

72. Kang, H., Freund, C., Duke-Cohan, J. S., Musacchio, A., Wagner, G., and Rudd, C. E. (2000) SH3 domain recognition of a proline-independent tyrosine-based RKxxYxxY motif in immune cell adaptor SKAP55, *EMBO J 19*, 2889-2899.

73. Kim, J., Lee, C. D., Rath, A., and Davidson, A. R. (2008) Recognition of non-canonical peptides by the yeast Fus1p SH3 domain: elucidation of a common mechanism for diverse SH3 domain specificities, *J Mol Biol 377*, 889-901.

74. Manser, E., Loo, T. H., Koh, C. G., Zhao, Z. S., Chen, X. Q., Tan, L., Tan, I., Leung, T., and Lim, L. (1998) PAK kinases are directly coupled to the PIX family of nucleotide exchange factors, *Mol Cell 1*, 183-192.

75. Kato, M., Miyazawa, K., and Kitamura, N. (2000) A deubiquitinating enzyme UBPY interacts with the Src homology 3 domain of Hrs-binding protein via a novel binding motif PX(V/I)(D/N)RXXKP, *J Biol Chem 275*, 37481-37487.

76. Ingley, E. (2008) Src family kinases: regulation of their activities, levels and identification of new pathways, *Biochim Biophys Acta 1784*, 56-65.

77. Samuels, A. L., Klinken, S. P., and Ingley, E. (2009) Liar, a novel Lyn-binding nuclear/cytoplasmic shuttling protein that influences erythropoietin-induced differentiation, *Blood 113*, 3845-3856.

78. Tibaldi, E., Venerando, A., Zonta, F., Bidoia, C., Magrin, E., Marin, O., Toninello, A., Bordin, L., Martini, V., Pagano, M. A., and Brunati, A. M. (2011) Interaction between the SH3 domain of Src family kinases and the proline-rich motif of HTLV-1 p13: a novel mechanism underlying delivery of Src family kinases to mitochondria, *Biochem J 439*, 505-516.

79. Shen, Z., Batzer, A., Koehler, J. A., Polakis, P., Schlessinger, J., Lydon, N. B., and Moran, M. F. (1999) Evidence for SH3 domain directed binding and phosphorylation of Sam68 by Src, *Oncogene 18*, 4647-4653.

80. Li, S. S. (2005) Specificity and versatility of SH3 and other proline-recognition domains: structural basis and implications for cellular signal transduction, *Biochem J 390*, 641-653.

81. Saksela, K., Cheng, G., and Baltimore, D. (1995) Proline-rich (PxxP) motifs in HIV-1 Nef bind to SH3 domains of a subset of Src kinases and are required for the enhanced growth of Nef+ viruses but not for down-regulation of CD4, *EMBO J 14*, 484-491.

82. Simon, J. A., and Schreiber, S. L. (1995) Grb2 SH3 binding to peptides from Sos: evaluation of a general model for SH3-ligand interactions, *Chem Biol 2*, 53-60.

83. Wunderlich, L., Goher, A., Farago, A., Downward, J., and Buday, L. (1999) Requirement of multiple SH3 domains of Nck for ligand binding, *Cell Signal 11*, 253-262.

84. Huang, R., Fang, P., and Kay, B. K. (2012) Isolation of monobodies that bind specifically to the SH3 domain of the Fyn tyrosine protein kinase, *N Biotechnol 29*, 526-533.

85. Liu, B. A., Jablonowski, K., Raina, M., Arce, M., Pawson, T., and Nash, P. D. (2006) The human and mouse complement of SH2 domain proteins-establishing the boundaries of phosphotyrosine signaling, *Mol Cell 22*, 851-868.

86. Pawson, T., Gish, G. D., and Nash, P. (2001) SH2 domains, interaction modules and cellular wiring, *Trends Cell Biol 11*, 504-511.

87. Waksman, G., Shoelson, S. E., Pant, N., Cowburn, D., and Kuriyan, J. (1993) Binding of a high affinity phosphotyrosyl peptide to the Src SH2 domain: crystal structures of the complexed and peptide-free forms, *Cell 72*, 779-790.

88. Songyang, Z., Shoelson, S. E., Chaudhuri, M., Gish, G., Pawson, T., Haser, W. G., King, F., Roberts, T., Ratnofsky, S., Lechleider, R. J., and et al. (1993) SH2 domains recognize specific phosphopeptide sequences, *Cell 72*, 767-778.

89. Xu, W., Harrison, S. C., and Eck, M. J. (1997) Three-dimensional structure of the tyrosine kinase c-Src, *Nature 385*, 595-602.

90. Sicheri, F., Moarefi, I., and Kuriyan, J. (1997) Crystal structure of the Src family tyrosine kinase Hck, *Nature 385*, 602-609.

91. Sicheri, F., and Kuriyan, J. (1997) Structures of Src-family tyrosine kinases, *Curr Opin Struct Biol 7*, 777-785.

92. Bossemeyer, D., Engh, R. A., Kinzel, V., Ponstingl, H., and Huber, R. (1993) Phosphotransferase and substrate binding mechanism of the cAMP-dependent protein kinase catalytic subunit from porcine heart as deduced from the 2.0 A structure of the complex with Mn2+ adenylyl imidodiphosphate and inhibitor peptide PKI(5-24), *EMBO J 12*, 849-859.

93. Zheng, J., Trafny, E. A., Knighton, D. R., Xuong, N. H., Taylor, S. S., Ten Eyck, L. F., and Sowadski, J. M. (1993) 2.2 A refined crystal structure of the catalytic subunit of cAMP-dependent protein kinase complexed with MnATP and a peptide inhibitor, *Acta Crystallogr D Biol Crystallogr 49*, 362-365.

94. Bakkenist, C. J., and Kastan, M. B. (2003) DNA damage activates ATM through intermolecular autophosphorylation and dimer dissociation, *Nature 421*, 499-506.

95. Fang, K. S., Barker, K., Sudol, M., and Hanafusa, H. (1994) A transmembrane protein-tyrosine phosphatase contains spectrin-like repeats in its extracellular domain, *J Biol Chem 269*, 14056-14063.

96. Hermiston, M. L., Xu, Z., and Weiss, A. (2003) CD45: a critical regulator of signaling thresholds in immune cells, *Annu Rev Immunol 21*, 107-137.

97. Ingley, E., Schneider, J. R., Payne, C. J., McCarthy, D. J., Harder, K. W., Hibbs, M. L., and Klinken, S. P. (2006) Csk-binding protein mediates sequential enzymatic down-regulation and degradation of Lyn in erythropoietin-stimulated cells, *J Biol Chem 281*, 31920-31929.

98. Harder, K. W., Parsons, L. M., Armes, J., Evans, N., Kountouri, N., Clark, R., Quilici, C., Grail, D., Hodgson, G. S., Dunn, A. R., and Hibbs, M. L. (2001) Gain- and loss-of-function Lyn mutant mice define a critical inhibitory role for Lyn in the myeloid lineage, *Immunity 15*, 603-615.

99. Okada, M., and Nakagawa, H. (1989) A protein tyrosine kinase involved in regulation of pp60c-src function, *J Biol Chem 264*, 20886-20893.

100. Zrihan-Licht, S., Lim, J., Keydar, I., Sliwkowski, M. X., Groopman, J. E., and Avraham, H. (1997) Association of csk-homologous kinase (CHK) (formerly MATK) with HER-2/ErbB-2 in breast cancer cells, *J Biol Chem 272*, 1856-1863.

101. Bjorge, J. D., Pang, A., and Fujita, D. J. (2000) Identification of protein-tyrosine phosphatase 1B as the major tyrosine phosphatase activity capable of dephosphorylating and activating c-Src in several human breast cancer cell lines, *J Biol Chem 275*, 41439-41446.

102. O'Brien, M. C., Fukui, Y., and Hanafusa, H. (1990) Activation of the proto-oncogene p60c-src by point mutations in the SH2 domain, *Mol Cell Biol 10*, 2855-2862.

103. Schaller, M. D., Hildebrand, J. D., Shannon, J. D., Fox, J. W., Vines, R. R., and Parsons, J. T. (1994) Autophosphorylation of the focal adhesion kinase, pp125FAK, directs SH2-dependent binding of pp60src, *Mol Cell Biol 14*, 1680-1688.

104. Sun, G., Sharma, A. K., and Budde, R. J. (1998) Autophosphorylation of Src and Yes blocks their inactivation by Csk phosphorylation, *Oncogene 17*, 1587-1595.

105. Sun, G., Ramdas, L., Wang, W., Vinci, J., McMurray, J., and Budde, R. J. (2002) Effect of autophosphorylation on the catalytic and regulatory properties of protein tyrosine kinase Src, *Arch Biochem Biophys 397*, 11-17.

106. Erpel, T., Superti-Furga, G., and Courtneidge, S. A. (1995) Mutational analysis of the Src SH3 domain: the same residues of the ligand binding surface are important for intra- and intermolecular interactions, *EMBO J 14*, 963-975.

107. Moarefi, I., LaFevre-Bernt, M., Sicheri, F., Huse, M., Lee, C. H., Kuriyan, J., and Miller, W. T. (1997) Activation of the Src-family tyrosine kinase Hck by SH3 domain displacement, *Nature 385*, 650-653.

108. Alexandropoulos, K., and Baltimore, D. (1996) Coordinate activation of c-Src by SH3- and SH2-binding sites on a novel p130Cas-related protein, Sin, *Genes Dev 10*, 1341-1355.

109. Young, M. A., Gonfloni, S., Superti-Furga, G., Roux, B., and Kuriyan, J. (2001) Dynamic coupling between the SH2 and SH3 domains of c-Src and Hck underlies their inactivation by C-terminal tyrosine phosphorylation, *Cell 105*, 115-126.

110. Ni, Q., Titov, D. V., and Zhang, J. (2006) Analyzing protein kinase dynamics in living cells with FRET reporters, *Methods 40*, 279-286.

111. Qayyum, T., McArdle, P. A., Lamb, G. W., Jordan, F., Orange, C., Seywright, M., Horgan, P. G., Jones, R. J., Oades, G., Aitchison, M. A., and Edwards, J. (2012) Expression and prognostic significance of Src family members in renal clear cell carcinoma, *Br J Cancer 107*, 856-863.

112. Wang, Y., Botvinick, E. L., Zhao, Y., Berns, M. W., Usami, S., Tsien, R. Y., and Chien, S. (2005) Visualizing the mechanical activation of Src, *Nature 434*, 1040-1045.

113. Garrett, S. C., Hodgson, L., Rybin, A., Toutchkine, A., Hahn, K. M., Lawrence, D. S., and Bresnick, A. R. (2008) A biosensor of S100A4 metastasis factor activation: inhibitor screening and cellular activation dynamics, *Biochemistry 47*, 986-996.

114. Gulyani, A., Vitriol, E., Allen, R., Wu, J., Gremyachinskiy, D., Lewis, S., Dewar, B., Graves, L. M., Kay, B. K., Kuhlman, B., Elston, T., and Hahn, K. M. (2011) A biosensor generated via high-throughput screening quantifies cell edge Src dynamics, *Nat Chem Biol 7*, 437-444.

115. Nussinov, R. (2012) How do dynamic cellular signals travel long distances?, *Mol Biosyst 8*, 22-26.

116. Marshall, C. J. (1995) Specificity of receptor tyrosine kinase signaling: transient versus sustained extracellular signal-regulated kinase activation, *Cell 80*, 179-185.

117. Ting, A. Y., Kain, K. H., Klemke, R. L., and Tsien, R. Y. (2001) Genetically encoded fluorescent reporters of protein tyrosine kinase activities in living cells, *Proc Natl Acad Sci U S A 98*, 15003-15008.

118. Karatan, E., Merguerian, M., Han, Z., Scholle, M. D., Koide, S., and Kay, B. K. (2004) Molecular recognition properties of FN3 monobodies that bind the Src SH3 domain, *Chem Biol 11*, 835-844.

119. Miyawaki, A., and Tsien, R. Y. (2000) Monitoring protein conformations and interactions by fluorescence resonance energy transfer between mutants of green fluorescent protein, *Methods Enzymol 327*, 472-500.

120. DeLano, W. (2002) The PYMOL molecular graphics system.

121. Smith, G. P. (1985) Filamentous fusion phage: novel expression vectors that display cloned antigens on the virion surface, *Science 228*, 1315-1317.

122. Gao, B., and Esnouf, M. P. (1996) Elucidation of the core residues of an epitope using membrane-based combinatorial peptide libraries, *J Biol Chem 271*, 24634-24638.

123. Sospedra, M., Pinilla, C., and Martin, R. (2003) Use of combinatorial peptide libraries for T-cell epitope mapping, *Methods 29*, 236-247.

124. Pershad, K., Wypisniak, K., and Kay, B. K. (2012) Directed evolution of the forkhead-associated domain to generate anti-phosphospecific reagents by phage-display, *J Mol Biol*.

125. Chu, R., Takei, J., Knowlton, J. R., Andrykovitch, M., Pei, W., Kajava, A. V., Steinbach, P. J., Ji, X., and Bai, Y. (2002) Redesign of a four-helix bundle protein by phage display coupled with proteolysis and structural characterization by NMR and X-ray crystallography, *J Mol Biol 323*, 253-262.

126. Grebien, F., Hantschel, O., Wojcik, J., Kaupe, I., Kovacic, B., Wyrzucki, A. M., Gish, G. D., Cerny-Reiterer, S., Koide, A., Beug, H., Pawson, T., Valent, P., Koide, S., and Superti-Furga, G. (2011) Targeting the SH2-kinase interface in Bcr-Abl inhibits leukemogenesis, *Cell 147*, 306-319.

127. Kridel, S. J., Chen, E., and Smith, J. W. (2001) A substrate phage enzyme-linked immunosorbent assay to profile panels of proteases, *Anal Biochem 294*, 176-184.

128. McCarter, J. D., Stephens, D., Shoemaker, K., Rosenberg, S., Kirsch, J. F., and Georgiou, G. (2004) Substrate specificity of the Escherichia coli outer membrane protease OmpT, *J Bacteriol 186*, 5919-5925.

129. Takahashi-Ando, N., Kakinuma, H., Fujii, I., and Nishi, Y. (2004) Directed evolution governed by controlling the molecular recognition between an abzyme and its haptenic transition-state analog, *J Immunol Methods 294*, 1-14.

130. Fernandez-Gacio, A., Uguen, M., and Fastrez, J. (2003) Phage display as a tool for the directed evolution of enzymes, *Trends Biotechnol 21*, 408-414.

131. Kamada, H., Okamoto, T., Kawamura, M., Shibata, H., Abe, Y., Ohkawa, A., Nomura, T., Sato, M., Mukai, Y., Sugita, T., Imai, S., Nagano, K., Tsutsumi, Y., Nakagawa, S., Mayumi, T., and Tsunoda, S. (2007) Creation of novel cell-penetrating peptides for intracellular drug delivery using systematic phage display technology originated from Tat transduction domain, *Biol Pharm Bull 30*, 218-223.

132. Gao, C., Mao, S., Ditzel, H. J., Farnaes, L., Wirsching, P., Lerner, R. A., and Janda, K. D. (2002) A cell-penetrating peptide from a novel pVII-pIX phage-displayed random peptide library, *Bioorg Med Chem 10*, 4057-4065.

133. Estephan, E., Larroque, C., Bec, N., Martineau, P., Cuisinier, F. J., Cloitre, T., and Gergely, C. (2009) Selection and mass spectrometry characterization of peptides targeting semiconductor surfaces, *Biotechnol Bioeng 104*, 1121-1131.

134. Moghaddam, A., Borgen, T., Stacy, J., Kausmally, L., Simonsen, B., Marvik, O. J., Brekke, O. H., and Braunagel, M. (2003) Identification of scFv antibody fragments that specifically recognise the heroin metabolite 6-monoacetylmorphine but not morphine, *J Immunol Methods 280*, 139-155.

135. Islam, M. O., Lim, Y. T., Chan, C. E., Cazenave-Gassiot, A., Croxford, J. L., Wenk, M. R., Macary, P. A., and Hanson, B. J. (2012) Generation and characterization of a novel recombinant antibody against 15-ketocholestane isolated by phage-display, *Int J Mol Sci 13*, 4937-4948.

136. Suzuki, M. M., Matsumoto, M., Yamamoto, A., Ochiai, M., Horiuchi, Y., Niwa, M., Omi, H., Kobayashi, T., and Takagi, T. (2010) Molecular design of LPS-binding peptides, *J Microbiol Methods 83*, 153-155.

137. Wang, X., Katayama, A., Wang, Y., Yu, L., Favoino, E., Sakakura, K., Favole, A., Tsuchikawa, T., Silver, S., Watkins, S. C., Kageshita, T., and Ferrone, S. (2011) Functional characterization of an scFv-Fc antibody that immunotherapeutically targets the common cancer cell surface proteoglycan CSPG4, *Cancer Res 71*, 7410-7422.

138. Cao, L., Zeller, M. K., Fiore, V. F., Strane, P., Bermudez, H., and Barker, T. H. (2012) Phage-based molecular probes that discriminate force-induced structural states of fibronectin in vivo, *Proc Natl Acad Sci U S A 109*, 7251-7256.

139. Kaneko, T., Huang, H., Cao, X., Li, X., Li, C., Voss, C., Sidhu, S. S., and Li, S. S. (2012) Superbinder SH2 Domains Act as Antagonists of Cell Signaling, *Sci Signal 5*, ra68.

140. Wojcik, J., Hantschel, O., Grebien, F., Kaupe, I., Bennett, K. L., Barkinge, J., Jones, R. B., Koide, A., Superti-Furga, G., and Koide, S. (2010) A potent and highly specific FN3 monobody inhibitor of the Abl SH2 domain, *Nat Struct Mol Biol 17*, 519-527.

141. Zahid, M., Phillips, B. E., Albers, S. M., Giannoukakis, N., Watkins, S. C., and Robbins, P. D. (2010) Identification of a cardiac specific protein transduction domain by in vivo biopanning using a M13 phage peptide display library in mice, *PLoS One 5*, e12252.

142. Sparks, A. B., Rider, J. E., and Kay, B. K. (1998) Mapping the specificity of SH3 domains with phage-displayed random-peptide libraries, *Methods Mol Biol 84*, 87-103.

143. Scholle, M. D., Kehoe, J. W., and Kay, B. K. (2005) Efficient construction of a large collection of phage-displayed combinatorial peptide libraries, *Comb Chem High Throughput Screen 8*, 545-551.

144. Koide, A., Bailey, C. W., Huang, X., and Koide, S. (1998) The fibronectin type III domain as a scaffold for novel binding proteins, *J Mol Biol 284*, 1141-1151.

145. Tolmachev, V., Velikyan, I., Sandstrom, M., and Orlova, A. (2010) A HER2-binding Affibody molecule labelled with 68Ga for PET imaging: direct in vivo comparison with the 111In-labelled analogue, *Eur J Nucl Med Mol Imaging 37*, 1356-1367.

146. Lewis, L., and Lloyd, C. (2012) Optimisation of antibody affinity by ribosome display using error-prone or site-directed mutagenesis, *Methods Mol Biol 805*, 139-161.

147. McCafferty, J., Griffiths, A. D., Winter, G., and Chiswell, D. J. (1990) Phage antibodies: filamentous phage displaying antibody variable domains, *Nature 348*, 552-554.

148. Clackson, T., and Wells, J. A. (1995) A hot spot of binding energy in a hormone-receptor interface, *Science 267*, 383-386.

149. Hoogenboom, H. R., Griffiths, A. D., Johnson, K. S., Chiswell, D. J., Hudson, P., and Winter, G. (1991) Multi-subunit proteins on the surface of filamentous phage: methodologies for displaying antibody (Fab) heavy and light chains, *Nucleic Acids Res 19*, 4133-4137.

150. Miller, K. R., Koide, A., Leung, B., Fitzsimmons, J., Yoder, B., Yuan, H., Jay, M., Sidhu, S. S., Koide, S., and Collins, E. J. (2012) T cell receptor-like recognition of tumor in vivo by synthetic antibody fragment, *PLoS One 7*, e43746.

151. Arbabi-Ghahroudi, M., Tanha, J., and MacKenzie, R. (2005) Prokaryotic expression of antibodies, *Cancer Metastasis Rev 24*, 501-519.

152. Nilsson, F. Y., and Tolmachev, V. (2007) Affibody molecules: new protein domains for molecular imaging and targeted tumor therapy, *Curr Opin Drug Discov Devel 10*, 167-175.

153. Silverman, J., Liu, Q., Bakker, A., To, W., Duguay, A., Alba, B. M., Smith, R., Rivas, A., Li, P., Le, H., Whitehorn, E., Moore, K. W., Swimmer, C., Perlroth, V., Vogt, M., Kolkman, J., and Stemmer, W. P. (2005) Multivalent avimer proteins evolved by exon shuffling of a family of human receptor domains, *Nat Biotechnol 23*, 1556-1561.

154. Skerra, A. (2008) Alternative binding proteins: anticalins - harnessing the structural plasticity of the lipocalin ligand pocket to engineer novel binding activities, *FEBS J 275*, 2677-2683.

155. Boersma, Y. L., and Pluckthun, A. (2011) DARPins and other repeat protein scaffolds: advances in engineering and applications, *Curr Opin Biotechnol 22*, 849-857.

156. Grabulovski, D., Kaspar, M., and Neri, D. (2007) A novel, non-immunogenic Fyn SH3-derived binding protein with tumor vascular targeting properties, *J Biol Chem 282*, 3196-3204.

157. Sechler, J. L., Corbett, S. A., and Schwarzbauer, J. E. (1997) Modulatory roles for integrin activation and the synergy site of fibronectin during matrix assembly, *Mol Biol Cell 8*, 2563-2573.

158. Batori, V., Koide, A., and Koide, S. (2002) Exploring the potential of the monobody scaffold: effects of loop elongation on the stability of a fibronectin type III domain, *Protein Eng 15*, 1015-1020.

159. Xu, L., Aha, P., Gu, K., Kuimelis, R. G., Kurz, M., Lam, T., Lim, A. C., Liu, H., Lohse, P. A., Sun, L., Weng, S., Wagner, R. W., and Lipovsek, D. (2002) Directed evolution of high-affinity antibody mimics using mRNA display, *Chem Biol 9*, 933-942.

160. Olson, C. A., Liao, H. I., Sun, R., and Roberts, R. W. (2008) mRNA display selection of a high-affinity, modification-specific phospho-IkappaBalpha-binding fibronectin, *ACS Chem Biol 3*, 480-485.

161. Lipovsek, D., Lippow, S. M., Hackel, B. J., Gregson, M. W., Cheng, P., Kapila, A., and Wittrup, K. D. (2007) Evolution of an interloop disulfide bond in high-affinity antibody mimics based on fibronectin type III domain and selected by yeast surface display: molecular convergence with single-domain camelid and shark antibodies, *J Mol Biol 368*, 1024-1041.

162. Hackel, B. J., Kapila, A., and Wittrup, K. D. (2008) Picomolar affinity fibronectin domains engineered utilizing loop length diversity, recursive mutagenesis, and loop shuffling, *J Mol Biol 381*, 1238-1252.

163. Koide, A., Tereshko, V., Uysal, S., Margalef, K., Kossiakoff, A. A., and Koide, S. (2007) Exploring the capacity of minimalist protein interfaces: interface energetics and affinity maturation to picomolar KD of a single-domain antibody with a flat paratope, *J Mol Biol 373*, 941-953.

164. Koide, A., Gilbreth, R. N., Esaki, K., Tereshko, V., and Koide, S. (2007) High-affinity single-domain binding proteins with a binary-code interface, *Proc Natl Acad Sci U S A 104*, 6632-6637.

165. Gilbreth, R. N., Truong, K., Madu, I., Koide, A., Wojcik, J. B., Li, N. S., Piccirilli, J. A., Chen, Y., and Koide, S. (2011) Isoform-specific monobody inhibitors of small ubiquitin-related modifiers engineered using structure-guided library design, *Proc Natl Acad Sci U S A 108*, 7751-7756.

166. Parker, M. H., Chen, Y., Danehy, F., Dufu, K., Ekstrom, J., Getmanova, E., Gokemeijer, J., Xu, L., and Lipovsek, D. (2005) Antibody mimics based on human fibronectin type three domain engineered for thermostability and high-affinity binding to vascular endothelial growth factor receptor two, *Protein Eng Des Sel 18*, 435-444.

167. Koide, A., Abbatiello, S., Rothgery, L., and Koide, S. (2002) Probing protein conformational changes in living cells by using designer binding proteins: application to the estrogen receptor, *Proc Natl Acad Sci U S A 99*, 1253-1258.

168. Huang, J., Koide, A., Makabe, K., and Koide, S. (2008) Design of protein function leaps by directed domain interface evolution, *Proc Natl Acad Sci U S A 105*, 6578-6583.

169. Koide, A., Wojcik, J., Gilbreth, R. N., Hoey, R. J., and Koide, S. (2012) Teaching an old scaffold new tricks: monobodies constructed using alternative surfaces of the FN3 scaffold, *J Mol Biol 415*, 393-405.

170. Richards, J., Miller, M., Abend, J., Koide, A., Koide, S., and Dewhurst, S. (2003) Engineered fibronectin type III domain with a RGDWXE sequence binds with enhanced affinity and specificity to human alphavbeta3 integrin, *J Mol Biol 326*, 1475-1488.

171. Liao, H. I., Olson, C. A., Hwang, S., Deng, H., Wong, E., Baric, R. S., Roberts, R. W., and Sun, R. (2009) mRNA display design of fibronectin-based intrabodies that detect and inhibit severe acute respiratory

syndrome coronavirus nucleocapsid protein, *J Biol Chem 284*, 17512-17520.

172. Gram, H., Marconi, L. A., Barbas, C. F., 3rd, Collet, T. A., Lerner, R. A., and Kang, A. S. (1992) In vitro selection and affinity maturation of antibodies from a naive combinatorial immunoglobulin library, *Proc Natl Acad Sci U S A 89*, 3576-3580.

173. Daugherty, P. S., Chen, G., Iverson, B. L., and Georgiou, G. (2000) Quantitative analysis of the effect of the mutation frequency on the affinity maturation of single chain Fv antibodies, *Proc Natl Acad Sci U S A 97*, 2029-2034.

174. Kummer, L., Parizek, P., Rube, P., Millgramm, B., Prinz, A., Mittl, P. R., Kaufholz, M., Zimmermann, B., Herberg, F. W., and Pluckthun, A. (2012) Structural and functional analysis of phosphorylation-specific binders of the kinase ERK from designed ankyrin repeat protein libraries, *Proc Natl Acad Sci U S A 109*, E2248-2257.

175. Hackel, B. J., Ackerman, M. E., Howland, S. W., and Wittrup, K. D. (2010) Stability and CDR composition biases enrich binder functionality landscapes, *J Mol Biol 401*, 84-96.

CHAPTER 2

IMPROVEMENTS TO THE KUNKEL MUTAGENESIS PROTOCOL FOR CONSTRUCTING PRIMARY AND SECONDARY PHAGE-DISPLAY LIBRARIES

Renhua Huang, Pete Fang, Brian K. Kay

Published in *Methods*, (2012), http://dx.doi.org/10.1016/j.ymeth.2012.08.008

2.1 Abstract

Site-directed mutagenesis is routinely performed in protein engineering experiments. One method, termed Kunkel mutagenesis, is frequently used for constructing libraries of peptide or protein variants in M13 bacteriophage, followed by affinity selection of phage particles. To make this method more efficient, the following two modifications were introduced: culture was incubated at 25 °C for phage replication, which yielded two- to sevenfold more single-stranded DNA template compared to growth at 37 °C, and restriction endonuclease recognition sites were used to remove non-recombinants. With both of the improvements, we could construct primary libraries of high complexity and that were 99ï 100% recombinant. Finally, with a third modification to the standard protocol of Kunkel mutagenesis, two secondary (mutagenic) libraries of a fibronectin type III (FN3) monobody were constructed with DNA segments that were amplified by error-prone and asymmetric PCR. Two advantages of this modification are that it bypasses the lengthy steps of restriction enzyme digestion and ligation, and that the pool of phage clones, recovered after affinity selection, can be used directly to generate a secondary library. Screening one of the two mutagenic libraries yielded variants that bound two- to fourfold tighter to human Pak1 kinase than the starting clone. The protocols described in this study should accelerate the discovery of phage-displayed recombinant affinity reagents.

2.2 Introduction

Several techniques are readily available for site-directed mutagenesis of proteins. Cassette mutagenesis (*1*), which requires restriction enzyme digestion and ligation to incorporate mutagenic sequences, has been supplanted by the "QuikChange" method (*2, 3*). In "QuikChange", a pair of complementary oligonucleotides, containing the desired mutation(s), are used to amplify the entire plasmid with a high-fidelity polymerase, followed by DpnI digestion to remove the parental strand. A third widely used technique is "Kunkel mutagenesis" (*4-8*), where one utilizes uracil-inserted, circular, single-stranded DNA (ssDNA) as a template to synthesize double-stranded DNA (dsDNA) *in vitro* with an oligonucleotide primer that introduces a mutation. After dsDNA is introduced into bacteria, recombinant clones predominate due to cleavage of the uracilated strand *in vivo*. Kunkel mutagenesis is particularly powerful in phage-display experiments that are based on M13 bacteriophage, as the viral particles contain a circular, single-stranded genome (*6, 9, 10*).

As the number of the theoretical permutations in a protein engineering experiment can be astronomical, it is desirable to construct phage-displayed libraries that comprise a vast number of mutants, as it has been observed that the size of a phage library is closely correlated with the affinity of the isolated mutants (*11*). While the size of the library is a limiting factor in isolating desired clones, the quality of the phage library (i.e., the percentage of the phage particles displaying the recombinant polypeptides out of the total phage pool), also significantly influences the efficiency and the outcome of affinity selections. For

example, some studies have found that non-recombinant clones, or target-unrelated clones, can overwhelm the target-binding clones in the library due to the advantages associated with steps of phage propagation or affinity selection (*12, 13*). Thus, it is widely believed that removing the wild-type clones from the final phage-displayed library should improve the efficiency of affinity selections.

Even with improvements in the size and quality of a phage-displayed library, affinity maturation experiments are usually necessary to fine-tune binders for improved specificity (*10, 14*), affinity (*10, 15, 16*), or both (*10*). One simple method is to generate secondary (i.e., mutant) libraries through an error-prone polymerase chain reaction (PCR) (*17, 18*), and repeat the affinity selections under more stringent conditions (i.e., less target, longer wash times, more washes). Nevertheless, generating each secondary library can be time-consuming, and unless large, may be inadequate for isolating mutants with dramatically improved properties.

In this study, we describe several modifications to the basic Kunkel mutagenesis protocol for constructing libraries that display the 10th subunit of human fibronectin type III repeat (FN3), also termed ómonobodyô(*19, 20*). With adjustments of the growth conditions of bacterial cultures, the yields of phage particles and single-stranded, circular DNA can be increased two- to sevenfold , which provides an ample source of template DNA for constructing libraries. Furthermore, with insertion of unique restriction endonuclease recognition sites in the FN3 coding region, non-recombinant clones are removed by restriction enzyme digestion, generating naïve (i.e., primary) libraries that are 99ï 100%

recombinant, which should improve the efficiency of affinity selection experiments and the discovery of high-affinity, selective affinity reagents. Finally, to improve the affinity of a previously isolated binder, we construct two secondary libraries using DNA segments generated by error-prone and asymmetric PCR. Affinity selection of one of these libraries yields three variants that exhibit two- to fourfold tighter binding to Pak1 kinase than the original clone.

2.3 Materials and methods

2.3.1 Phagemids and Escherichia coli strains

The sequence of the 10^{th} subunit of human fibronectin type III repeat (FN3) was amplified by PCR from a plasmid (*21*), and subcloned into the pAP-III_6 vector (*22, 23*). In this phagemid vector, the Flag (DYKDDDDK) epitope is fused at the N-terminus of the FN3 coding region, thereby allowing convenient detection of the displayed FN3 domain with an anti-Flag antibody (Sigmaï Aldrich; St. Louis, MO).

The *E. coli* strain, CJ236 (New England BioLabs; Ipswich, MA), which lacks functional dUTPase and uracil-N glycosylase, was used for generating uracilated single-stranded DNA template. In *E. coli*, dUTPase and uracil-N glycosylase serve to play roles in DNA repair and ensure fidelity of DNA replication by removing any uracils incorporated into the bacterial genome (*24*). Here in this study, the *E. coli* strain, TG1 (Lucigen, Madison, WI), which encodes wild-type versions of dUTPase and uracil-N glycosylase, was used to favor propagation of the newly synthesized (i.e., mutated or recombinant) strand. For the sake of

clarity, in this report we refer to the circular, single-stranded phagemid genome and the *in vitro* synthesized circular, double-stranded, heteroduplex product as ssDNA and dsDNA, respectively.

2.3.2 Extraction of uracilated single-stranded DNA from bacterial cultures grown in different conditions

CJ236 cells, carrying the phagemid, were streaked on a petri plate containing 2×YT medium (per liter 16 g tryptone, 10 g yeast extract, 5 g NaCl), 1.5% agar (mass/volume), carbenicillin (50 µg/mL), and chloramphenicol (15 µg/mL). After an overnight incubation at 37 °C, three fresh colonies were used to inoculate 10 mL 2×YT medium, containing carbenicillin (50 µg/ml) and chloramphenicol (15 µg/mL). The culture was incubated at 37 °C, and shaken at 250 rpm overnight. The next day, 1.8 mL of overnight culture was diluted into 180 mL of fresh 2×YT medium with carbenicillin (50 µg/mL). After 3ï 4 h incubation at 37 °C with 250 rpm shaking, when the culture reached an OD_{600nm}= 0.4ï 0.6, M13-K07 helper phage (New England BioLabs) was added at a multiplicity of infection (MOI) of 10. The cells were infected for 1 h at 150 rpm, pelleted, and resuspended in 180 mL fresh 2×YT medium, containing carbenicillin (50 µg/mL) and kanamycin (50 µg/mL). The infected cells were aliquoted into six 250 mL flasks, 30 mL each. The following six different growth conditions in different combinations were tested for phage replication: incubation at 37 °C or 25 °C, with shaking at 280 rpm or 200 rpm, and in baffled or non-baffled flasks. After 22 h incubation, cells were centrifuged three times to clarify the supernatant, of which 2.5 mL was used for

extraction of ssDNA with the QIAprep Spin M13 kit (Qiagen). The isolated ssDNA was quantified with a Nanodrop spectrophotometer (Thermo Fisher Scientific Co.; Waltham, MA), and evaluated by agarose gel electrophoresis. Phage particles were precipitated from the remaining 25 mL of culture supernatant by adjusting the solution to 5% (mass/volume) PEG 8000 and 300 mM NaCl. The pellet of phage particles was resuspended in phosphate buffered saline (PBS; 137 mM NaCl, 3 mM KCl, 8 mM Na_2HPO_4, 1.5 mM KH_2PO_4), and processed with the QIAprep Spin M13 kit (Qiagen), which has a binding capacity of 10 µg ssDNA per column.

2.3.3 Construction of phage-display libraries

2.3.3.1 Creation of a phagemid with stop codons and restriction endonuclease recognition sites inserted into FN3 sequence

Based on a modified protocol of Kunkel mutagenesis (7), two stop codons (TAA and TGA) and a SacII (5ôCCGC$^{\acute{Z}}$GG-3ô), SmaI (5ôCCC$^{\acute{Z}}$GGG-3ô), or StuI (5ôAGG$^{\acute{Z}}$CCT-3ô), site was introduced into each of the BC and FG loop regions of the FN3 coding sequence (Each vector had two copies of the SacII, SmaI, or StuI sites). First, two oligonucleotides (13.2 pmol each; IDT DNA, Coralville, Iowa), each containing the two stop codons and one of the three different restriction endonuclease recognition sites, were phosphorylated by T4 polynucleotide kinase (5 units; New England BioLabs) at 37 °C, for 1 h, in 50 mM Trisï HCl (pH 7.5), 10 mM $MgCl_2$, 1 mM ATP and 5 mM dithiothreitol (DTT). In 50 mM Trisï HCl and 10 mM $MgCl_2$, the phosphorylated oligonucleotides were annealed to

uracilated ssDNA template, at a molar ratio of 3 (oligonucleotide/ssDNA), by heating the mixture at 90 °C for 2 minutes (min), followed by a temperature decrease of 1 °C /min to 25 °C in a thermal cycler. In a solution containing 0.55 mM ATP, 0.8 mM dNTPs, 5 mM DTT, 15 Weiss units of T4 DNA ligase, and 15 units of T7 DNA polymerase (New England BioLabs), the two phosphorylated and annealed oligonucleotides were used to prime *in vitro* DNA synthesis at 20 °C for 3 h, yielding dsDNA, which was purified with the QIAquick PCR purification kit (Qiagen; Valencia, CA). In a pre-chilled 0.2 cm cuvette (BioExpress; Kaysville, UT), DNA was electroporated into TG1 cells at 2400 V, with an electroporator (Eppendorf; Hauppauge, NY). The next day, six single bacterial colonies were inoculated for preparation of phagemid DNA and sequencing analysis.

2.3.3.2 Comparing different reaction conditions of in vitro dsDNA synthesis for their influences on mutation rate

To examine if different annealing ratios of oligonucleotide to ssDNA and different extension times would change the mutation rate, the following nine different reaction conditions were tested in parallel: three different annealing molar ratios of oligonucleotide to ssDNA (3, 20 and 100), were paired individually with three different extension times (30 min, 3 h and 16 h). Heteroduplex dsDNA, which was generated in these nine parallel reactions, was purified with the QIAquick PCR purification kit (Qiagen) before being electroporated into TG1 cells (Lucigen).

Forty-six bacterial colonies, obtained from transformations with dsDNA product from each of the nine different reaction conditions, were inoculated into a 96 deep-well plate (Thermo Fisher Scientific Co.) and grown overnight in the presence of M13-K07 helper virus particles (New England BioLabs). Anti-M13 bacteriophage antibody (GE Healthcare; Piscataway, NJ) was diluted in PBS to 5 ng/εL for overnight immobilization in the wells of Nunc^{TM} microtiter plates (Thermo-Fisher Scientific Co.). The next day, non-specific binding sites on the plates were blocked for 1 h with casein (Thermo Fisher Scientific Co.), followed by addition of clarified phage supernatant from overnight cultures in the deep-well plates. After 1 h incubation, microtiter plates were washed five times with PBS-0.1% Tween (volume/volume), followed by addition of 100 ng/mL anti-Flag antibody, conjugated to horseradish peroxidase (Sigmaï Aldrich). The microtiter plates were washed after 30 min incubation, and the chromogenic substrate, 2,2'-Azino-bis (3-Ethylbenzothiazoline-6-Sulfonic Acid) (ABTS), mixed with hydrogen peroxide, was added and the resulting absorbance was measured at 405 nm with a microtiter plate spectrophotometer (POLARstar OPTIMA; BMG Labtech, Cary, NC). A clone displaying a positive ELISA signal was considered as a recombinant (i.e., both BC and FG loops replaced by mutagenic sequences), whereas a negative ELISA signal was interpreted as the starting template (i.e., carries two stop codons in the coding regions for the two loops). Only phage clones with positive ELISA signals were selected for DNA sequencing. The nine different reaction conditions were tested three times.

2.3.3.3 Construction of phage libraries that were 99–100% recombinant

Following the protocol described above, dsDNA was synthesized *in vitro* with oligonucleotides encoding five NNK (where N is an equimolar mixture of A, G, C, and T, and K is an equimolar mixture of G and T) codons in the BC and FG loop regions of the FN3 coding sequence. The purified heteroduplex dsDNA was then electroporated into TG1 cells and spread on agar plates containing 2×YT and carbenicillin (50 µg/mL). After overnight incubation at 30 °C, colonies were scraped together and DNA was extracted with the Wizard Plus SV Mini-Prep kit (Promega; Madison, WI). The DNA was then digested with SacII, SmaI or StuI for 8 h (New England BioLabs), purified with the QIAquick PCR purification kit (Qiagen), and used to transform TG1 cells. After transformation, cells were recovered at 37 °C with 200 rpm shaking for 30 min, before serial dilutions of the recovered cells were plated (to determine transformation efficiency) on 2×YT agar plates with carbenicillin (50 µg/mL), and incubated overnight at 30 °C. The resulting colonies were inoculated into 96 deep-well plates (Thermo Fisher Scientific Co.) and grown overnight in 2×YT medium, containing carbenicillin (50 µg/mL), kanamycin (50 µg/mL), and helper virus, M13-K07 (New England BioLabs). Phage enzyme-linked immunosorbent assays (ELISA) and DNA sequencing of selected clones were carried out as described above.

2.3.3.4 Construction of two mutagenic libraries with DNA segments generated by error-prone and asymmetric PCR

Screening a phage display library of FN3 monobodies with the kinase domain of Pak1 kinase (*25*) led to isolation of a monobody, C12, which bound to the ώpenôform of the protein (*26*). A secondary mutant library based on the C12 monobody was created and a variant was isolated that bound twice as tight as the original clone. To further increase the affinity of the C12 variant, a mutagenic library of this clone was constructed with a modified protocol of Kunkel mutagenesis. Briefly, 0.3 fmol (1 ng) of phagemid DNA from the C12 variant was mixed with 2.5 units of Mutazyme II (Agilent; Santa Clara, CA), and amplified by PCR over 34 cycles (95 °C for 1 min, 62 °C for 1 min, and 72 °C for 1 min). The resulting DNA segment was resolved by agarose gel electrophoresis and purified with the QIAquick gel extraction kit (Qiagen). Following heat denaturation of the purified DNA segment and annealing to the ssDNA template, the *in vitro* dsDNA synthesis was performed under the reaction conditions described in above, and the resulting dsDNA was electroporated into TG1 cells (Lucigen). Cells were allowed to recover for 30 min at 37 °C with 200 rpm shaking, followed by serial dilutions, spreading on petri plates, and overnight incubation at 30ºC.

To investigate if the mutation rate and the transformation efficiency of heteroduplex dsDNA could be increased by using a long single-stranded DNA as a primer for *in vitro* DNA synthesis, we employed asymmetric PCR (*27*) to amplify the preferred strand. One pmol (200 ng) of the purified DNA segment, generated under mutagenic conditions, and 400 pmol of the reverse primer were

mixed and incubated for 40 cycles (95 °C for 1 min, 58 °C for 1 min, and 72 °C for 1 min) of asymmetric amplification. The amplified DNA segments were purified with the QIAquick PCR purification kit (Qiagen). Following the same procedure mentioned above, purified DNA segments were phosphorylated and annealed to the ssDNA template. After DNA extension, the resulting heteroduplex dsDNA was electroporated into TG1 cells (Lucigen). The bacterial cells were spread on agar plates, and the next day, 46 colonies from the secondary library were picked and subjected to phage ELISA and DNA sequencing analysis, as described above.

To increase the mutation rate of error-prone PCR, Mutazyme II was used to amplify the FN3 coding region under conditions that increased the mutation rate of *Taq* DNA polymerase (*28*). Briefly, 0.3 fmol (1 ng) of DNA template was incubated in a solution containing 7 mM $MgCl_2$, 0.1 mM $MnCl_2$, 1 mM dCTP, dTTP and 200 µM dGTP and dATP, 2.5 units of Mutazyme II and 38 pmol of oligonucleotide primers. Thermal cycling consisted of 36 cycles: 95 °C for 30 s, 62 °C for 30 s, and 72 °C for 30 s. Kunkel mutagenesis and electroporation of the resulting dsDNA were performed as described above.

2.3.3.5 Affinity selection of tighter binders from a secondary mutagenic library

Phage particles, displaying monobody variants, were amplified and resuspended in Tris-buffered saline (TBS; 50 mM Trisï HCl, 150 mM NaCl, pH 7.5) containing 0.5% Tween (volume/volume) + 0.5% bovine serum albumin

(BSA; mass/volume). The suspension of phage particles was then mixed with the target, biotinylated ópenôform of human Pak1 kinase (25 nM, final concentration). After 2 h incubation, streptavidin-coated magnetic beads (Promega) were added to the phage solution. Beads were collected with a magnet after 15 min tumbling, followed by six washes with PBS-0.5% Tween, three washes with PBS-0.1% Tween, and three washes with PBS (All the solutions contained the non-biotinylated form of the Pak1 kinase protein at 160 nM). Bound phage particles were eluted with 50 mM glycine (pH 2) for 10 min, which was neutralized with Trisï HCl (pH 10) and used to infect mid-log phase TG1 cells for 30 min at 37 °C with 100 rpm shaking. Infected cells were spun down and spread on 2×YT agar plates with carbenicillin (50 µg/mL), and incubated overnight at 30 °C. The next day, bacterial colonies were scraped from the plate and inoculated into cultures for amplifying viral particles, which would be used for the next round of affinity selection. To increase the stringency, the second and third rounds of selections were performed with reduced concentration of the target protein (500 pM) and with additional washes (to remove weak and non-binding clones).

2.3.3.6 Phage ELISA for identifying FN3 variants that bound tighter to Pak1 kinase

The phage ELISA was performed with a similar protocol as described above. The target protein, the ópenôform of human Pak1 kinase, was immobilized directly on the Nunc™ microtiter plate (Thermo Fisher Scientific Co.). The blocking reagent, casein, was used as the control of background binding. Among

the eighty-eight clones tested in the initial phage ELISA, three clones (C2, D3, and E10) together with the original clone were picked for further testing their binding to the Pak1 kinase. First a phage ELISA was performed with anti-Flag antibody (Sigmaï Aldrich), so that the amount of phage particles could be normalized in assays that monitored binding of FN3 monobodies to the Pak1 kinase.

2.4 Results and discussion

2.4.1 Overview of the Kunkel mutagenesis

One method frequently used to construct phage-display libraries is Kunkel mutagenesis (Figure 2.1). First, a phagemid genome is introduced into *E. coli* CJ236 cells, which lack functional dUTPase and uracil-N glycosylase. With the aid of a helper virus, M13-K07, the transformed CJ236 cells secretes phage particles, from which single-stranded, circular DNA (ssDNA), containing uracil in place of thymine (i.e., uracilated), is recovered. A pair of mutagenic oligonucleotides are phosphorylated and annealed to the ssDNA template for *in vitro* synthesis of heteroduplex, double-stranded DNA (dsDNA) with T7 DNA polymerase and T4 DNA ligase. The resulting product is purified and evaluated by agarose gel electrophoresis; as seen in Figure 2.2, the ssDNA can be quantitatively converted to the larger dsDNA species by this technique. The dsDNA is electroporated into *E. coli* TG1 cells, where the parental uracilated strand is cleaved *in vivo* by uracil-N glycosylase, so that only the recombinant strand survives.

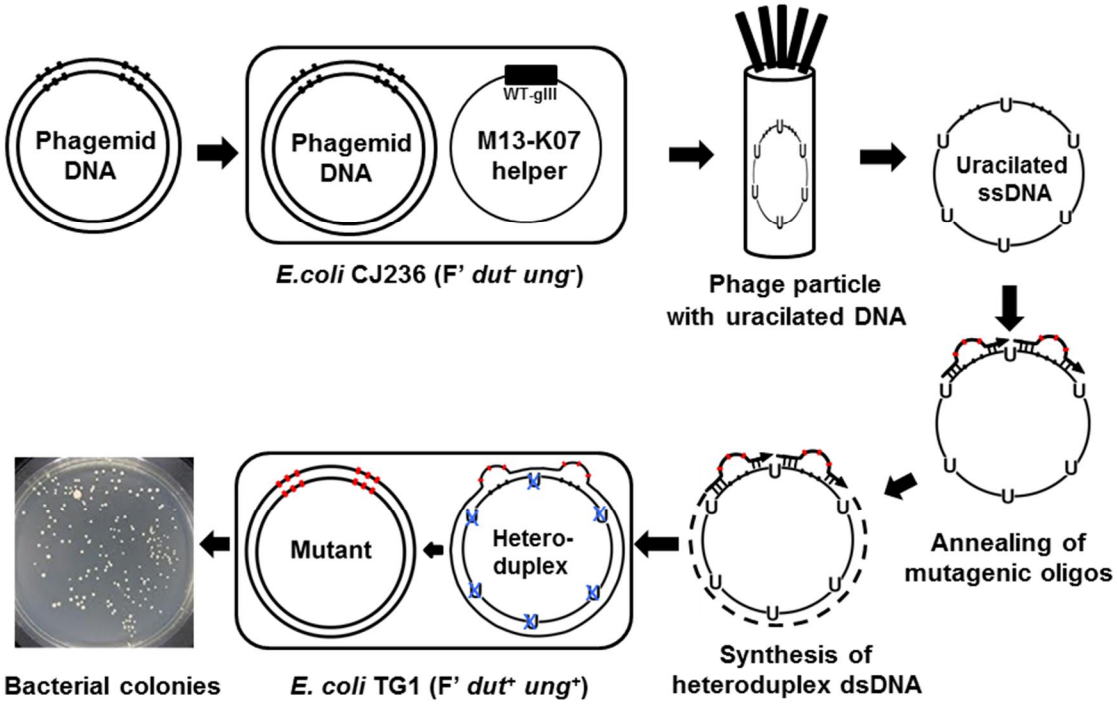

Figure 2.1. Overview of the Kunkel mutagenesis. Phagemid DNA is electroporated into the CJ236 strain of *E. coli*. These cells are then infected with M13-K07 helper virus for amplifying phage particles that yielded uracilated (U) single-stranded DNA (ssDNA). The ssDNA is annealed to two phosphorylated mutagenic oligonucleotides, which prime the synthesis of heteroduplex, double-stranded DNA (dsDNA) in the presence of T7 DNA polymerase, T4 DNA ligase, and deoxynucleotides. The resulting dsDNA is purified and electroporated into TG1 cells, where the uracilated parental strand is degraded and the mutant strand is preserved and converted into the replicative form of phagemid DNA.

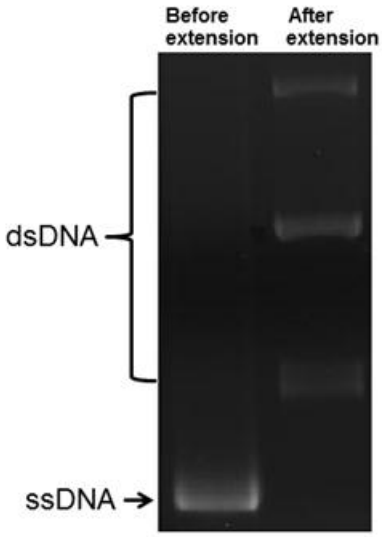

Figure 2.2. Synthesis of heteroduplex dsDNA *in vitro*. Purified uracilated ssDNA was converted into dsDNA by T7 DNA polymerase and T4 DNA ligase. The extended heteroduplex dsDNA was purified and resolved by agarose gel electrophoresis. The relative mobility of ssDNA and dsDNA are noted with an arrow and a parenthesis, respectively.

2.4.2 Phage replication at lower temperature improved yields of ssDNA

Infected CJ236 cells often have low yields of ssDNA, and of low purity (*7*). To find conditions leading to higher yields and better purity, multiple settings (i.e., growing temperature, shaking speed, different type of flasks) were evaluated. Incubation at 25 °C for 22 h consistently yielded two- to sevenfold more ssDNA than cultures grown at 37 °C (Figure 2.3). A similar increase in ssDNA yields was also observed for cultures of TG1 cells carrying the M13 bacteriophage genome (data not shown). However, if cells were resuspended in a much higher volume (i.e., 30 fold) of fresh medium after infection, the same growing conditions did not lead to higher yields.

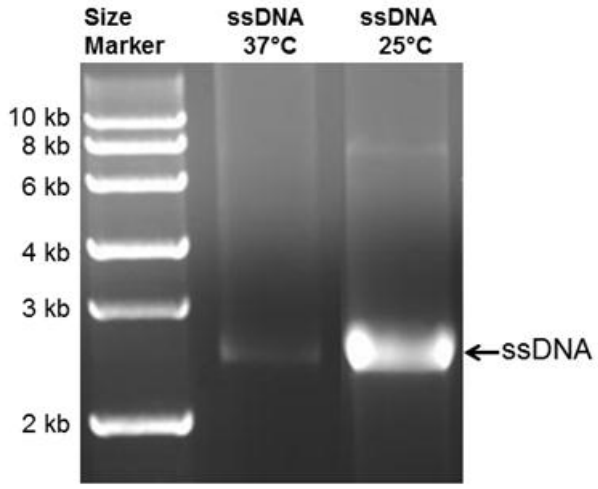

Figure 2.3. Single-stranded DNA extracted from bacterial cultures grown at two different temperatures. Bacterial cultures, which were grown at 37 °C and 25 °C, were clarified by centrifugation. Single-stranded DNA (ssDNA) were extracted from clarified supernatant and resolved in a 1% agarose gel. The ssDNA depicted here migrates with a size of 5830 nucleotides and its position in the gel is denoted with an arrow. As shown in the figure, the yields of ssDNA from a culture grown at 25 °C were sevenfold higher than that grown at 37 °C.

The effects of shaking speed and flask shape on phage yields were also examined. High shaking speed (i.e., 280 rpm), with 37 °C incubation, led to lower yields of ssDNA due to excessive degradation of DNA (data not shown). As both greater aeration and higher temperatures lead to rapid cell growth and potential cell lysis (*29*), these conditions are not recommended for phage replication. When cultures were grown in baffled and non-baffled flasks, there was no significant change in the yields or purity of the ssDNA (data not shown). In summary, keeping the culture volume the same after infection and incubating it for 22 h at 25 °C, with a shaking speed of 200 rpm, contributed to the best results, among all the conditions tested.

2.4.3 Different reaction conditions for *in vitro* dsDNA synthesis exhibited minimal influences on mutation rate

As mentioned above, it is beneficial to reduce or eliminate phage particles displaying the ówild-typeôform of a scaffold protein, thereby increasing the diversity of a library and enhancing its effectiveness in yielding binders. One way to reduce the number of wild-type clones in a phage library is to identify conditions that improve the efficiency of *in vitro* synthesis of dsDNA during Kunkel mutagenesis. To learn what modifications of the extension step might lead to enhanced yields, nine different conditions, ranging from different annealing ratios of oligonucleotide/ssDNA (3, 20, and 100) to different extension times (30 min, 3 h, and 16 h), were tested. While none of these conditions appeared to increase significantly the mutation rate, there are two points worth

noting. First, the average mutation rate (i.e., replacement of both loops with degenerate sequences) for all nine conditions was 38 ± 3%. Second, for reactions of all three annealing ratios, as the extension time went from 30 min, 3 h to 16 h, there was a 1ï 8% increase in the mutation rate from 30 min to 3 h, and then a 3ï 6% decrease from 3 h to 16 h (data not shown). A 16 h extension not only led to a lower mutation rate, but also a significantly lower yield of dsDNA (data not shown). Based on our results, an annealing ratio of 3:1 (oligonucleotide/ssDNA template), with an extension time of 3 h, is recommended for the synthesis of heteroduplex dsDNA *in vitro*.

Curiously, even in the absence of any synthesized oligonucleotide primer, ssDNA is still able to self-prime and generate dsDNA (*6*) during the extension reaction, which can be how the non-recombinant dsDNA is synthesized. To test the possibility that one could outcompete self-priming with longer oligonucleotide primers to reduce the synthesis of non-recombinant dsDNA, primers of different lengths were tested. No significant difference in the mutation rate was observed, indicating that once a minimum length requirement was met (T_m=50ï 55 °C), longer primers offered no advantage in boosting the mutation rate compared to shorter ones. We also hypothesized that degraded small DNA segments, which might be present in preparations of the ssDNA template, could be responsible for the self-priming. To test this notion, ssDNA was resolved by agarose gel electrophoresis and extracted from any contaminating DNA segments. However, this extra purification step only slightly raised the mutation rate (i.e., from 40% to

50%), implying that the persistence of non-recombinants was somehow inherent to the ssDNA template itself.

2.4.4 Removal of non-recombinant clones by restriction enzyme digestion

To enhance the efficiency of Kunkel mutagenesis, a set of three phagemid vectors were devised with stop codons and restriction endonuclease recognition sites inserted in the BC and FG loop coding regions. The stop codons are intended to prevent the display of wild-type FN3 domain and its N-terminal fused Flag epitope, whereas inclusion of restriction endonuclease cleavage sites is to permit differential destruction of non-recombinant DNA by digestion with restriction endonucleases.

Three restriction endonucleases were chosen because their recognition sequences were absent from the original phagemid genome and their activities were robust. Vectors were designed with SacII (5ôCCGC$^{\acute{Z}}$GG-3ô), SmaI (5ô CCC$^{\acute{Z}}$GGG-3ô), or StuI (5ôAGG$^{\acute{Z}}$CCT-3ô) sites in the BC and FG coding regions. (Note that each vector carried two recognition sites for the same enzyme). For StuI recognition site, even though it contains thymine, which can be replaced by uracil when ssDNA genome is propagated in the CJ236 *E. coli* strain, and thus can make non-recombinant dsDNA resistant to StuI cleavage, we rationalized that the chance that one or both thymines in the StuI site are replaced by uracil is low (i.e., 3ï 4%), given that only 20ï 30 uracils are inserted in each ssDNA genome when propagated in CJ236 cells (*30*).

When the three vectors were used for *in vitro* synthesis of dsDNA, digestion of the dsDNA with the cognate restriction enzyme prior to electroporation led to only a 10% increase in the frequency of recombinants (51% to 61%) obtained. At the moment, we cannot account for this result, even though it is reproducible. However, we noted that the phagemid carrying the two StuI sites consistently yielded larger transformation outputs, compared to the phagemids with SacII or SmaI sites; consequently, we used the phagemid DNA with the two StuI sites throughout this study.

Since we could not selectively degrade the *in vitro* synthesized, non-recombinant dsDNA molecules by restriction enzyme cleavage, we decided to first electroporate the dsDNA into TG1 cells, and then digest the purified, replicated DNA. After re-electroporating the digested DNA into bacteria, the resulting transformants were observed to be entirely recombinant (Figure 2.4). By this approach, a phage-display library, with 10^{10} members and >99% recombinant, has been recently constructed in the lab by performing 140 electroporations (i.e., 100 electroporations of the *in vitro* synthesized dsDNA, followed by 40 electroporations of the digested DNA, into bacteria).

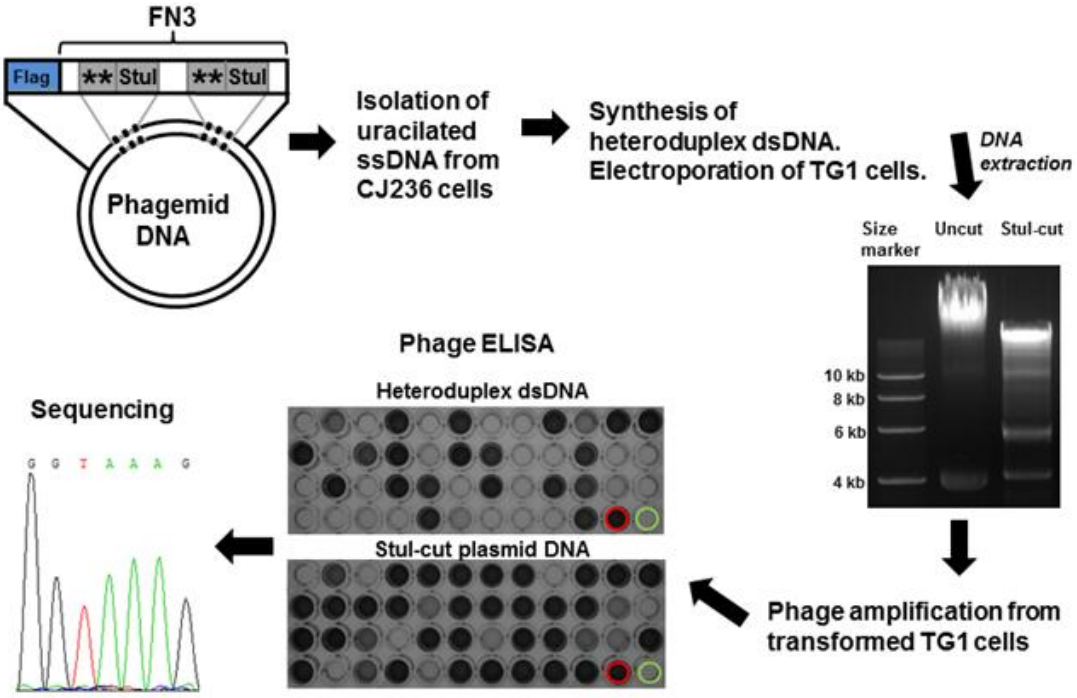

Figure 2.4. Removal of non-recombinant clones by digestion with StuI. The phagemid modified with sequences of stop codons and StuI restriction enzyme sites was electroporated into CJ236 bacterial cells for generating uracilated ssDNA, which was annealed to mutagenic oligonucleotides (With NNK codons) and converted to dsDNA *in vitro*. Heteroduplex dsDNA was electroporated into TG1 cells, and the next day, transformed cells were scraped off the surface of agar plates. Plasmid DNA was then extracted from the scraped cells, digested with StuI, and electroporated back into TG1 cells. Bacterial colonies from electroporation of the synthesized dsDNA and the digested DNA were picked and grown up for phage replication. The following day, a phage ELISA was performed with anti-Flag antibody to identify mutant clones for sequencing analysis. Due to the presence of two amber stop codons encoded by the NNK codons, some recombinant clones appeared negative in the ELISA assay. On the microtiter plate of phage ELISA, the red-circled and green-circled wells correspond to positive and negative controls, respectively.

2.4.5 Kunkel mutagenesis with DNA segments generated by error-prone and asymmetric PCR

To bypass the time-consuming steps of restriction enzyme digestion, gel purification, and ligation in the conventional approach for generating a secondary mutagenic library, a protocol was devised that utilizes DNA segments amplified from PCR in lieu of oligonucleotide primers. First, an error-prone PCR was carried out with Mutazyme II, a mixture of two mutant DNA polymerases that introduce point mutations at high frequency in the targeted gene (*31*). The amplified DNA segments were resolved by agarose gel electrophoresis, gel purified, denatured, and annealed to the ssDNA template. After DNA synthesis *in vitro*, the resulting dsDNA was electroporated into TG1 cells. But as revealed by phage ELISA and DNA sequencing, only 3ï 8% of the transformants were recombinants. With this method, a secondary library with a diversity of 1.0×10^8 was constructed (Figure 2.5). To investigate whether digestion by StuI could elevate the incorporation of the mutated strand, the dsDNA was subjected to digestion with StuI before transformation. Although digestion did increase the mutation rate to 17ï 28%, the transformation efficiency decreased five- to sevenfold.

As Kunkel mutagenesis is usually conducted with one to several 30ï 60 nucleotide long oligonucleotide primers, we rationalized that a double-stranded 300-bp DNA segment might not anneal efficiently to the ssDNA template for *in vitro* DNA synthesis because of the equimolar presence of its complementary

DNA strand. Therefore, we decided to generate DNA segments that were predominately single-stranded through asymmetric PCR (*27, 32*), and use the resulting mixture to prime DNA synthesis on the template strand (Figure 2.5A). DNA segments that were predominantly single-stranded were generated through 40 cycles of DNA synthesis with Mutazyme II. They were subsequently annealed to the uracilated ssDNA template, converted to dsDNA *in vitro*, and electroporated into TG1 cells. A library consisting of 4×10^8 recombinants was created, with a transformation efficiency of 7.4×10^8 cfu/µg dsDNA (Figure 2.5B), which is comparable to the transformation efficiency, 5ï 6 $\times 10^8$ cfu/µg, obtained with dsDNA synthesized with oligonucleotide primers ordered from commercial vendor (data not shown). Upon sequencing 24 recombinants, we observed equal numbers of transition mutations and transversion mutations, 18/35 compared to 17/35, respectively, and an overall point mutation rate of 5.3 mutations per kilobase (i.e., 0.5%).

While conducting our experiments, we witnessed that asymmetric PCR amplification was very sensitive to many factors (i.e., type of DNA polymerase, buffer, thermal cycling conditions). Even with a third primer to perform a nested asymmetric PCR (*32*), amplification results were not consistent (i.e., the yields of single-stranded product varied). Thus, when asymmetric PCR fails to generate high-quality single-stranded DNA, the double-stranded segment from the error-prone PCR can be used instead for constructing a secondary library.

To elevate the mutation rate, error-prone PCR was performed with Mutazyme II under conditions reported to increase the mutation rate of *Taq* DNA

polymerase (*28*). The resulting DNA segment was used directly as the primer for *in vitro* dsDNA synthesis, as described above (Figure 2.5A). Electroporation of the dsDNA yielded 2.8×10^9 transformants, with a transformation efficiency of 5.3×10^8 cfu/μg dsDNA. Among the transformants, 3.5% were recombinant, and on the average each recombinant clone had 6.5 mutations, which is equal to a point mutation rate of 2.5% (i.e., 25 mutations/per kb) (Figure 2.5B). While the fraction of recombinants among the transformants is low, the diversity of the resulting library is still sufficient (i.e., 1.0×10^8) for generating enhanced binders.

A.

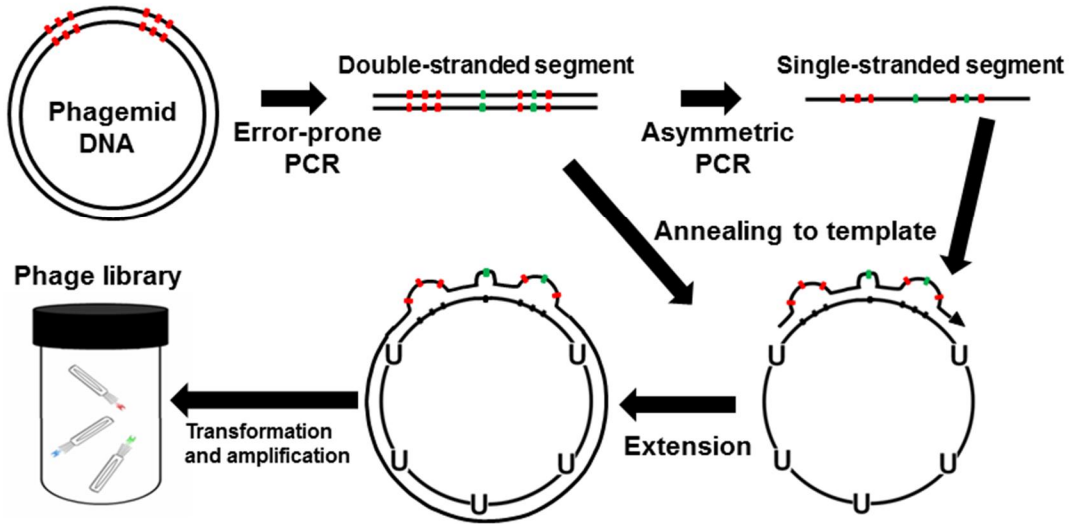

B.

Type of DNA segment	Number of transformants	Percentage of recombinant	Library diversity	Mutation rate of recombinants (mutations/kb)
Double-stranded	2.8×10^9	3.5%	1.0×10^8	25.0
Single-stranded	2.1×10^9	18%	4.0×10^8	5.3

Figure 2.5. Construction of two secondary mutagenic libraries with DNA segments amplified by error-prone and asymmetric PCR. A. Error-prone PCR was performed to amplify the coding region of an FN3 variant that had been evolved to bind to Pak1 kinase. The DNA segment, which was gel purified, was either used directly as primer for annealing to the uracilated ssDNA template, or was used as template to carry out asymmetric PCR, yielding DNA segments that were mostly single-stranded. This mixture of DNA segments was purified free of oligonucleotide primers and annealed to uracilated ssDNA. The annealed ssDNA template, either to the double-stranded or the single-stranded segments, was converted into dsDNA *in vitro* by the action of T7 DNA polymerase and T4 DNA ligase. The extended, circular dsDNA was purified and electroporated into TG1 cells, thereby generating a secondary library. **B.** Two mutagenic libraries were constructed with the modified protocol of Kunkel mutagenesis. The number of transformants is the estimated total number of bacterial colonies produced through electroporation. The percentage of recombinants is the ratio of recombinants to the total pool of transformants, as a fraction of 100. The library diversity is the estimated total number of recombinants in this mutagenic library. Mutations/kb is the average number of point mutations per kilobase (kb).

2.4.6 Identification of stronger binders through affinity selection of a mutagenic library

The mutagenic library containing 4×10^8 variants was screened through three rounds of affinity selection under stringent conditions. After the third round of selection, eighty-eight clones were evaluated by phage ELISA: ~50% of the clones showed tighter binding to Pak1 kinase than the original clone (data not shown). Three clones with the greatest ELISA signals were chosen for further testing, and two variants, C2 and D3, were observed to bind fourfold stronger to Pak1 kinase than the original clone, while a third variant, E10, bound twofold better (Figure 2.6). Compared to the primary structure of the original binder, each of the three FN3 variants had three amino acid substitutions (data not shown). Thus, with this example, we demonstrate the utility of our modifications to the Kunkel mutagenesis protocol in generating high quality recombinant affinity reagents.

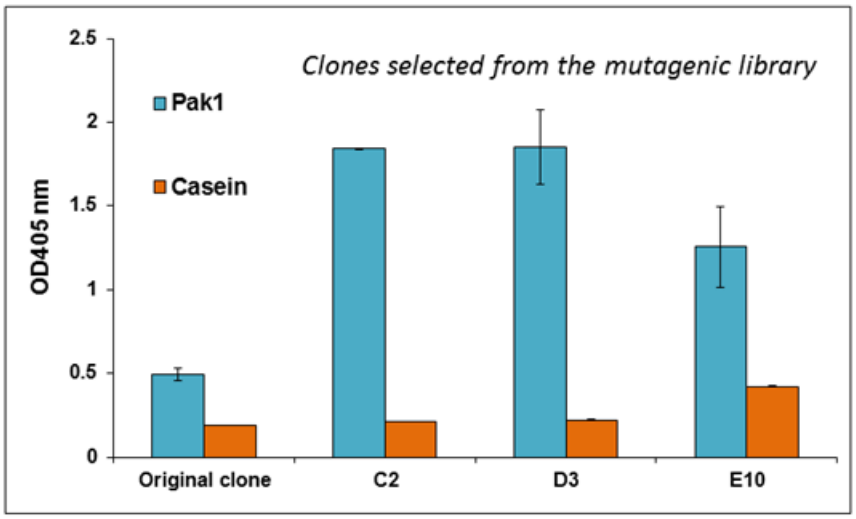

Figure 2.6. Comparing the original clone and its three variants for binding to Pak1 kinase. The blue bars represent the binding of phage particles to the Pak1 kinase (target), and the orange bars represent binding to casein (negative control). All binding values were normalized to the display level of the Flag-epitope, which is at the N-terminus of the displayed FN3 monobody. The error bars represent the standard deviation of duplicate measurements.

2.5 Conclusions

Kunkel mutagenesis is one of the most frequently used methods for constructing phage-displayed libraries. To make this technique more efficient, we optimized the yields of ssDNA by growing infected cells for 22 h at 25 °C, with a shaking speed of 200 rpm. By introducing StuI recognition sites in the FN3 coding sequence, we were able to remove non-recombinant clones by restriction endonuclease digestion and subsequently created libraries that were >99% recombinant. Finally, two mutagenic phage libraries were constructed with DNA segments amplified by error-prone and asymmetric PCR. Screening one of the secondary libraries identified three variants that bound two- to fourfold tighter to the Pak1 kinase than the original clone. In the future, we envision that a phage pool, enriched for binders via affinity selection of the primary library, can be used directly as template for mutagenic PCR, and the resulting mutated DNA segment can be used to prime dsDNA synthesis *in vitro*. Thus, in one weekôs time a secondary library can be constructed and screened to yield enhanced binders.

2.6 References

1. Wells, J. A., and Estell, D. A. (1988) Subtilisin--an enzyme designed to be engineered, *Trends Biochem Sci 13*, 291-297.

2. Vandeyar, M. A., Weiner, M. P., Hutton, C. J., and Batt, C. A. (1988) A simple and rapid method for the selection of oligodeoxynucleotide-directed mutants, *Gene 65*, 129-133.

3. Sugimoto, M., Esaki, N., Tanaka, H., and Soda, K. (1989) A simple and efficient method for the oligonucleotide-directed mutagenesis using plasmid DNA template and phosphorothioate-modified nucleotide, *Anal Biochem 179*, 309-311.

4. Kunkel, T. A. (1985) Rapid and efficient site-specific mutagenesis without phenotypic selection, *Proc Natl Acad Sci U S A 82*, 488-492.

5. Kunkel, T. A., Roberts, J. D., and Zakour, R. A. (1987) Rapid and efficient site-specific mutagenesis without phenotypic selection, *Methods Enzymol 154*, 367-382.

6. Scholle, M. D., Kehoe, J. W., and Kay, B. K. (2005) Efficient construction of a large collection of phage-displayed combinatorial peptide libraries, *Comb Chem High Throughput Screen 8*, 545-551.

7. Tonikian, R., Zhang, Y., Boone, C., and Sidhu, S. S. (2007) Identifying specificity profiles for peptide recognition modules from phage-displayed peptide libraries, *Nature Protocols 2*, 1368-1386.

8. Wojcik, J., Hantschel, O., Grebien, F., Kaupe, I., Bennett, K. L., Barkinge, J., Jones, R. B., Koide, A., Superti-Furga, G., and Koide, S. (2010) A potent and highly specific FN3 monobody inhibitor of the Abl SH2 domain, *Nat Struct Mol Biol 17*, 519-527.

9. Fellouse, F. A., Esaki, K., Birtalan, S., Raptis, D., Cancasci, V. J., Koide, A., Jhurani, P., Vasser, M., Wiesmann, C., Kossiakoff, A. A., Koide, S., and Sidhu, S. S. (2007) High-throughput generation of synthetic antibodies from highly functional minimalist phage-displayed libraries, *J Mol Biol 373*, 924-940.

10. Huang, R., Fang, P., and Kay, B. K. (2011) Isolation of monobodies that bind specifically to the SH3 domain of the Fyn tyrosine protein kinase, *N Biotechnol*.

11. Ling, M. M. (2003) Large antibody display libraries for isolation of high-affinity antibodies, *Comb Chem High Throughput Screen 6*, 421-432.

12. Menendez, A., and Scott, J. K. (2005) The nature of target-unrelated peptides recovered in the screening of phage-displayed random peptide libraries with antibodies, *Anal Biochem 336*, 145-157.

13. Brammer, L. A., Bolduc, B., Kass, J. L., Felice, K. M., Noren, C. J., and Hall, M. F. (2008) A target-unrelated peptide in an M13 phage display library traced to an advantageous mutation in the gene II ribosome-binding site, *Anal Biochem 373*, 88-98.

14. Fagete, S., Ravn, U., Gueneau, F., Magistrelli, G., Kosco-Vilbois, M. H., and Fischer, N. (2009) Specificity tuning of antibody fragments to neutralize two human chemokines with a single agent, *MAbs 1*, 288-296.

15. Yang, W. P., Green, K., Pinz-Sweeney, S., Briones, A. T., Burton, D. R., and Barbas, C. F., 3rd. (1995) CDR walking mutagenesis for the affinity maturation of a potent human anti-HIV-1 antibody into the picomolar range, *J Mol Biol 254*, 392-403.

16. Groves, M., Lane, S., Douthwaite, J., Lowne, D., Rees, D. G., Edwards, B., and Jackson, R. H. (2006) Affinity maturation of phage display antibody populations using ribosome display, *J Immunol Methods 313*, 129-139.

17. Gram, H., Marconi, L. A., Barbas, C. F., 3rd, Collet, T. A., Lerner, R. A., and Kang, A. S. (1992) In vitro selection and affinity maturation of antibodies from a naive combinatorial immunoglobulin library, *Proc Natl Acad Sci U S A 89*, 3576-3580.

18. Daugherty, P. S., Chen, G., Iverson, B. L., and Georgiou, G. (2000) Quantitative analysis of the effect of the mutation frequency on the affinity maturation of single chain Fv antibodies, *Proc Natl Acad Sci U S A 97*, 2029-2034.

19. Koide, A., Bailey, C. W., Huang, X., and Koide, S. (1998) The fibronectin type III domain as a scaffold for novel binding proteins, *J Mol Biol 284*, 1141-1151.

20. Koide, S., Koide, A., and Lipovsek, D. (2012) Target-binding proteins based on the 10th human fibronectin type III domain ((1)(0)Fn3), *Methods Enzymol. 503*, 135-156.

21. Karatan, E., Merguerian, M., Han, Z., Scholle, M. D., Koide, S., and Kay, B. K. (2004) Molecular recognition properties of FN3 monobodies that bind the Src SH3 domain, *Chem Biol 11*, 835-844.

22. Pershad, K., Sullivan, M. A., and Kay, B. K. (2011) Drop-out phagemid vector for switching from phage displayed affinity reagents to expression formats, *Analytical Biochemistry 412*, 210-216.

23. Haidaris, C. G., Malone, J., Sherrill, L. A., Bliss, J. M., Gaspari, A. A., Insel, R. A., and Sullivan, M. A. (2001) Recombinant human antibody single chain variable fragments reactive with Candida albicans surface antigens, *J Immunol Methods 257*, 185-202.

24. Lindahl, T., Ljungquist, S., Siegert, W., Nyberg, B., and Sperens, B. (1977) DNA N-glycosidases: properties of uracil-DNA glycosidase from Escherichia coli, *J. Biol. Chem. 252*, 3286-3294.

25. Manser, E., Leung, T., Salihuddin, H., Zhao, Z. S., and Lim, L. (1994) A brain serine/threonine protein kinase activated by Cdc42 and Rac1, *Nature 367*, 40-46.

26. Parrini, M. C., Lei, M., Harrison, S. C., and Mayer, B. J. (2002) Pak1 kinase homodimers are autoinhibited in trans and dissociated upon activation by Cdc42 and Rac1, *Mol Cell 9*, 73-83.

27. Tessier, D. C., and Thomas, D. Y. (1996) PCR-assisted mutagenesis for site-directed insertion/deletion of large DNA segments, *Methods Mol. Biol. 57*, 229-237.

28. Cadwell, R. C., and Joyce, G. F. (1994) Mutagenic PCR, *PCR Methods Appl. 3*, S136-140.

29. Ellis, E., and Delbrück, M. (1938) The growth of bacteriophage *J Gen Physiol 22*, 365-384

30. Sagher, D., and Strauss, B. (1983) Insertion of nucleotides opposite apurinic/apyrimidinic sites in deoxyribonucleic acid during in vitro synthesis: uniqueness of adenine nucleotides, *Biochemistry 22*, 4518-4526.

31. Rasila, T. S., Pajunen, M. I., and Savilahti, H. (2009) Critical evaluation of random mutagenesis by error-prone polymerase chain reaction protocols, Escherichia coli mutator strain, and hydroxylamine treatment, *Anal Biochem 388*, 71-80.

32. Pai, J. C., Entzminger, K. C., and Maynard, J. A. (2012) Restriction enzyme-free construction of random gene mutagenesis libraries in Escherichia coli, *Anal Biochem 421*, 640-648.

CHAPTER 3

ISOLATION OF MONOBODIES THAT BIND SPECIFICALLY TO THE SH3 DOMAIN OF THE FYN TYROSINE PROTEIN KINASE

Renhua Huang, Pete Fang, and Brian K. Kay

Part of this work has been published in *New Biotechnology*, Volume 29 (5), pages 526-533 (2012)

3.1 Abstract

Fyn is a non-receptor protein tyrosine kinase that belongs to a highly conserved kinase family, Src family kinases (SFKs). Fyn plays an important role in inflammatory processes and neuronal functions. To generate a synthetic affinity reagent that can be used to probe Fyn, a phage-display library of fibronectin type III (FN3) monobodies was affinity selected with the SH3 domain of Fyn and three binders were isolated. One of the three binders, G9, is specific in binding to the SH3 domain of Fyn, but not to the other members of the Src family (i.e., Blk, Fgr, Hck, Lck, Lyn, Src, Yes), even though they share 51-81% amino acid identity. The other two bind principally to the Fyn SH3 domain, with some cross-reactivity to the Yes SH3 domain. The G9 binder has a dissociation constant of 166 ± 6 nM, as measured by isothermal titration calorimetry, and binds only to the Fyn SH3 domain out of 150 human SH3 domains examined in an array. Interestingly, although the G9 monobody lacks proline in its randomized BC and FG loops, it binds at the same site on the SH3 domain as proline-rich ligands, as revealed by competition assays. Active Fyn kinase was successfully pulled down by the G9 monobody, demonstrating its potential as a highly selective probe for detecting active cellular Fyn kinase.

3.2 Introduction

While recombinant antibodies continue to be a fruitful source of affinity reagents, there has been a great deal of interest in engineering useful affinity reagents from other scaffolds. Several other scaffold proteins have been engineered into affinity reagents (*1*). These include three Ŭ-helix bundles of the Z domain of protein A, called affibodies (*2*), avimers (*3*), cystine-knot peptides (*4*), green fluorescent protein (GFP) (*5*), lipocalin (*6*), camelid V_{HH} (*7*), and designed ankyrin repeat proteins (DARPins) (*8*), to name a few. The scaffold I have exploited is the fibronectin type III (FN3) domain, which is 94 amino acids in length, and has a three-dimensional structure similar to that of the immunoglobulin fold. There are over 8000 examples of this domain in GenBank, making it one of the most prevalent domains known. It should be pointed out that the tenth repeat of the domain in fibronectin contains the Arg-Gly-Asp (RGD) motif in one loop, which interacts with the fibronectin receptor on cell surfaces (*9*) . Protein engineering experiments have shown it is possible to substitute amino acids within five of the six loops without loss of stability (*10*); in particular, from libraries of variants with combinatorial peptides within two loops on one side of the domain, one generates libraries of synthetic affinity reagents, termed ñmonobodiesò. Through phage display, RNA display, or yeast display, FN3 monobodies have been generated for binding to a variety of targets, such as the estrogen receptor (*11*), integrin (*12*), lysozyme (*13*), a phosphorylated IəBŬ peptide (*14*), small ubiquitin-like modifier 4 (SUMO4) (*15*), streptavidin (*16*), tumor necrosis factor (*17*), ubiquitin (*18*), and vascular endothelial growth factor

receptor 2 (*19*). In addition, the FN3 domain can be expressed inside eukaryotic cells, where it can fold properly and bind to its target (*10*). It is also possible to combine a monobody with a protein interaction module to create affinity reagents that can ñclampò short peptides with picomolar affinity (*20, 21*). Three advantages of the FN3 domain are that it lacks disulfide bonds, it can be highly overexpressed (Ó50 mg/L culture) in *E. coli*, and it is thermally stable (T_m = 88ºC).

Recently, I have screened a phage-display library of monobodies for variants that bind to the Src Homology 3 (SH3) domain (*16*). This 60 amino acid domain is involved in protein-protein interactions (*22*), and is present in many different eukaryotic proteins that are involved in signal transduction (*23*), cytoskeleton assembly (*24*), and endocytosis (*25*). In mammals, the Src family of protein tyrosine kinases (Figure 3.1) plays an important role in cell signaling pathways, by transferring signals from activated receptors to downstream signaling proteins. This family of kinases shares a common architecture that consists of an N-terminal myristic acid, a unique region, a Src Homology 3 (SH3) domain, a Src homology 2 (SH2) domain, a linker, and a C-terminal catalytic kinase domain. Generally, these proteins have two conformations: a catalytically inactive conformation, in which the protein is folded into a 'closed' state, due to intramolecular interactions, and a catalytically active conformation, in which the protein is in an extended, 'open' state (*26*). The Fyn protein has been proposed to play a role in T-cell receptor activation (*27*), lipid utilization (*28*), exit from meiotic and mitotic metaphases (*29*), mast cell signaling (*30*), and

carcinogenesis (*31, 32*).

This work extends prior efforts in which I identified monobodies that bind to the Src SH3 domain (*16*), and one of the isolated monobodies was converted into a biosensor of *in situ* activation of Src in cultured cells (*33*). I was interested in extending this approach to other members of the Src family, which consists of Blk, Fgr, Fyn, Hck, Lck, Lyn, Src, and Yes (*34*). I report the isolation of monobodies that are specific in binding to the Fyn SH3 domain. One of the isolated monobodies, G9, is highly selective and can be potentially developed into a biosensor of Fyn kinase activation.

3.3 Materials & methods

3.3.1 Construction of a phage display library

A library of FN3 monobodies was constructed by oligonucleotide-directed mutagenesis (*35, 36*). Briefly, the FN3 coding region was subcloned into a drop-out phagemid vector (*37*), which encodes a truncated form of gene III of the M13 bacteriophage and the DsbA signal sequence (*38*). The recombinant phagemid construct was transformed into the bacterial strain CJ236 (New England BioLabs, Ipswich, MA), an *Escherichia coli* host used for producing uracil-containing single-stranded DNA (ssDNA). The ssDNA was annealed to two mutagenic oligonucleotides (IDT DNA, Coralville, Iowa), which encoded five NNK codons in the BC loop and FG loop (Figure 3.2A). (N is an equimolar distribution of A, G, C, or T, whereas K is G or T. NNK allows incorporation of all 20 amino acids, plus

the TAG amber codon.) With T7 DNA polymerase (New England BioLabs) and T4 DNA ligase (New England BioLabs), the ssDNA was converted into the double-stranded DNA (dsDNA) using the two annealed degenerate oligonucleotides. Synthesized dsDNA was recovered with a PCR clean-up kit (Qiagen, Valencia, CA), and electroporated into TG1 *E. coli* cells (Lucigen, Madison, WI). Transformed cells were immediately transferred to pre-warmed recovery medium (Lucigen), incubated at 37ºC at 200 rpm for 35 min, and then aliquots were taken out for determining the transformation efficiency. To ensure optimal recovery, cells were allowed to recover for an additional 25 min, before being centrifuged and plated for overnight growth at 30ºC. The output of 85 electroporations was pooled to generate a library containing $2.8x10^{10}$ transformants. The result of DNA sequencing of 60 clones from the library showed that both BC and FG loops were replaced by mutagenic sequences in 46% of the transformants. The library was estimated to have a diversity of $1.3x10^{10}$ recombinant clones (46% of $2.8x10^{10}$).

To amplify the phage particles displaying the recombinant FN3 monobodies, approximately 1.3×10^{11} cells were diluted into Luria Broth (LB; 10 g/L tryptone, 5 g/L yeast extract, 10 g/L NaCl) - 50 εg/mL carbenicillin to a final density of OD_{600nm}= 0.05. After 2 h incubation at 37ºC at 250rpm, the cells were infected with M13KO7 helper phage (New England BioLabs) at a multiplicity of infection (MOI) of 10, and then incubated at 37ºC for 2 h at 150 rpm. Infected cells were recovered by centrifugation, resuspended in fresh LB (supplemented with 50 εg/mL carbenicillin and 100 εg/mL kanamycin), and incubated overnight at 30ºC.

The next day, secreted phage particles were separated from bacterial cells by centrifugation, followed by precipitation with 5% PEG8000 - 300 mM NaCl (final concentrations). The phage particle pellet was dissolved in phosphate buffered saline (PBS; 137 mM NaCl, 3 mM KCl, 8 mM Na_2HPO_4, 1.5 mM KH_2PO_4), and stored in 16% glycerol (with PBS) at -80ºC.

3.3.2 Gene synthesis, plasmid preparation, protein overexpression, and purification

The coding sequences of FN3 monobodies and the Fyn SH3 domain were amplified by polymerase chain reaction (PCR), and subcloned into a modified form of the pET-14b expression vector (Gift of Dr. Arnon Lavie, University of Illinois at Chicago), which carries a His_6-tag that is fused in frame to the small ubiquitin-like modifier (SUMO) at the N-terminus. The coding sequences of the other seven human SH3 domains of the SFKs were synthesized commercially (GenScript, Piscataway, NJ) and subcloned into the same vector.

All expression constructs were transformed into the BL21-DE3 (Novagen, Rockland, MA) or C41-DE3 (*39*) strains of *E. coli*. Cells were used to inoculate into 10 mL LB with 50 ε g/mL carbenicillin, and incubated at 37ºC overnight. After a 30:1 dilution in auto-induction medium (Novagen), the cells were grown for 20-24 h at 30ºC. The cell pellet was lysed with Bugbuster detergent (Novagen), which was supplemented with rLysosme (Novagen) and ethylenediaminetetraacetic acid (EDTA)-free protease inhibitor (Roche). After 10

min of sonication (Thermo Fisher Scientific), the clarified lysate was incubated with nickel-nitriloacetic acid (Ni-NTA) resin (Qiagen) for immobilized metal affinity chromatography of the His_6-tagged proteins. The SUMO fusion proteins (SH3 domain and monobody) were subsequently chromatographed through a Superdex 200 column (GE Healthcare, Piscataway, NJ) to attain >95% purity, with yields of 50-200 mg/L of cell culture.

3.3.3 Affinity selection

Three rounds of affinity selection were used to select monobodies binding to the Fyn SH3 domain. A Fyn SH3 domain fusion to glutathione-S-transferase (GST) was purified with GST bind resin (GE Healthcare) and chemically biotinylated with the EZ-link NHS biotinylation kit (Thermo Fisher Scientific). NeutrAvidin® (Thermo Fisher Scientific) was diluted in PBS (25 ng/εL) and incubated in Nunc microtiter plate wells (Thermo Fisher Scientific) overnight at 4ºC. The next day, after washing the wells, biotinylated Fyn SH3 domain-GST fusion protein (25 ng/εL) was added to microtiter plate wells for 20min at room temperature, followed by blocking of non-specific binding sites with casein (Thermo Fisher Scientific), which was supplemented with 10 εM biotin. In the affinity selection experiment, ~$5x10^{12}$ phage particles, which displayed variants of the FN3 monobody, were incubated in microtiter plate wells for 2 h, followed by three washes with PBS-0.1% Tween (PBST) and three washes with PBS. Bound phage particles were eluted with 50 mM glycine (pH 2.0). Eluted phages were

neutralized with Tris-HCl (pH 10) and used to infect TG1 cells (OD_{600nm}=0.4-0.6) for 1 h at 37ºC at 150 rpm. Infected cells were spread onto Petri plates containing 1.5% agar, LB, and 50 εg/mL carbenicillin, and incubated overnight at 30ºC. The next day, colonies were scraped from plates and ~5 x 10^8 cells were inoculated into 50 mL of LB + 50 εg/mL carbenicillin and grown for 2-3 h at 37ºC at 250 rpm. When the culture reached an OD_{600nm} =0.4-0.6, the cells were infected with M13K07 helper phage (MOI = 10) for 1 h, transferred to fresh LB + 50 εg/mL carbenicillin and 100 εg/mL kanamycin, and incubated overnight at 30ºC. The next day, phage particles were harvested from the culture supernatant, precipitated with 5% PEG8000 and 300 mM NaCl (final concentrations), dissolved in PBS, and used for the next round of affinity selection. The second and third rounds of affinity selection were conducted in the same manner, except that PBS-suspended phage particles was supplemented with soluble GST for binding to the Fyn SH3 domain in the microtiter plate wells, as a means of eliminating recovery of FN3 monobodies that bind to the GST portion of the fusion protein. After the third round of affinity selection, individual clones were picked for phage amplification, followed by enzyme-linked immunosorbent assay (ELISA) to identify binders to the Fyn SH3 domain. Subsequently, positive binding clones were sequenced.

3.3.4 Phage ELISA and mapping of binding location

Phage ELISA assays were performed as described in previous work (*16*).

Briefly, the SH3 domain fusion proteins were directly immobilized on Nunc microtiter plate (Thermo Fisher Scientific), by aliquoting 5 εg/mL solutions (in PBS) into triplicate wells, and incubating the plates overnight at 4ºC. The following day, non-specific binding sites in the wells were blocked with excess casein (in PBS) for 1 h. After washing the wells with PBST, culture supernatants, which contained phage particles, were added to wells for 1 h incubation, followed by washes of microtiter plate and incubation with an anti-phage antibody that is conjugated to horseradish peroxidase (GE Healthcare). After 1 h incubation, the wells were washed, and the chromogenic substrate, 2,2'-Azino- bis(3-Ethylbenzothiazoline-6-Sulfonic Acid (ABTS), in the presence of hydrogen peroxide, was added and the resulting absorbance was determined at 405 nm with a microtiter plate spectrophotometer (BMG Labtech, Germany).

To determine if the isolated monobodies bind to the Fyn SH3 domain at the same site used for binding to proline-rich peptides, a competition binding assay was devised. First, I optimized the phage ELISA assay, with respect to signal generation for the lowest amount of phage binding particles. Second, a proline-rich peptide (VSLARRPLPPLPGGK), which is a peptide ligand for the Fyn SH3 domain (*40*), was added over a range of concentrations, from 0.1 εM to 512 εM, along with the phage particles to the wells. After 1 h of incubation, the wells were washed with PBST, and phage particles that were retained in the wells were detected by ELISA, as described above. A second peptide (VSAARAALAPLAGGK), in which several residues were substituted with alanine, served as a negative control. In a separate experiment (data not shown), I

confirmed that the VSLARRPLPPLPGGK peptide bound to the Fyn SH3 domain and the VSAARAALAPLAGGK control peptide did not. In a parallel set of experiments, the binding of G9 to the Fyn SH3 was competed over a range of concentrations with the 1F11 monobody, a ligand with proline-rich binding motif.

3.3.5 Probing of an SH3 domain array

Four PVDF membranes, spotted with a total of 150 human SH3 domains, were purchased from Panomics (Freemont, CA). The membranes were probed according to the manufacturerôs instructions. Briefly, the four membranes were soaked in the wash buffer, provided by the manufacturer, for 1 h until the membrane was completely wet. The soaked membranes were blocked for 2 h, prior to the addition of the His_6-tagged SUMO-G9 monobody fusion at a final concentration of 1 nM. After overnight incubation at 4ºC, the membranes were washed four times with PBST, followed by the addition of an anti-his_6-tag antibody, conjugated to HRP (diluted 1:1200). After 1 h incubation, the membranes were washed 10 times with PBST and then incubated with a substrate for enhanced chemiluminescence (ECL-Plus, GE Healthcare). The four membranes were scanned simultaneously with a blue fluorescence filter on the Storm 860 PhosphorImager (GE Healthcare).

3.3.6 Isothermal titration calorimetry

His_6-tagged SUMO-FN3 monobody fusions and His_6-tagged SUMO-SH3 domain fusions were purified to homogeneity of >95% and dialyzed in the same beaker against 25 mM Tris-HCl (pH 7.5), 150 mM NaCl, and 100 mM imidazole. After overnight dialysis, their concentrations were determined with a NanoDrop ND-1000 spectrophotometer. Degassed samples were added to the loading cell (1.4 mL) and syringe (300 µL) of a VP-ITC (GE Healthcare). FN3 monobodies were loaded into the syringe at 200 µM and SH3 domains were loaded into the cell at 22 µM. The reference well was loaded with water. FN3 monobodies were injected into the cell with a volume of 10 µL per injection at 25ºC, with a reference power of 10 µcal/s. The heat change of each injection was recorded, and analyzed with Origin software (GE Healthcare).

3.3.7 Pull-down experiments with the G9 monobody

To test the possibility that the G9 monobody can bind the full-length Fyn, pull-down experiments were performed with recombinant Fyn kinase (Invitrogen; Carlsbad, CA). All experiments were performed in duplicate. One µL of Fyn kinase protein (200 nM) was mixed with 2 µL of biotinylated G9 or wild-type FN3 monobodies (45 µM), and incubated at room temperature for 1 h. Separately, 100 µL of streptavidin-coated magnetic beads (Promega; Madison, WI) were washed with phosphate buffered saline (PBS; 137 mM NaCl, 3 mM KCl, 8 mM Na_2HPO_4, 1.5 mM KH_2PO_4) three times, followed by a 30 min incubation in Tris-

buffered saline (TBS; 50 mM Trisï HCl, 150 mM NaCl, pH 7.5) containing 0.5% Tween (volume/volume) + 0.5% bovine serum albumin (BSA; mass/volume). Blocked beads were resuspended in 10 µL PBS and were added to the two mixtures of kinase with monobodies. After 15 min tumbling at room temperature, the beads were captured with a magnet, washed five times with PBS, and resuspended in 20 µL SDS sample buffer (Invitrogen). The bead were heated for 10 min incubation at 95°C.

The heat-denatured samples were resolved by SDS-polyacrylamide gel electrophoresis (SDS-PAGE), with an Any-KD pre-stained gel (Bio-rad; Hercules, CA) run for 45 min at 150 V. The gel image was captured with a Gel Doc EZ imager (Bio-Rad). Proteins in the gel were transferred to a nitrocellulose membrane (Thermo Fisher Scientific) by a 30 min semi-dry transfer on a Trans-blot Turbo transfer system (Bio-Rad). The nitrocellulose membrane was incubated in blocking buffer (Li-Cor bioscience; Lincoln, NE) for 1 h, followed by addition of anti-Fyn antibody (Final concentration, 2 µg/mL; Santa Cruz biotech, Santa Cruz, CA) for a 1 h incubation. After five washes with PBS+ 0.1% Tween 20 (PBST), the membrane was incubated with an anti-mouse IR-800 conjugated antibody (Li-Cor Bioscience), diluted with 1:10,000. After 1 h incubation, the membrane was washed three times with PBST, and scanned with the Odyssey infrared imaging system (Li-Cor Bioscience).

For pull-down experiments with cell lysates containing overexpressed Fyn kinase (Genway Bio; San Diego, CA), 35 µL of lysate (1 µg/µL) was mixed with 10 µL of biotinylated G9 and wild-type FN3 monobodies (Both at 45 µM),

respectively, and the mixture was incubated for 1 h at room temperature. The sample was processed as described above.

3.4 Results & discussion

One of the criteria of an affinity reagent's usefulness is its specificity. This is especially difficult to achieve when generating affinity reagents to members of a closely related protein family. Members of human SFKs are evolved from the same kinase, Src64, and thus share a highly conserved sequence with one another (*41*). Based on the sequence identity of the catalytic domain (*42*), the SFKs are divided into two groups (Figure 3.1A): the SrcA group (Fgr, Fyn, Src, and Yes) and the SrcB group (Blk, Hck, Lck, and Lyn). In general, the Fyn, Src, and Yes protein kinases are ubiquitously expressed in different types of tissues while the other members are expressed mostly in myeloid-lineage cells (*43*). Like the catalytic domain, the SH3 domain is highly conserved among the SFKs; for example, the SH3 domain of Fyn shares 51-81% identity with the SH3 domains of the other SFKs (Figure 3.1B). As recombinant antibodies have the prospect of being more specific than natural antibodies, due to the ability to control the selection process *in vitro (44)*, I decided to engineer a synthetic affinity reagent to the SH3 domain of Fyn.

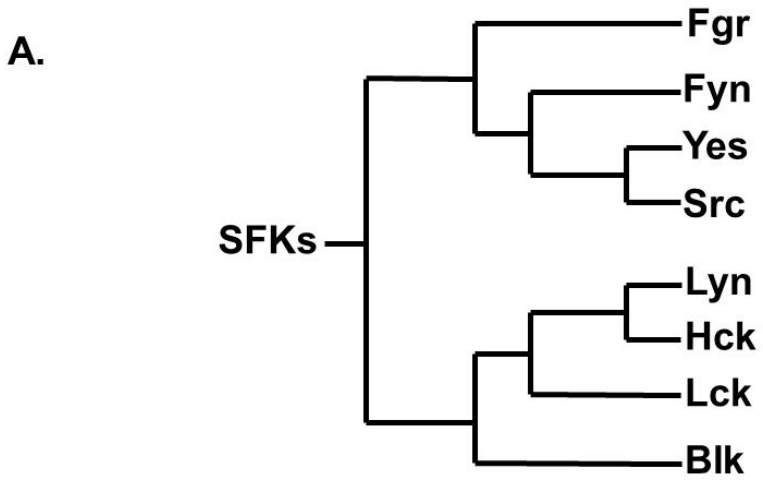

B.

```
                                                                %Match
Fyn SH3  -FVALYDYEARTEDDLSFHKGEKFQILNSSEGDWWEARSLTTGETGYIPSNYVAP  —
Fgr SH3  -FIALYDYEARTEDDLTFTKGEKFHILNNTEGDWWEARSLSSGKTGCIPSNYVAP  81
Yes SH3  -FVALYDYEARTTEDLSFKKGERFQIINNTEGDWWEARSIATGKNGYIPSNYVAP  79
Src SH3  -FVALYDYESRTETDLSFKKGERLQIVNNTEGDWWLAHSLSTGQTGYIPSNYVAP  77
Hck SH3  IVVALYDYEAIHHEDLSFQKGDQMVVLEES-GEWWKARSLATRKEGYIPSNYVAR  60
BLK SH3  FVVALYDYTAMNDRDLQMLKGEKLQVLKGT-GDWWLARSLVTGREGYVPSNFVAR  58
Lyn SH3  IVVALYPYDGIHPDDLSFKKGEKMKVL-EEHGEWWKAKSLLTKKEGFIPSNYVAK  54
Lck SH3  -VIALHSYEPSHDGDLGFEKGEQLRILEQS-GEWWKAQSLTTGQEGFIPFNFVAK  51
```

Figure 3.1. Cladogram of human Src family kinases (SFKs) and sequence alignment of their SH3 domains. A. A phylogenetic tree of human SFKs, which is based on the similarity of their catalytic domains, and adapted from another publication (*42*). **B.** The sequences of SH3 domains of SFKs were aligned to reveal their level of amino acid identity to the Fyn SH3 domain; conserved residues are highlighted in the gray columns, and gaps (dashes) are introduced to maximize alignment.

3.4.1 Isolation of FN3 monobodies to Fyn SH3 domain

The coding sequence of FN3 monobody was subcloned into a new phagemid vector (*37*), fusing it with the truncated gene III of M13 bacteriophage, which allows monovalent display of the monobody protein on the phage surface. Diversifying the 5 residues of each of the BC and FG loops of the FN3 scaffold (Figure 3.2A), by a modified form of Kunkel mutagenesis (*36, 44*), generated a library containing 1.3×10^{10} variants. The library was affinity selected for binders to the Fyn SH3 domain. The first screening yielded one binding FN3 monobody, D10, and when repeated, yielded two more, G9 and H4. A follow-up ELISA of all three clones confirmed binding to the Fyn SH3 domain (Figure 3. 2C). The sequencing revealed that all three clones were different, with four residues shared between clones G9 and D10 (Figure 3.2B). Interestingly, two of the clones, G9 and H4, contained no proline residues in either BC or FG loops, while the third clone, D10, had a single proline residue in the FG loop. The absence of proline is unexpected, as most cellular ligands for SH3 domains contain a proline-rich motif (i.e., PxxP, where x is any amino acid) (*22, 40, 45, 46*). However, the G9 clone contains an RxxK motif in its FG loop (RY-SK), which is found in a non-canonical SH3-binding ligand (*47*). Mutagenesis experiments and three-dimensional structural determinations will ultimately be necessary to learn the finer details of binding.

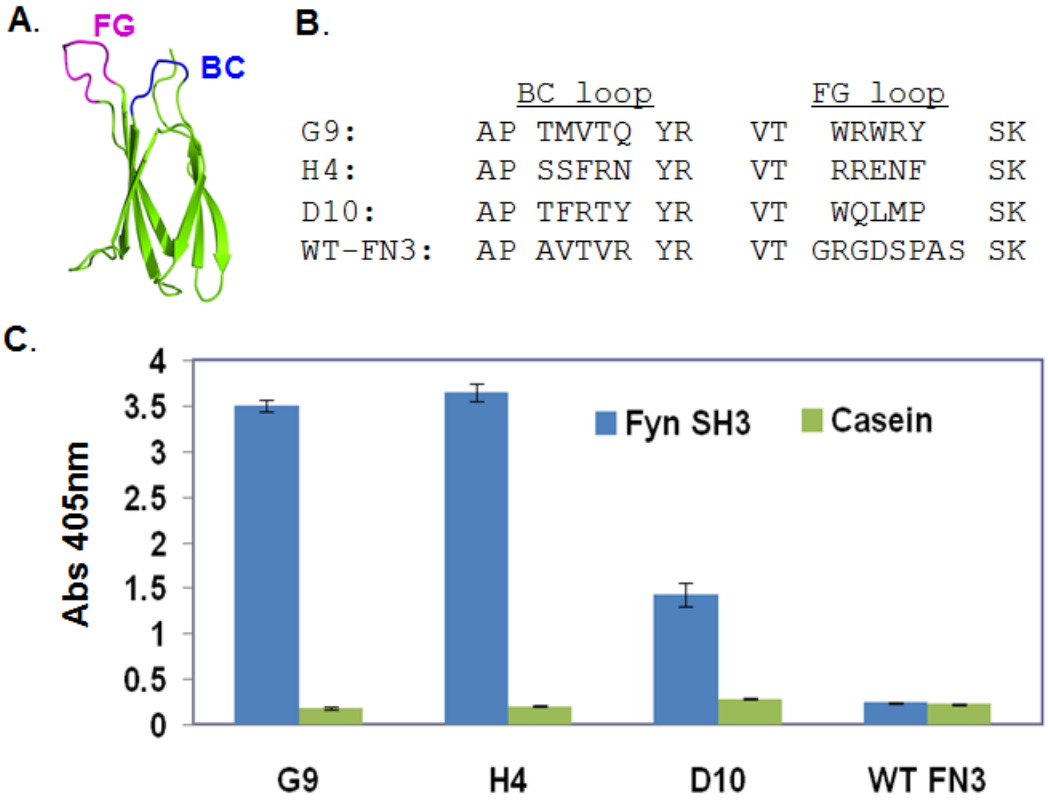

Figure 3.2. Characterization of three FN3 monobodies that bind to the Fyn SH3 domain. **A.** Cartoon of the FN3 scaffold with its randomized BC and FG loops labeled. The beta-sheet secondary structures of FN3 are shown as arrows in the figure, which was generated with the PyMol program (*48*), using published coordinates (PDB: 1TTG structure) (*49*). **B.** Sequences of the BC and FG loops of the three isolated monobodies and the wild-type domain. The length of the FG loop of wild-type (WT) FN3 was shortened from eight residues to five residues in the library design. **C.** Phage ELISA results of the three binders and the wild-type monobody (WT FN3) binding to the Fyn SH3 domain. Casein served as the negative control target.

3.4.2 Characterization of binding specificity

As the SH3 domains of SFKs are highly conserved in sequence, cross-reactivity is an important parameter to evaluate. To assess the binding specificity of the three monobodies, the SH3 domains of all eight SFKs were used in an ELISA experiment (Figure 3.3). Phage particles that displayed the G9 monobody bound exclusively to the Fyn SH3 domain with no cross-reactivity to the other seven SH3 domains, even though they share a common three-dimensional structure and are 51-81% identical in amino acid sequence to the Fyn SH3 domain. The same binding specificity was observed in the binding assays performed with purified protein of G9 monobody. The monobodies H4 and D10 bound principally to the Fyn SH3 domain, with some cross-reactivity to the Yes SH3 domain. The binding of the D10 clone was improved through mutagenesis and affinity selection, resulting in 25-fold tighter binding (measured by isothermal titration calorimetry, data not shown) to the Fyn SH3 domain and loss of binding to the Yes SH3 domain (data not shown).

As there are 297 SH3 domains encoded in the human genome (*50*), it would be desirable to profile the cross-reactivity of the isolated monobody to all of them. Toward that end, a protein array containing 150 human SH3 domains was probed with the G9 monobody. Among the 150 SH3 domains arrayed on the four membranes, G9 bound exclusively with the Fyn SH3 domain but not to the other 149 (Figure 3.4). This level of selectivity is remarkable given the relatively small size (i.e., 60 amino acids) and the highly conserved primary structure of SH3 domains. It should be noted that when G9 was fused to bacterial alkaline

phosphatase, it bound predominantly to the Fyn SH3 domain, but showed some binding to three other SH3 domains in the array (i.e. Yes, Src, Grap-2-D2; data not shown). I interpret the slightly broadened specificity of the fusion protein to be caused by avidity effect, due to dimerization of bacterial alkaline phosphatase (*51*).

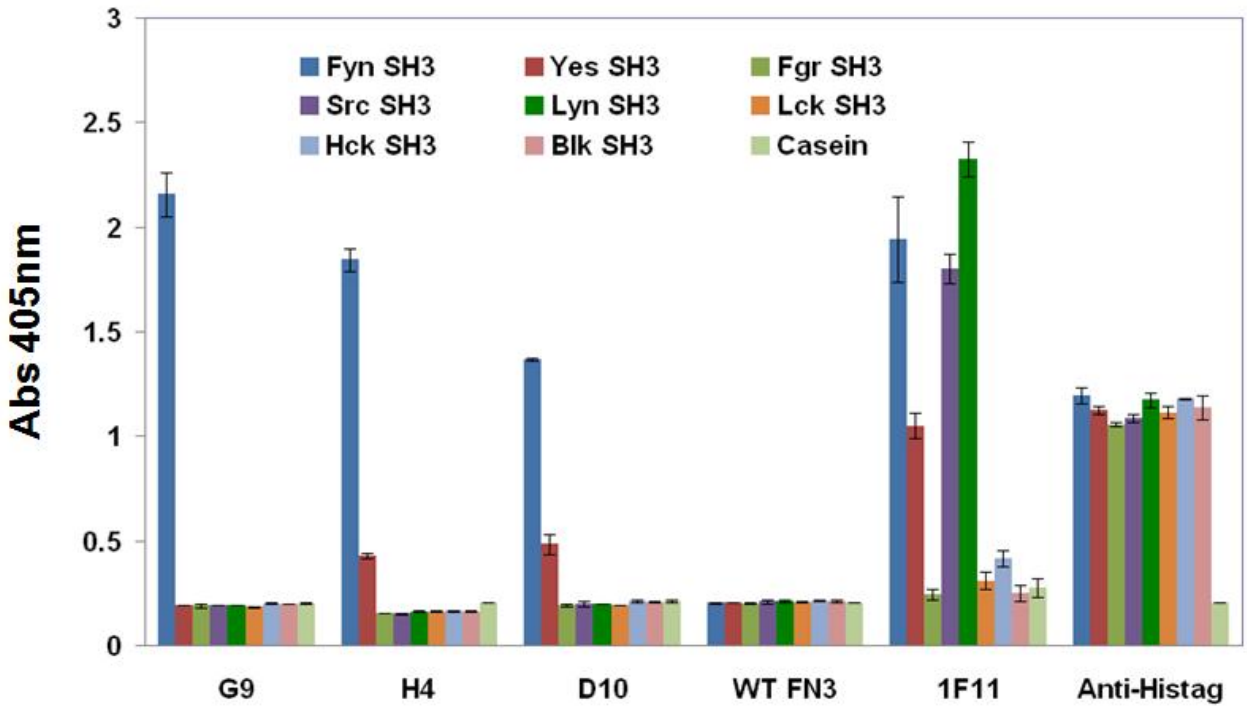

Figure 3.3. Phage ELISA of monobodies to the SH3 domains of all eight human SFKs. Microtiter plate wells were coated with equal amounts of target or casein (negative control), and probed with equivalent amounts of phage particles displaying the various binding monobodies. Phage particles displaying wild-type monobody (WT FN3) served as the non-binding negative control. 1F11 is a monobody that binds to several, but not all, SFKs SH3 domains. An anti-his_6 tag antibody, conjugated to horseradish peroxidase (HRP), was used to normalize the amount of SH3 domain protein immobilized in the microtiter plate wells. Error bars correspond to standard deviation of triplicate measurements.

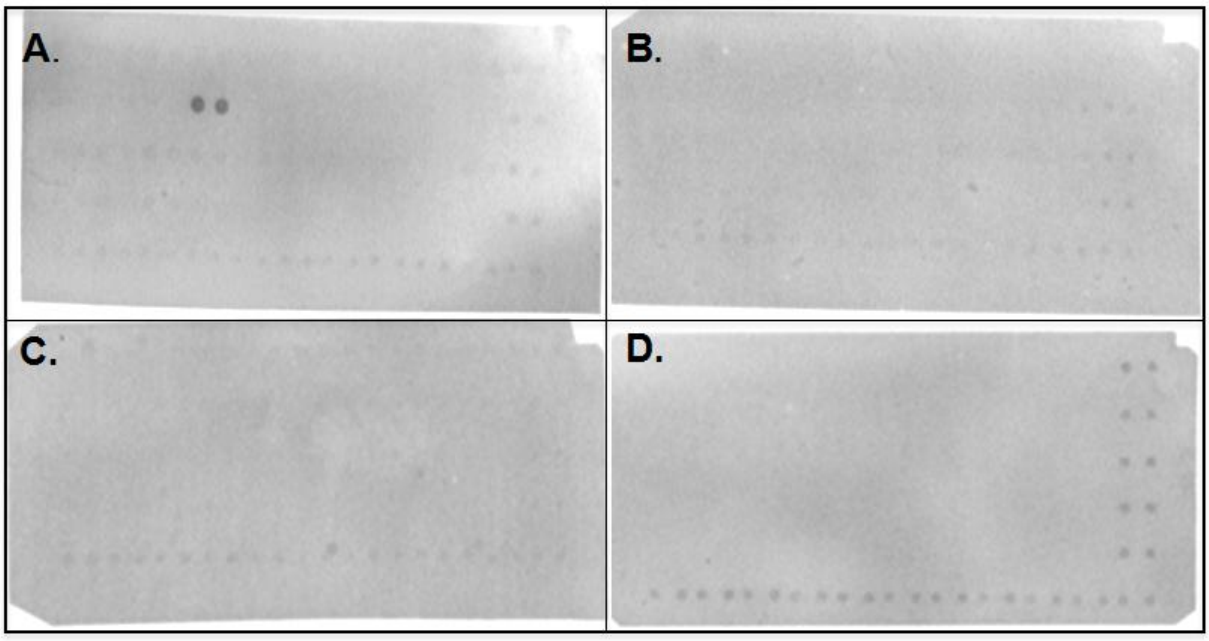

Figure 3.4. Probing of an SH3 domain array with the G9 monobody. Four membranes (purchased from Panomics) were incubated with a His_6-tagged SUMO fusion of the G9 monobody, washed, incubated with an anti-His_6-tag antibody conjugated to HRP, followed by detection with Enhanced Chemiluminescence-Plus (ECL-Plus). Panels A-D correspond to Panomics Arrays I-IV, respectively. Of the 150 SH3 domains tested, only the Fyn SH3 domain (duplicate, adjacent spots in panel A) bound to the G9 monobody. A His_6-tagged ligand has been spotted in duplicate along the right side and the bottom of each membrane; these positive control spots are intended for alignment.

3.4.3 Measurement of dissociation constant

To determine the binding strength of the monobodies to the Fyn SH3 domain, isothermal titration calorimetry (ITC) was performed, in which the amount of heat change upon binding was plotted as a titration curve for calculating the dissociation constant (K_D). Purified monobodies were injected into the sample cell loaded with the Fyn SH3 domain, and the K_D of G9 binding to the Fyn SH3 domain was determined to be 166 ± 6 nM (Figure 3.5). This binding affinity approximately 10-fold stronger than those of most peptide ligands (*40*). The clone D10 bound to the Fyn SH3 domain with a K_D = 8.2 ± 0.5 μM, making it less attractive than G9 as an affinity reagent. However, the dissociation constant of an affinity-matured derivative of D10 could be lowered 25-fold to 325 ± 21 nM (data not shown), demonstrating that enhanced binding can be obtained through second round of protein engineering. To verify the selectivity exhibited in the ELISA and the array probing experiment, ITC was carried out for G9 bindin to the SH3 domains of Fgr and Yes, the two closest relatives of Fyn. However, due to the small amount of heat released during the titrations, I could not determine dissociation constants of G9 binding to these two SH3 domains (data not shown).

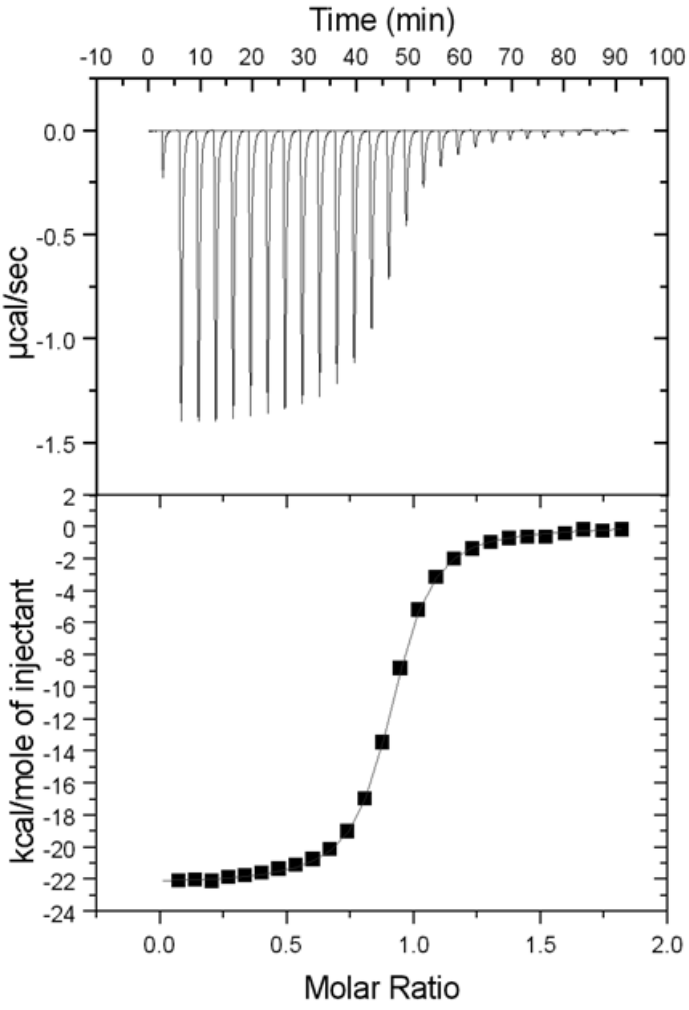

Figure 3.5. Isothermal titration calorimetry (ITC) measurements of the G9 monobody binding to the Fyn SH3 domain. The thermogram (top panel) and the plotted titration curve (bottom panel) were obtained with a Microcal VP-ITC. The observed N, qH, qS, and dissociation constants for this interaction are 0.89, -2.22x10^4 cal/mole, -43.37 Joule/ºK, and 160 nM, respectively.

3.4.4 Mapping the binding location on the SH3 domain

SH3 domains of SFKs contain a shallow groove that, upon kinase activation (*52-55*), binds to proline-rich peptides (*46, 56-58*). Thus, ligands that bind to this region of the SH3 domain can be potentially used as biosensors for SFKs activation. As the monobody G9 does not contain such a proline-rich motif, it is of interest to learn if it binds to the Fyn SH3 domain in the same location or not. To that aim, a class I proline-rich peptide, VSLARRPLPPLPGGK, which binds to the Fyn SH3 with a K_D of 0.6 µM (*40*), and a negative control peptide, VSAARAALAPLAGGK, were tested for their ability to compete with G9 for binding to the Fyn SH3 domain. In Figure 3.6A, it is shown that the Fyn SH3-binding peptide competed with G9 for binding to the SH3 domain in a dose-dependent manner, with an IC_{50} value of ~440 nM, while the negative control peptide did not compete at all.

To confirm the above finding, 1F11, a monobody with a sequence of GISQG (BC loop) and SRPLP (FG loop) (*16*), was also used in the competition experiment. The 1F11 monobody binds to several SH3 domains of SFKs, including Src and Fyn. The chemical shift of residues in Src SH3 upon binding to 1F11 has been mapped by NMR, which exhibited the same profile upon binding to a proline-rich peptide (*16*). In the competition assay, 1F11 competed with G9 for binding to the Fyn SH3 domain with an IC_{50} value of ~210 nM (Figure 3.6B). The wild-type FN3 (WT FN3) didn't compete with G9 for binding to the SH3 domain and served as the non-competitive control.

As some cellular proline-rich ligands bind to the SH3 domains to activate or inhibit the activities of SFKs (*59, 60*) , the above competition binding experiments suggest that G9 monobody may be a potential activator or inhibitor of Fyn kinase. A kinase assay with the presence of G9 monobody can determine if G9 interferes the kinase activity of Fyn. As G9 bears a sequence that is not present in known cellular ligands, its sequence information may be used for the search of potential interacting proteins in the cells. Furthermore, as PxxP-containing ligands inhibits Fyn kinase (*60*), G9 may even serve as a blueprint for designing drugs to inhibit Fyn kinase activities.

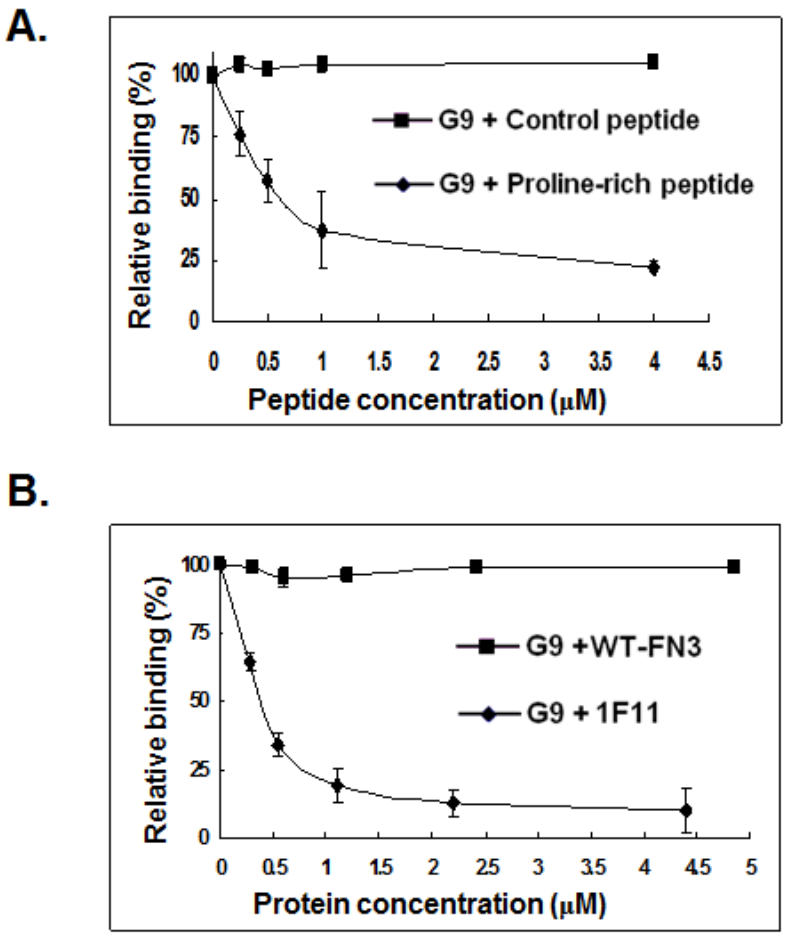

Figure 3.6. Mapping the binding location of the G9 monobody. **A.** Competition binding of the G9 monobody to the Fyn SH3 domain in the presence of a proline-rich peptide (VSLARRPLPPLPGGK) or a control peptide, a less proline-rich form of the same peptide (VSAARAALAPLAGGK). **B.** Competition binding of G9 monobody to the Fyn SH3 domain by the 1F11 monobody, which contains a proline-rich motif in its FG loop (*16*). Wild type monobody (WT-FN3) served as the non-competitive control.

3.4.5 Pull-down experiments with G9 monobody

To determine if the G9 monobody was able to bind to full-length, active Fyn kinase, the biotinylated G9 monobody was used in pull-down experiments. The G9 protein was incubated in solution with active Fyn protein, followed by capture of the protein complex with streptavidin-coated magnetic beads. Proteins that were released through heating the magnetic beads were resolved in an SDS-PAGE gel, and transferred to nitrocellulose membrane for western blotting with anti-Fyn antibody. Figure 3.7 demonstrates that the G9 monobody was able to pull down recombinant active Fyn kinase from solution, whereas the wild-type FN3 did not. Based on the above competition assays and pull-down experiments, I suggest that G9 can potentially serve as a biosensor for monitoring the activation of Fyn kinase inside cells.

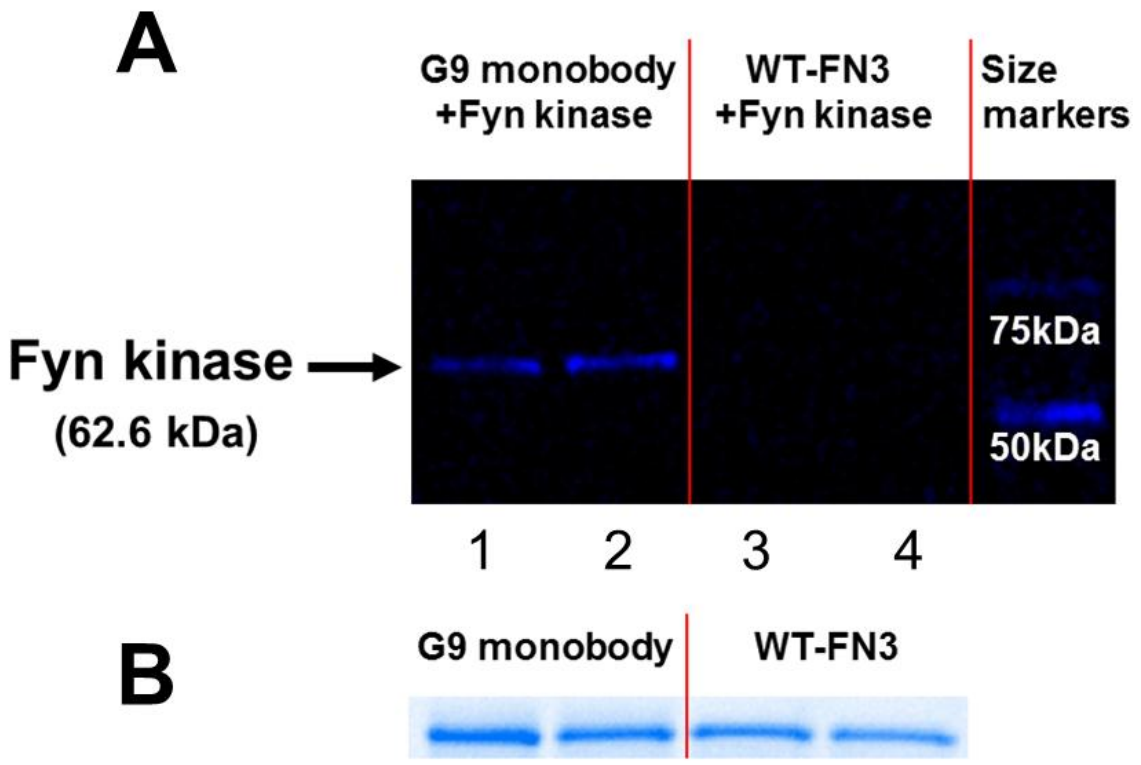

Figure 3.7. Pull-down experiment with active recombinant Fyn kinase purified from insect cells. A. Image of a western blot acquired with Li-Cor infrared imager. Lanes 1 and 2 are duplicates of pull-down experiments with G9 monobody; lanes 3 and 4 are duplicates of pull-down experiments with wild-type FN3 monobody (WT-FN3), which was the non-binding negative control. **B**. Image of the biotinylated monobodies boiled off the streptavidin beads and resolved on SDS-PAGE gel, acquired with Gel Doc EZ imager, Bio-Rad).

Recently with the advancement of phage display technology, highly selective reagents have been generated that distinguish closely related proteins. McCafferty and his colleagues (*61*) have isolated antibodies that can differentiate SH2 domains of Abl1 and Abl2, which share 89% identity. In addition, Koide and his coworkers (*62*) have identified a FN3 monobody that is capable of discriminating between the SH2 domains of Abl (1 and 2) and the other 82 SH2 domains, demonstrating an impressive level of selectivity. Here, I report the discovery of a FN3 monobody, which not only discriminated between Fyn SH3 domain and its closest relative, Fgr SH3 domain (81% sequence identity), but also exhibited exquisite selectivity to the SH3 domain of Fyn out of 150 SH3 domains in the human genome. In an unpublished work, I isolated monobodies that could differentiate between the SH3 domains of Abl1 and Abl2, which have 91% sequence identity. All of the above evidence suggests that FN3 monobody, even with a relatively small binding face due to its small molecular size (10 kDa), is a valuable scaffold for generating affinity reagents with high selectivity.

3.5 References

1. Gebauer, M., and Skerra, A. (2009) Engineered protein scaffolds as next-generation antibody therapeutics, *Curr Opin Chem Biol 13*, 245-255.

2. Nilsson, F. Y., and Tolmachev, V. (2007) Affibody molecules: new protein domains for molecular imaging and targeted tumor therapy, *Curr Opin Drug Discov Devel 10*, 167-175.

3. Silverman, J., Liu, Q., Bakker, A., To, W., Duguay, A., Alba, B. M., Smith, R., Rivas, A., Li, P., Le, H., Whitehorn, E., Moore, K. W., Swimmer, C., Perlroth, V., Vogt, M., Kolkman, J., and Stemmer, W. P. (2005) Multivalent avimer proteins evolved by exon shuffling of a family of human receptor domains, *Nat Biotechnol 23*, 1556-1561.

4. Kolmar, H. (2008) Alternative binding proteins: biological activity and therapeutic potential of cystine-knot miniproteins, *FEBS J 275*, 2684-2690.

5. Dai, M., Temirov, J., Pesavento, E., Kiss, C., Velappan, N., Pavlik, P., Werner, J. H., and Bradbury, A. R. (2008) Using T7 phage display to select GFP-based binders, *Protein Eng Des Sel 21*, 413-424.

6. Skerra, A. (2008) Alternative binding proteins: anticalins - harnessing the structural plasticity of the lipocalin ligand pocket to engineer novel binding activities, *FEBS J 275*, 2677-2683.

7. Muyldermans, S., Baral, T. N., Retamozzo, V. C., De Baetselier, P., De Genst, E., Kinne, J., Leonhardt, H., Magez, S., Nguyen, V. K., Revets, H., Rothbauer, U., Stijlemans, B., Tillib, S., Wernery, U., Wyns, L., Hassanzadeh-Ghassabeh, G., and Saerens, D. (2009) Camelid immunoglobulins and nanobody technology, *Vet Immunol Immunopathol 128*, 178-183.

8. Boersma, Y. L., and Pluckthun, A. (2011) DARPins and other repeat protein scaffolds: advances in engineering and applications, *Curr Opin Biotechnol 22*, 849-857.

9. Xiong, J. P., Stehle, T., Zhang, R., Joachimiak, A., Frech, M., Goodman, S. L., and Arnaout, M. A. (2002) Crystal structure of the extracellular

segment of integrin alpha Vbeta3 in complex with an Arg-Gly-Asp ligand, *Science 296*, 151-155.

10. Batori, V., Koide, A., and Koide, S. (2002) Exploring the potential of the monobody scaffold: effects of loop elongation on the stability of a fibronectin type III domain, *Protein Eng 15*, 1015-1020.

11. Koide, A., Abbatiello, S., Rothgery, L., and Koide, S. (2002) Probing protein conformational changes in living cells by using designer binding proteins: application to the estrogen receptor, *Proc Natl Acad Sci U S A 99*, 1253-1258.

12. Richards, J., Miller, M., Abend, J., Koide, A., Koide, S., and Dewhurst, S. (2003) Engineered fibronectin type III domain with a RGDWXE sequence binds with enhanced affinity and specificity to human alphavbeta3 integrin, *J Mol Biol 326*, 1475-1488.

13. Hackel, B. J., Kapila, A., and Wittrup, K. D. (2008) Picomolar affinity fibronectin domains engineered utilizing loop length diversity, recursive mutagenesis, and loop shuffling, *J Mol Biol 381*, 1238-1252.

14. Olson, C. A., Liao, H. I., Sun, R., and Roberts, R. W. (2008) mRNA display selection of a high-affinity, modification-specific phospho-IkappaBalpha-binding fibronectin, *ACS Chem Biol 3*, 480-485.

15. Gilbreth, R. N., Truong, K., Madu, I., Koide, A., Wojcik, J. B., Li, N. S., Piccirilli, J. A., Chen, Y., and Koide, S. (2011) Isoform-specific monobody inhibitors of small ubiquitin-related modifiers engineered using structure-guided library design, *Proc Natl Acad Sci U S A 108*, 7751-7756.

16. Karatan, E., Merguerian, M., Han, Z., Scholle, M. D., Koide, S., and Kay, B. K. (2004) Molecular recognition properties of FN3 monobodies that bind the Src SH3 domain, *Chem Biol 11*, 835-844.

17. Xu, L., Aha, P., Gu, K., Kuimelis, R. G., Kurz, M., Lam, T., Lim, A. C., Liu, H., Lohse, P. A., Sun, L., Weng, S., Wagner, R. W., and Lipovsek, D. (2002) Directed evolution of high-affinity antibody mimics using mRNA display, *Chem Biol 9*, 933-942.

18. Koide, A., Bailey, C. W., Huang, X., and Koide, S. (1998) The fibronectin type III domain as a scaffold for novel binding proteins, *J Mol Biol 284*, 1141-1151.

19. Parker, M. H., Chen, Y., Danehy, F., Dufu, K., Ekstrom, J., Getmanova, E., Gokemeijer, J., Xu, L., and Lipovsek, D. (2005) Antibody mimics based on human fibronectin type three domain engineered for thermostability and high-affinity binding to vascular endothelial growth factor receptor two, *Protein Eng Des Sel 18*, 435-444.

20. Huang, J., Koide, A., Makabe, K., and Koide, S. (2008) Design of protein function leaps by directed domain interface evolution, *Proc Natl Acad Sci U S A 105*, 6578-6583.

21. Huang, J., Makabe, K., Biancalana, M., Koide, A., and Koide, S. (2009) Structural basis for exquisite specificity of affinity clamps, synthetic binding proteins generated through directed domain-interface evolution, *J Mol Biol 392*, 1221-1231.

22. Mayer, B. J. (2001) SH3 domains: complexity in moderation, *J Cell Sci 114*, 1253-1263.

23. Li, S. S. (2005) Specificity and versatility of SH3 and other proline-recognition domains: structural basis and implications for cellular signal transduction, *Biochem J 390*, 641-653.

24. Buday, L., Wunderlich, L., and Tamas, P. (2002) The Nck family of adapter proteins: regulators of actin cytoskeleton, *Cell Signal 14*, 723-731.

25. McPherson, P. S. (1999) Regulatory role of SH3 domain-mediated protein-protein interactions in synaptic vesicle endocytosis, *Cell Signal 11*, 229-238.

26. Engen, J. R., Wales, T. E., Hochrein, J. M., Meyn, M. A., 3rd, Banu Ozkan, S., Bahar, I., and Smithgall, T. E. (2008) Structure and dynamic regulation of Src-family kinases, *Cell Mol Life Sci 65*, 3058-3073.

27. Salmond, R. J., Filby, A., Qureshi, I., Caserta, S., and Zamoyska, R. (2009) T-cell receptor proximal signaling via the Src-family kinases, Lck and Fyn,

influences T-cell activation, differentiation, and tolerance, *Immunol Rev 228*, 9-22.

28. Vatish, M., Yamada, E., Pessin, J. E., and Bastie, C. C. (2009) Fyn kinase function in lipid utilization: a new upstream regulator of AMPK activity?, *Arch Physiol Biochem 115*, 191-198.

29. Levi, M., and Shalgi, R. (2010) The role of Fyn kinase in the release from metaphase in mammalian oocytes, *Mol Cell Endocrinol 314*, 228-233.

30. Siraganian, R. P., de Castro, R. O., Barbu, E. A., and Zhang, J. (2010) Mast cell signaling: the role of protein tyrosine kinase Syk, its activation and screening methods for new pathway participants, *FEBS Lett 584*, 4933-4940.

31. Saito, Y. D., Jensen, A. R., Salgia, R., and Posadas, E. M. (2010) Fyn: a novel molecular target in cancer, *Cancer 116*, 1629-1637.

32. Schenone, S., Brullo, C., Musumeci, F., Biava, M., Falchi, F., and Botta, M. (2011) Fyn kinase in brain diseases and cancer: the search for inhibitors, *Curr Med Chem 18*, 2921-2942.

33. Gulyani, A., Vitriol, E., Allen, R., Wu, J., Gremyachinskiy, D., Lewis, S., Dewar, B., Graves, L. M., Kay, B. K., Kuhlman, B., Elston, T., and Hahn, K. M. (2011) A biosensor generated via high-throughput screening quantifies cell edge Src dynamics, *Nat Chem Biol 7*, 437-444.

34. Thomas, S. M., and Brugge, J. S. (1997) Cellular functions regulated by Src family kinases, *Annu Rev Cell Dev Biol 13*, 513-609.

35. Kunkel, T. A. (1985) Rapid and efficient site-specific mutagenesis without phenotypic selection, *Proc Natl Acad Sci U S A 82*, 488-492.

36. Weiss, G. A., Watanabe, C. K., Zhong, A., Goddard, A., and Sidhu, S. S. (2000) Rapid mapping of protein functional epitopes by combinatorial alanine scanning, *Proc Natl Acad Sci U S A 97*, 8950-8954.

37. Pershad, K., Sullivan, M. A., and Kay, B. K. (2011) Drop-out phagemid vector for switching from phage displayed affinity reagents to expression formats, *Anal Biochem 412*, 210-216.

38. Steiner, D., Forrer, P., Stumpp, M. T., and Pluckthun, A. (2006) Signal sequences directing cotranslational translocation expand the range of proteins amenable to phage display, *Nat Biotechnol 24*, 823-831.

39. Miroux, B., and Walker, J. E. (1996) Over-production of proteins in Escherichia coli: mutant hosts that allow synthesis of some membrane proteins and globular proteins at high levels, *J Mol Biol 260*, 289-298.

40. Rickles, R. J., Botfield, M. C., Zhou, X. M., Henry, P. A., Brugge, J. S., and Zoller, M. J. (1995) Phage display selection of ligand residues important for Src homology 3 domain binding specificity, *Proc Natl Acad Sci U S A 92*, 10909-10913.

41. Liu, B. A., Shah, E., Jablonowski, K., Stergachis, A., Engelmann, B., and Nash, P. D. (2011) The SH2 domain-containing proteins in 21 species establish the provenance and scope of phosphotyrosine signaling in eukaryotes, *Sci Signal 4*, ra83.

42. Manning, G., Whyte, D. B., Martinez, R., Hunter, T., and Sudarsanam, S. (2002) The protein kinase complement of the human genome, *Science 298*, 1912-1934.

43. Parsons, S. J., and Parsons, J. T. (2004) Src family kinases, key regulators of signal transduction, *Oncogene 23*, 7906-7909.

44. Tonikian, R., Zhang, Y., Boone, C., and Sidhu, S. S. (2007) Identifying specificity profiles for peptide recognition modules from phage-displayed peptide libraries, *Nat Protoc 2*, 1368-1386.

45. Sparks, A. B., Rider, J. E., and Kay, B. K. (1998) Mapping the specificity of SH3 domains with phage-displayed random-peptide libraries, *Methods Mol Biol 84*, 87-103.

46. Lim, W. A., and Richards, F. M. (1994) Critical residues in an SH3 domain from Sem-5 suggest a mechanism for proline-rich peptide recognition, *Nat Struct Biol 1*, 221-225.

47. Berry, D. M., Nash, P., Liu, S. K., Pawson, T., and McGlade, C. J. (2002) A high-affinity Arg-X-X-Lys SH3 binding motif confers specificity for the interaction between Gads and SLP-76 in T cell signaling, *Curr Biol 12*, 1336-1341.

48. DeLano, W. (2002) The PYMOL molecular graphics system.

49. Main, A. L., Harvey, T. S., Baron, M., Boyd, J., and Campbell, I. D. (1992) The three-dimensional structure of the tenth type III module of fibronectin: an insight into RGD-mediated interactions, *Cell 71*, 671-678.

50. Karkkainen, S., Hiipakka, M., Wang, J. H., Kleino, I., Vaha-Jaakkola, M., Renkema, G. H., Liss, M., Wagner, R., and Saksela, K. (2006) Identification of preferred protein interactions by phage-display of the human Src homology-3 proteome, *EMBO Rep 7*, 186-191.

51. Schlesinger, M. J., and Andersen, L. (1968) Multiple molecular forms of the alkaline phosphatase of Escherichia coli, *Ann N Y Acad Sci 151*, 159-170.

52. Sicheri, F., Moarefi, I., and Kuriyan, J. (1997) Crystal structure of the Src family tyrosine kinase Hck, *Nature 385*, 602-609.

53. Williams, J. C., Weijland, A., Gonfloni, S., Thompson, A., Courtneidge, S. A., Superti-Furga, G., and Wierenga, R. K. (1997) The 2.35 A crystal structure of the inactivated form of chicken Src: a dynamic molecule with multiple regulatory interactions, *J Mol Biol 274*, 757-775.

54. Xu, W., Harrison, S. C., and Eck, M. J. (1997) Three-dimensional structure of the tyrosine kinase c-Src, *Nature 385*, 595-602.

55. Yamaguchi, H., and Hendrickson, W. A. (1996) Structural basis for activation of human lymphocyte kinase Lck upon tyrosine phosphorylation, *Nature 384*, 484-489.

56. Lim, W. A., Richards, F. M., and Fox, R. O. (1994) Structural determinants of peptide-binding orientation and of sequence specificity in SH3 domains, *Nature 372*, 375-379.

57. Yu, H., Chen, J. K., Feng, S., Dalgarno, D. C., Brauer, A. W., and Schreiber, S. L. (1994) Structural basis for the binding of proline-rich peptides to SH3 domains, *Cell 76*, 933-945.

58. Musacchio, A., Saraste, M., and Wilmanns, M. (1994) High-resolution crystal structures of tyrosine kinase SH3 domains complexed with proline-rich peptides, *Nat Struct Biol 1*, 546-551.

59. Trible, R. P., Emert-Sedlak, L., and Smithgall, T. E. (2006) HIV-1 Nef selectively activates Src family kinases Hck, Lyn, and c-Src through direct SH3 domain interaction, *J Biol Chem 281*, 27029-27038.

60. Briggs, S. D., Lerner, E. C., and Smithgall, T. E. (2000) Affinity of Src family kinase SH3 domains for HIV Nef in vitro does not predict kinase activation by Nef in vivo, *Biochemistry 39*, 489-495.

61. Pershad, K., Pavlovic, J. D., Graslund, S., Nilsson, P., Colwill, K., Karatt-Vellatt, A., Schofield, D. J., Dyson, M. R., Pawson, T., Kay, B. K., and McCafferty, J. (2010) Generating a panel of highly specific antibodies to 20 human SH2 domains by phage display, *Protein Eng Des Sel 23*, 279-288.

62. Wojcik, J., Hantschel, O., Grebien, F., Kaupe, I., Bennett, K. L., Barkinge, J., Jones, R. B., Koide, A., Superti-Furga, G., and Koide, S. (2010) A potent and highly specific FN3 monobody inhibitor of the Abl SH2 domain, *Nat Struct Mol Biol 17*, 519-527.

CHAPTER 4

DIRECTED EVOLUTION OF HIGHLY SELECTIVE FN3 MONOBODIES THAT BIND TO THE SH3 DOMAIN OF THE LYN PROTEIN TYROSINE KINASE

4.1 Abstract

Affinity reagents of high affinity and specificity are of great use in studying cellular proteins. To generate specific affinity reagents for monitoring the activation of Lyn tyrosine kinase, a phage library of FN3 monobodies was affinity selected with the SH3 domain of Lyn and three binders were isolated. Two of the isolates, TA1 and TA8, selectively bound to the Lyn SH3 domain out of 150 SH3 domains examined. An isothermal titration calorimetry experiment was performed to determine the dissociation constants (K_D) of TA1 and TA8 to be 3 μM and 5 μM, respectively. To improve the binding affinity of TA8, a secondary library containing 1.1×10^9 variants was created and screened, leading to the discovery of three variants that bound more than 8-fold tighter to the Lyn SH3 domain. One of the variants bound selectively to the SH3 domain of Lyn out of the nine SH3 domains tested, as revealed by phage ELISA. A competition-binding assay showed that both TA1 and TA8 competed with a proline-rich peptide, Tip, for binding to the Lyn SH3 domain. As a proof-of-concept experiment, one monobody was converted into a biosensor that increased fluorescence upon binding to the Lyn SH3 domain in solution.

4.2 Introduction

As the number of protein targets for biological research increases rapidly due to the decoding of genomes (*1*), there is a growing demand for antibodies or affinity reagents for studying such newly discovered genes. In some cases when many targets share conserved primary and tertiary structures, it is challenging to isolate affinity reagents that selectively target only one of them. One group of reagents that permits exquisite discrimination between antigens is recombinant affinity reagents. For example, antibody fragments have been generated through phage display that can distinguish lysozymes that differ by four amino acid residues (*2*) or 20 closely related human SH2 domains (*3*).

Unlike hybridoma technology, phage display also permits directed evolution of existing affinity reagents, increasing their affinity or changing their specificity. Through phage display, the affinity of existing antibody fragments has been increased by 420-fold (*4*) and 1230-fold (*5*), and the specificity of antibody fragments has also been correspondingly narrowed (*6, 7*) or broadened (*8, 9*). There are several methods to construct secondary libraries for directed evolution of existing affinity reagents. One method is to perform a mutagenic polymerase chain reaction (PCR) to introduce random mutations in the gene of the existing clone and create a secondary library (*10*). Another method is to use oligonucleotide to randomize certain residues at the binding interface of the existing binder and create a secondary library (*11, 12*). A third approach is to create a new mutagenic library by shuffling mutagenized loops between clones recovered through affinity selection (*11, 13*).

Besides antibody fragments, phage display has been also very successful in adapting alternative scaffolds into affinity reagents with high affinity and specificity. These scaffolds *include* affibodies (*14*), avimers (*15*), lipocalin (*16*), designed ankyrin repeat proteins (*17*), SH3 domains (*18*), SH2 domains (*19*), and FN3 monobody (*20*), which is used in this study. The FN3 scaffold, 94 amino acids in size, contains seven beta-strands, which folds into a structure that resembles the variable domain of the immunoglobulin heavy chain, leading to the name ómonobodyô(*20*). Other *in vitro* display methods, such as mRNA display (*21, 22*), and yeast display (*11, 23*), have been used with phage display to engineer FN3 scaffold for binding to a wide variety of targets, such as ubiquitin (*20*), maltose binding protein (*24*), estrogen receptor (*25*), lysozyme (*11*), streptavidin (*26*), hSUMO (*27*), Phosphor-IəBŬ peptide (*22*) and Abl SH2 domain (*28*).

In our previous studies, we have engineered FN3 monobodies for binding to SH3 domains of Fyn (*7*) and Src (*26*). The SH3 domain, a protein domain of 60 amino acid residues, has 300 relatives in the human proteome (*29*). They interact with proline-rich (PxxP; x is any reside) ligands in cells and are involved in a variety of cellular processes, such as signal transduction (*30*), cytoskeleton assembly (*31*), and endocytosis (*32*). In SFKs, the SH3 domain engages in an intramolecular interaction with a proline-rich linker to hold the SFKs in an inactive configuration (*33, 34*). Upon activation of SFKs, this intramolecular interaction of SH3 is disrupted, exposing the binding interface on the SH3 domain to the cytoplasm (*35*). One of our FN3 monobodies, which binds to the Src SH3 domain,

has been converted into a biosensor for Src activation in living cells (*36*). As the SFKs members may share a similar mechanism for activation (*35, 37*), we wanted to extend our effort to another member of the family, Lyn tyrosine kinase. Lyn kinase is mainly expressed in hematopoietic cells (*38*) and plays an important role in regulating the activation of mast (*39*) and B cells (*40*), apoptosis (*41*), and wound response (*42*). Elevated expression and activity of Lyn are also associated with several types of cancers (*43-45*) and autoimmune diseases (*46*).

In this study, I generate affinity reagents to the Lyn SH3 domain, which can be potentially developed into biosensors of Lyn activation. Affinity selections of a phage library identified two FN3 monobodies, TA1 and TA8, which bind selectively to the Lyn SH3 domain out of 150 SH3 domains examined. Their affinities were measured to be 3 μM and 5 μM, respectively. Affinity selection of a secondary library of TA8 isolated variants than bound eightfold tighter than the starting clone, while keeping its specificity to the Lyn SH3 domain. A prototype sensor was developed and documented to increase in fluorescence upon binding to the Lyn SH3 domain in solution.

4.3 Materials & methods

4.3.1 *Escherichia coli* strains, plasmids and phagemids

E. coli strains BL21-DE3 (Novagen, Rockland, MA) and C41-DE3 (Dr. Arnon Lavie, Univ. of IL at Chicago) were used to overexpress proteins in bacteria. TG1 (Lucigen; Madison, WI) was used for construction of phage-display libraries. CJ236 bacterial cells (New England BioLabs; Ipswich, MA), which lack functional dUTPase and uracil-N glycosylase, were used for generating uracilated single-stranded DNA template to perform Kunkel mutagenesis (*7, 47*). Plasmids derived from pGEX-2T, pKP300 without gene III (*48*), and pET14b were used for overexpressing proteins fused to the glutathione-S-transferase (GST), alkaline phosphatase, and small ubiquitin-like modifier (SUMO), respectively. A Flag epitope (DYKDDDDK) was fused to the N-terminal of FN3 gene in the pKP300 phagemid, thereby permitting convenient detection of the displayed FN3 domain with an anti-Flag antibody (Sigma-Aldrich; St. Louis, MO). Phagemid pHEN4 (*26, 49*) was used for construction of a primary phage-display library. Full-length pKP300 (with gene III) (*7, 50*) was used for constructing a secondary mutagenic phage-display library.

4.3.2 Construction of the FN3 coding region and the primary phage library

The construction of the FN3 gene and the primary phage library was detailed in a previous study (*26*). Briefly, the open-reading frame of the FN3 gene was assembled from 6 oligonucleotides using a modified protocol, described by Koide et al. (*20*) and subcloned into a phagemid vector pHEN4 (*49*) to generate the

recombinant plasmid pHEN4:FN3. To construct the phage library, overlap PCR was performed with oligonucleotides containing NNK degenerate codons to diversify five residues each within the BC and the FG loops of the FN3 scaffold (Figure 4.2A). (N is an equimolar distribution of A, G, C, or T, whereas K is G or T. NNK allows incorporation of all 20 amino acids, plus the TAG amber codon.) In this manner, a phage library containing $2x10^9$ variants of FN3 was constructed.

4.3.3 Gene synthesis, plasmid preparation, protein overexpression, and purification

The pGEX-2T-derived plasmids for overexpressing GST-SH3 domains of Lyn, Abl, Src and Fyn were constructed by previous co-workers in the Kay Lab (*51*). The construction of pET14b-derived plasmids, which expressed SUMO fusion proteins of FN3 monobodies and 8 SFKs SH3 domains, were described in a previous study (*7*). Briefly, the coding sequences of FN3 monobodies and the Lyn SH3 domain were amplified by PCR, and subcloned into a modified form of the pET-14b expression vector, which carries a His_6-tag that is fused in frame to the N-terminus of SUMO. The coding sequences of the other seven human SH3 domains of the SFKs were synthesized commercially (GenScript, Piscataway, NJ) and subcloned into the same vector. To generate a construct expressing an alkaline phosphatase fusion protein of a particular monobody, Kunkel mutagenesis was performed (*52*) with oligonucleotides (IDT DNA; Coralville, Iowa) that mutated the BC and FG loops of FN3 gene encoded in the pKP300 plasmid (*7, 48*). The resultant plasmid was used to transform into BL21-DE3

E.coli cells for overexpression of the fusion protein.

The procedures for overexpressing SUMO and GST fusion proteins of SH3 domains were described in a previous study (*7*). For expressing alkaline phosphatase fusion to FN3 monobodies, BL21-DE3 bacterial cells (Novagen) containing the expression constructs were used to inoculate 300 mL low phosphate medium (*48*) with 50 ε g/mL carbenicillin, and incubated at 30 °C at 270 rpm for 24 h. The next day, bacterial cells were pelleted and resuspended in PBS supplemented with ethylenediaminetetraacetic acid (EDTA)-free protease inhibitor (Roche). After 10 min of sonication (Thermo Fisher Scientific), the cell lysate was clarified by centrifugation and incubated with nickel-nitriloacetic acid (Ni-NTA) resin (Qiagen) for purification by immobilized metal affinity chromatography (IMAC). SUMO fusions to SH3 domains were purified following the same protocol. For purification of the GST-SH3 proteins, clarified bacterial cell lysates were incubated with GST-bind resin (GE Healthcare, Piscataway, NJ), to capture the fusion protein.

4.3.4 Affinity selection

Three rounds of affinity selection were performed to select monobodies binding to the Lyn SH3 domain. The target was the GST-Lyn SH3 domain, which was chemically biotinylated with the EZ-link NHS biotinylation kit (Thermo Fisher Scientific). (All the affinity selection steps were performed at room temperature.) First, ~$2x10^{12}$ phage particles, displaying FN3 variants, were depleted by

incubating with 100 µL of streptavidin-coated magnetic beads (Promega; Madison, WI) for 30 min, followed by 1 h blocking with 4% dry milk, dissolved in phosphate buffered saline (PBS; 137 mM NaCl, 3 mM KCl, 8 mM Na_2HPO_4, 1.5 mM KH_2PO_4). During the incubation step, 40 µg (1.2 nmol) of biotinylated GST-Lyn SH3 protein was mixed with 100 µL of streptavidin-coated magnetic beads (Promega) for 45 min, followed by 1 h blocking in 4% dry milk dissolved in PBS. Next, the magnetic beads with the bound GST-Lyn SH3 protein were mixed with the depleted phage particles for 90 min, followed by three washes with PBS-0.1% Tween 20 (PBST) and three washes with PBS. Bound phage particles were eluted with 100 µL of 50 mM glycine (pH 2.0) for 10 min, followed by neutralization with 20 µL of 1 M Tris-HCl (pH 8) and infection of TG1 cells (OD_{600nm}=0.4-0.6) for 30 min at 37 °C. Infected cells were used to inoculate 2×YT + 50 ε g/mL carbenicillin and 1% glucose for overnight incubation at 37 °C at 250 rpm. The next day, 50 µL cells from an overnight culture were used to inoculate 5 mL of 2×YT + 50 ε g/mL carbenicillin and grown at 37ºC at 250 rpm for 2 h. When the culture reached an OD_{600nm} =0.4-0.6, the cells were infected with M13-K07 helper phage (MOI = 10) for 40 min, spun down and resuspended in fresh 5 mL of 2×YT + 50 ε g/mL carbenicillin, 100 ε g/mL kanamycin and 200 µM IPTG, overnight incubation at 30ºC. The next day, 800 µL of phage particles was harvested from the culture supernatant and used for the next round of affinity selection. The second and third rounds of affinity selection were conducted in the same manner, except that the no depletion step was included and the amount of target was reduced to 20 µg (0.6 nmol) for second round and 10 µg (0.3 nmol) for

the third round of selection. After the third round of affinity selection, bacterial single colonies were picked for phage amplification, followed by phage enzyme-linked immunosorbent assay (ELISA) to identify binders to the Lyn SH3 domain. Subsequently, positive binding clones were sequenced.

4.3.5 Phage ELISA and mapping of binding location by ELBA

Phage ELISA assays were performed as described in previous studies (*7, 26*). Briefly, NeutrAvidin® (Thermo Fisher Scientific) was immobilized on Nunc microtiter plate (Thermo Fisher Scientific), by aliquoting 5 εg/mL solutions (in PBS) into triplicate wells, and incubating the plates overnight at 4ºC. The next day, the microtiter plate wells were washed once with PBS, followed by addition of biotinylated SH3 domain for 15-min incubation with shaking. Later, non-specific binding sites in the wells were blocked with excess casein (Thermo Fisher Scientific) for 1 h. After washing the wells with PBS+0.1%Tween, culture supernatants, which contained phage particles, were added to wells for 1 h incubation, followed by washing of the wells and incubation with an anti-phage antibody that is conjugated to horseradish peroxidase (GE Healthcare). After 1 h incubation, the wells were washed, and the chromogenic substrate, 2, 2'-Azino-bis (3-Ethylbenzothiazoline-6-Sulfonic Acid (ABTS), in the presence of hydrogen peroxide, was added and the resulting absorbance was determined at 405 nm with a microtiter plate spectrophotometer (BMG Labtech, Cary, NC).

To determine if the isolated monobodies bind to the Lyn SH3 domain at the

same site used for binding to a proline-rich peptide (*53*), a competition enzyme-linked binding assay (ELBA) was devised. First, the GST-Lyn SH3 protein was immobilized on the surface of Nunc plate wells. Then, a synthesized proline-rich peptide (GMPTPPLPPRPANLGERQA), part of the tyrosine kinase Interacting protein (TIP) of herpesvirus saimiri that interacts with the Lyn SH3 domain (*53*), was added over a range of concentrations (0.1 ε M to 50 ε M), along with the FN3-alkaline phosphatase to the wells. After 1 h of incubation, the wells were washed with PBST, and FN3-alkaline phosphatase retained in the wells was detected by adding a chromogenic substrate, para-nitrophenyl phosphate (pNPP; Sigma-Aldrich, St. Louis, MO). The resulting absorbance was determined at 405 nm with a microtiter plate spectrophotometer (BMG Labtech). In the experiment, negative controls consisted of a second peptide (GMPTAPLAPRPANLGERQA), in which two proline residues were substituted with alanine, and a third non-related peptide (DYKDDDDKLTVYHSKVNLP) of the same length.

4.3.6 Probing an SH3-domain array

Four Polyvinylidene fluoride (PVDF) membranes, spotted with a total of 150 human SH3 domains, were purchased from Panomics (Freemont, CA). The membranes were probed according to the manufacturerôs instructions. Briefly, the four membranes were soaked in the wash buffer, provided by the manufacturer, for 1 h until the membrane was completely wet. The soaked membranes were blocked for 2 h, prior to the addition of the purified fusion

protein of FN3-alkaline phosphatase at a final concentration of 1 nM. After overnight incubation at 4 °C, the membranes were washed 10 times with PBST and then incubated with a substrate for enhanced chemifluorescence (ECF; GE Healthcare). The four membranes were scanned simultaneously with a blue fluorescence filter on the Storm 860 PhosphorImager (GE Healthcare). The probing experiments were repeated two times for each monobody.

4.3.7 Mutagenesis analysis of monobodies by alanine scanning

Kunkel mutagenesis (*47, 52*) was performed to replace ten residues, one at a time with alanine (When alanine is present, glycine is used instead), of the BC and FG loops of monobodies. This mutagenesis is also called alanine scanning mutagenesis (*54*) and is often used to determine the contribution of each amino acid residue in a binding interface. For each monobody, ten alanine mutants were created based on the pKP300 phagemid that expressed the fusion protein of FN3+alkaline phosphatase. The original clones, together with the ten mutants, were overexpressed and purified side by side with one another to minimize variances associated with preparation of the protein samples. Purified protein samples were resolved by SDS-polyacrylamide gel electrophoresis (SDS-PAGE) and their concentrations were determined by the Bradford assay (*55*) (Thermo-Fisher Scientific Co.). The ELBA experiment was performed as described above. An anti-Flag antibody (Sigma-Aldrich) was used to normalize the amount of FN3-alkaline phosphatase fusion protein present in the wells.

4.3.8 Isothermal titration calorimetry

His_6-tagged SUMO-FN3 monobody fusions and His_6-tagged SUMO-SH3 domain fusions were purified to homogeneity of >95% and dialyzed in a beaker against 25 mM Tris-HCl (pH 7.5), 150 mM NaCl, and 100 mM imidazole. After overnight dialysis, their concentrations were measured with a NanoDrop ND-1000 spectrophotometer. Degassed samples were added to the loading cell (200 µL) and syringe (40 µL) of an ITC200 instrument (GE Healthcare). FN3 monobodies were loaded into the syringe at 500 µM and SH3 domains were loaded into the cell at 50 µM. The reference well was loaded with water. FN3 monobodies were injected into the cell with a volume of 2 µL per injection at 25ºC, with a reference power of 10 µcal/s. The heat change of each injection was recorded, and analyzed with Origin software (GE Healthcare).

4.3.9 Affinity maturation of TA8 monobody

Kunkel mutagenesis was performed (as described in Chapter 2) to diversify three residues in each of the BC and FG loops of the TA8 monobody with all 20 amino acids using NNK codons in the oligonucleotides. A secondary library, containing 1.1×10^9 recombinants was generated as described in Chapter 2, and subjected to affinity selection.

Phage particles displaying monobody variants were amplified and resuspended in Tris-buffered saline (TBS; 50 mM Trisï HCl, 150 mM NaCl, pH

7.5) containing 0.5% Tween (volume/volume) and 0.5% bovine serum albumin (BSA; mass/volume). The suspension of phage particles was then mixed with the target, the biotinylated GST-SH3 domain of Lyn (300 nM, final concentration), the non-biotinylated GST-SH3 domain of Hck (600 nM, final concentration) and SUMO-SH3 domain of Bruton's tyrosine kinase (Btk) (600 nM, final concentration). After 1 h incubation, streptavidin-coated magnetic beads (Promega) were added to the solution. Beads were collected with a magnet after 15 min tumbling, followed by seven washes with PBS-0.5% Tween, seven washes with PBS-0.1% Tween (containing 300 nM SUMO-Lyn SH3, 10 µM SUMO-Btk SH3 and 2.4 µM of GST-Hck SH3), and three washes with PBS. Bound phage particles were eluted with 50 mM glycine buffer (pH 2) for 10 min. The elution solution was neutralized with Trisï HCl (pH 10) and used to infect mid-log phase TG1 cells for 30 min at 37 °C, with 100 rpm shaking. Infected cells were spun down and spread on 2×YT agar plates with carbenicillin (50 µg/mL), and incubated overnight at 30°C. The next day, bacterial colonies were scraped from the surface of the plate and transferred into flasks for amplifying viral particles, which were used for the second round of affinity selection. The second round of selection was carried out in the same manner, except the concentration of the Lyn SH3 domain was reduced to 3 nM.

4.4 Results and discussion

4.4.1 Src family kinases and the sequence alignment of their SH3 domains

Src family kinases (SFKs), a group of protein tyrosine kinases, are active participants of many cellular pathways and are implicated in wide variety of diseases, especially cancers (*56*). SFKs are highly similar in overall structure and contain an N-terminal unique domain, followed by a SH3 domain, SH2 domain, proline-rich linker, kinase domain and a C-terminal tail containing a conserved tyrosine residue. Based on the sequence identity of the kinase domain (*57*), SFKs can be divided into two groups (Figure 4.1A): the SrcA group (Fgr, Fyn, Src, and Yes) and the SrcB group (Blk, Hck, Lck, and Lyn). The SH3 domain, like the kinase domain, is highly conserved among SFKs. Sequence alignment shows that the Lyn SH3 domain is 50% to 72% identical with the SH3 domains of other SFKs (Figure 4.1B).

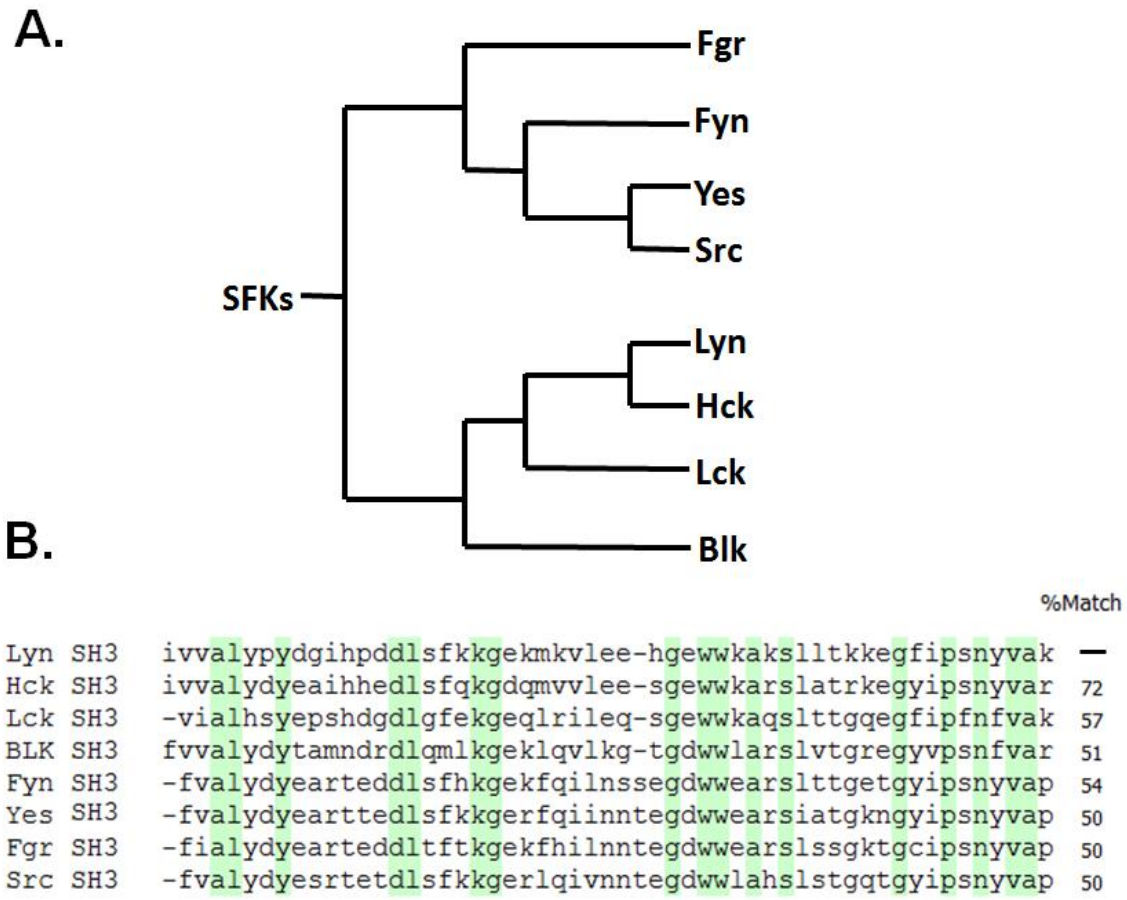

Figure 4.1. Cladogram of human Src family kinases (SFKs) and sequence alignment of their SH3 domains. A. A phylogenetic tree of human SFKs, which was constructed based on the similarity of their catalytic domains, and adapted from another publication (*57*). **B.** The sequences of SH3 domains of SFKs were aligned to reveal their amino acid identity to the Lyn SH3 domain; conserved residues are highlighted in green columns. Dashes have been introduced to maximize alignment of the primary structures.

4.4.2 Isolation of FN3 monobodies that bind to Lyn SH3 domain

A phage library containing 2×10^9 FN3 variants was previously created (*26*) by diversifying five residues in each BC and FG loops of the FN3 scaffold (Figure 4.2A) by overlap PCR. The phage library was selected for three rounds, which led to the discovery of five monobodies of unique sequence that bound the Lyn SH3 domain. Two of the monobodies contained PxxP motifs and cross-reacted with multiple SH3 domains (data not shown). Two other monobodies, TA1 and TA8, contained proline residues in their FG loops, but lacked the canonical PxxP motif that present in ligands for most SH3 domains (Figure 4.2B). Both TA1 and TA8 selectively bound to the Lyn SH3 domain among the four SH3 domains examined (Figure 4.2C). The fifth monobody, TA7, did not contain proline in the BC or FG loops (Figure 4.2B), and while it exhibited good specificity in the initial phage ELISA (Figure 4.2C), it was found to cross react with Hck, the closest relative of Lyn, and, therefore, was not evaluated further. In contrast, neither TA1 nor TA8 bound the Hck SH3 domain.

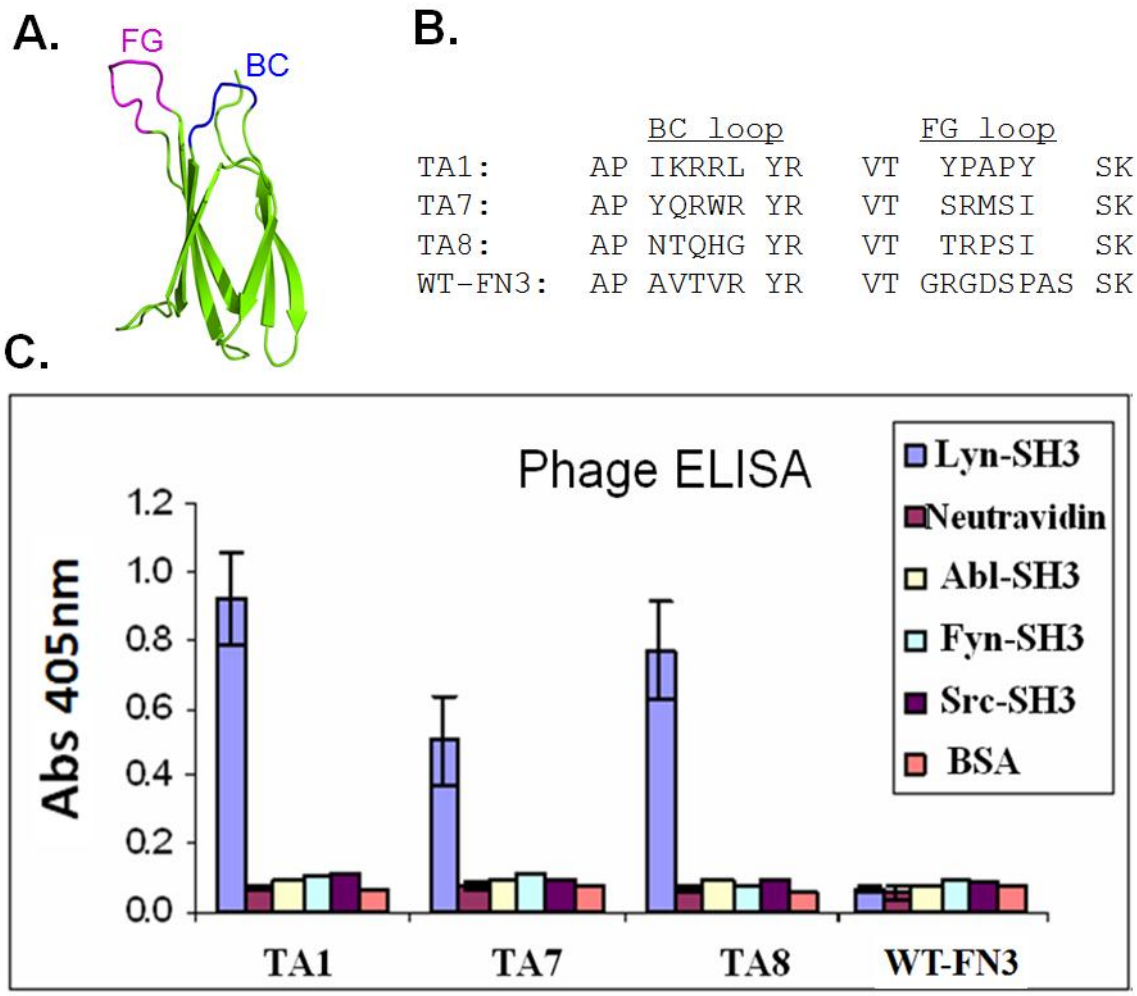

Figure 4.2. Characterization of three FN3 monobodies that bound to the Lyn SH3 domain. A. A cartoon of the FN3 scaffold with its diversified BC and FG loops labeled. The beta-sheet secondary structures of FN3 are shown as arrows in the figure, which was generated with the PyMol program (*58*), using published coordinates (PDB: 1TTG structure) (*59*). **B.** Sequences of the BC and FG loops of the three isolated monobodies and the wild-type domain. The length of the FG loop of wild-type (WT) FN3 was shortened from eight residues to five residues in the library design. **C.** Phage ELISA of the three binders, TA1, TA7 and TA8, and the wild-type monobody (WT FN3) for testing their binding to four different SH3 domains. Both BSA and NeutrAvidin served as negative controls in the assay.

4.4.3 Characterization of TA1 and TA8 monobodies

While phage ELISA experiments indicated that both TA1 and TA8 bound selectively to Lyn SH3 domain among the five SH3 domains examined, there are more than 300 SH3 domains encoded by the human genome (*29*). Thus, it is desirable to test the two monobodies against a much larger number of SH3 domains. To that purpose, alkaline phosphatase fusion proteins of TA1 and TA8 were used to probe a commercially prepared array of 150 human SH3 domains. Out of the 150 SH3 domains, both TA1 and TA8 bound principally to Lyn SH3 domain, with minimal cross-reactivity to SH3 domains of Hck, Btk and Y124 (TA1) (Figure 4.3). It is interesting to note that in phage ELISA, both TA1 and TA8 did not bind to the Hck SH3 domain, whereas there was some cross-reactivity to the Hck SH3 domain in the array probing experiment. I suspect that this may be due to avidity, as bacterial alkaline phosphatase is a homodimer (*60*). The binding of TA1 and TA8 is particularly interesting, as they lack the conventional proline-rich motif present in most SH3 domain ligands. Understanding the molecular recognition properties of these two monobodies will likely require solving the three-dimensional structure of the monobody complexed with the Lyn SH3 domain by X-ray diffraction.

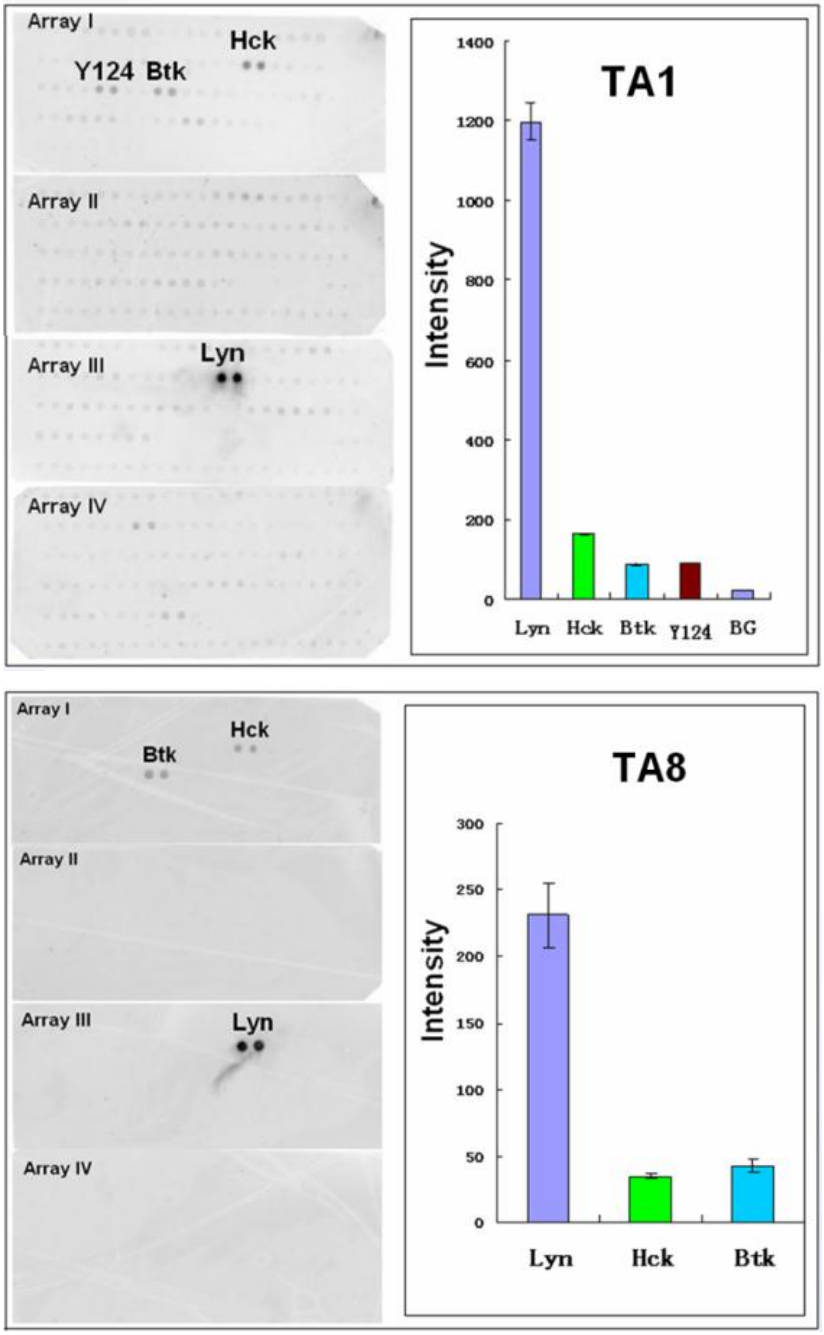

Figure 4.3. Probing an array of 150 human SH3 domains by TA1 and TA8 monobodies. TA1 and TA8 were expressed as fusion proteins to alkaline phosphatase (AP) and purified with Nickel affinity column. The purified AP-monobodies were incubated with the protein arrays, followed by washes and reaction with ECF substrate (GE-healthcare). The membranes were immediately scanned using Storm™ imager (GE-Life Science). The intensity of the spots was quantitated with ImageQuant software (GE Life Science).

To be useful in biological experiments, TA1 and TA8 must possess good binding affinity for their target. To measure the affinity of TA1 and TA8, the proteins were overexpressed *in E. coli* and purified by immobilized metal affinity chromatography. For the TA8 monobody, isothermal titration calorimetry (ITC) (*61*) was performed to measure the dissociation constant (K_D) of its interaction with the Lyn SH3 domain. Purified TA8 monobody was injected into the sample cell, which was loaded with the Lyn SH3 domain, and a K_D of ~ 5 µM was measured (Figure 4.4). This interaction is considered weak, as this value is similar to those of peptide ligands for binding to SH3 domains (*62*). The affinity of TA1 for the Lyn SH3 domain was measured by surface plasmon resonance, using a BIAcore biosensor (*63*), and observed also to be weak (~3 µM) (data not shown).

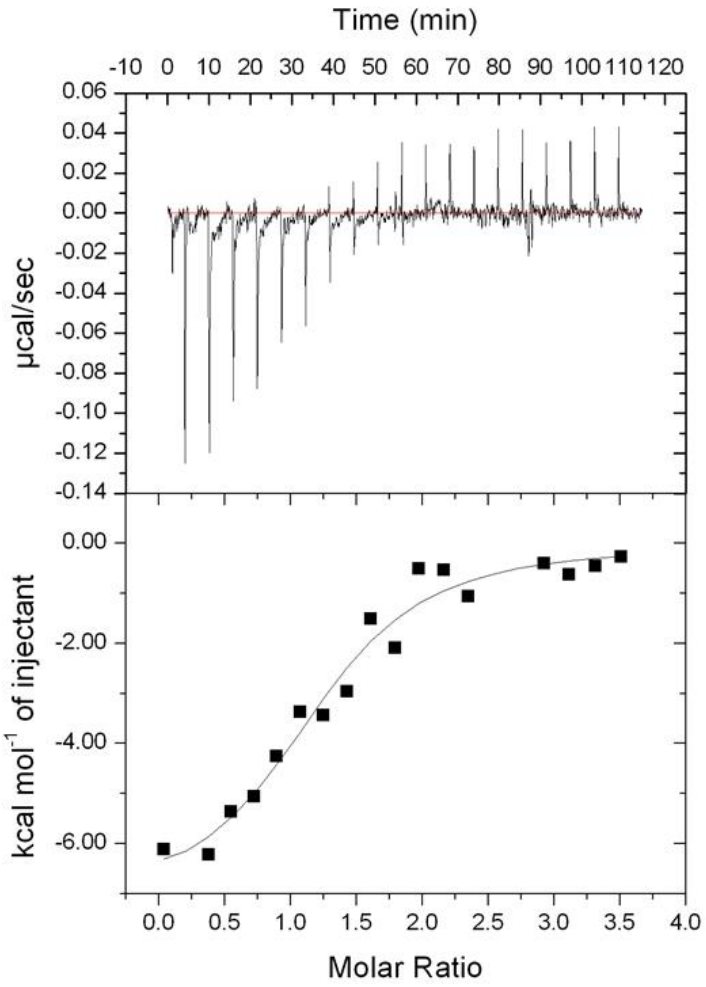

Figure 4.4. Isothermal titration calorimetry (ITC) measurements of the dissociation constant (K_D) of TA8 monobody to the Lyn SH3 domain. The thermogram (top panel) and the plotted titration curve (bottom panel) were obtained with an ITC200 (GE healthcare). The observed N, ΔH, ΔS, and dissociation constants for this interaction are 1.23, -7.25x10^3 cal/mole, 0.147Joule/ºK, and 4.5 µM, respectively.

4.4.4 Alanine-scanning of the diversified loops of monobodies

Unfortunately, the measured affinities of both TA1 and TA8, are too weak to be useful in biological experiments, as K_D values below 50 nM are necessary to immunoprecipitate a target from cell lysates (*64, 65*), and values close to 500 nM are needed for biosensor experiment (*36*). Thus, my plan was to find mutations in TA1 and/or TA8 that improved their affinity for the Lyn SH3 domain by directed evolution. To do so, I first designed an experiment in which I identified residues in the BC and FG loops that contributed to monobody binding. Residues of the BC and FG loops of monobodies were replaced with alanine (*54*), one at a time, and variants were compared side by side for their binding to the Lyn SH3 domain. The enzyme-linked binding assay showed that among the ten residues replaced by alanine, mutations in nine of them in TA1 and eight in TA8 caused significant loss of binding to the Lyn SH3 domain (Figure 4.5). Thus, the majority of the residues in the BC and FG loops contributed to binding to the Lyn SH3 domain.

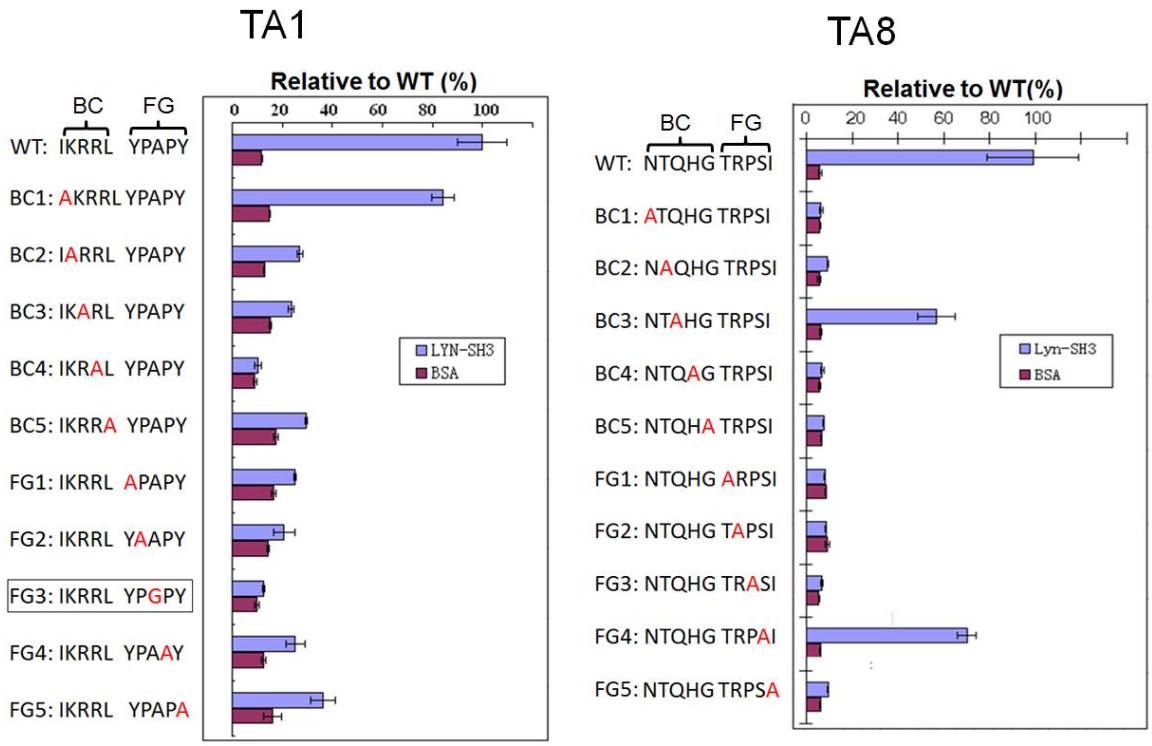

Figure 4.5. Alanine-scanning mutagenesis to reveal important residues of monobodies for binding to Lyn SH3 domain. Mutants of TA1 and TA8 monobodies with alanine substitute (At FG3 of TA1, AŸ G) were evaluated by enzyme-linked binding assay for their binding to Lyn SH3 domain. The binding values of the mutants were converted to the percentage of the value of WT monobodies. The amount of the fusion proteins of FN3+alkaline phosphatase used in the assay was normalized to the binding value of anti-flag antibody. BSA served as the non-binding control.

4.4.5 Directed evolution of TA8 monobody for tighter binding

To improve the affinity of TA8 monobody, I constructed a library of variants in which I randomized three residues in the BC loop and three residues in the FG loop. To avoid dramatically changing the binding specificity of TA8, I only randomized the two residues determined by alanine scanning to be non-critical for binding. To build in additional contact points at the binding interface, two residues flanking the BC and FG loops were also mutated. A secondary library was constructed with a diversity of 1.1×10^9. It should be noted that this library is close in size to my primary library (2×10^9) and is considerably larger than most of the secondary libraries constructed by other groups (*66-69*).

After two rounds of affinity selection, 184 clones were selected for phage ELISA, of which 65% bound at least 3-fold tighter to the Lyn SH3 domain than the wild-type TA8 (data not shown). Eight clones with the highest binding values were selected for further evaluation, of which three (i.e., 2H7, 2H10 and 3C12), bound > 8-fold tighter than the wild-type TA8 while retaining their specificity for the Lyn SH3 domain (Figure 4.6A). Although all three variants carry unique sequences in their loops (Figure 4.6B), one position (TRP**S**ISK) in their FG loops seems to favor arginine and lysine (K/R), whereas another position (TRPSI**S**K) prefers exclusively glycine.

Clone 2H7 was picked for further evaluation. In a phage ELISA with SH3 domains of all eight SFKs, 2H7 bound only to Lyn SH3 domain (Figure 4.6C). It will be interesting in the future to use it to probe an array of 150 SH3 domains, as

well as determine its dissociation constant by ITC. If desired, 2H7 can be used as a starting point for discovering point mutants that enhance its binding properties further.

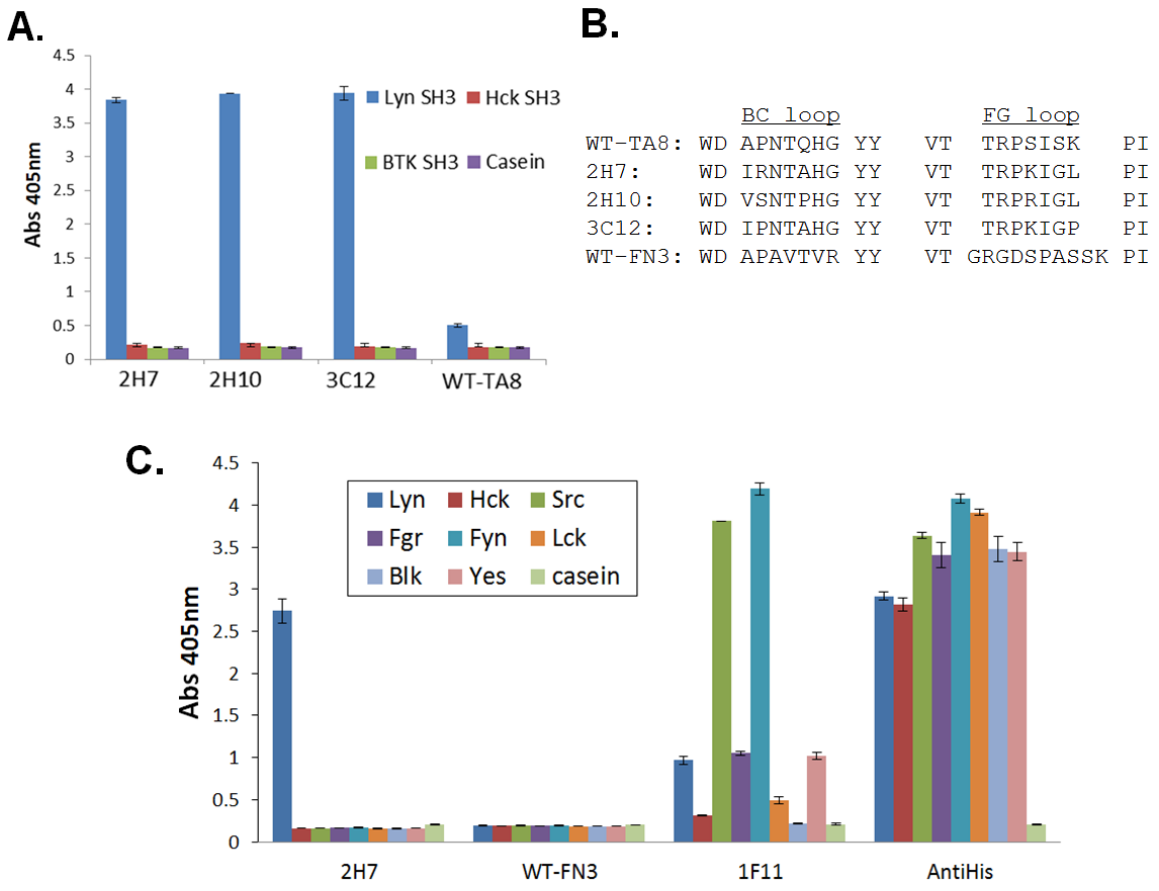

Figure 4.6. Phage ELISA of FN3 monobodies to the SH3 domains. A. Phage ELISA comparing wild-type (WT) TA8 with its variants for their binding to the SH3 domains of Lyn, Hck and Btk**.** The binding values were normalized to the display level of the Flag-epitope. Casein served as the non-binding negative control. **B.** Amino acid sequences of the BC and FG loops of WT-TA8, its variants and WT-FN3. **C.** Phage ELISA of FN3 monobodies to the SH3 domains of SFKs. Microtiter plate wells were coated with equal amounts of target or casein (negative control), and probed with equivalent amounts of phage particles displaying the various binding monobodies. Phage particles displaying wild-type monobody (WT FN3) served as the non-binding negative control. 1F11 is a monobody that binds to several, but not all, SFKs SH3 domains. An anti-his_6 tag antibody, conjugated to horseradish peroxidase (HRP), was used to normalize the amount of SH3 domain protein immobilized in the microtiter plate wells. Error bars correspond to standard deviation of triplicate measurements.

4.4.6 Mapping the binding epitope on the SH3 domain

Many SH3 domains, including the Lyn SH3 domain, interact with proline-rich (PxxP) ligands (*53, 70-72*). The SH3 domains bind to the PxxP motifs via a shallow groove that contains two binding pockets, one for each conserved proline residue in the motif (*73, 74*). As shown by NMR (*53*) (Figure 4.7A), the Lyn SH3 domain contains a similar groove that interacts with a class II proline-rich peptide (GMPTPPLPPRPANLGERQA), which is part of the tyrosine kinase interacting protein (Tip) of herpesvirus saimiri (*75*), To determine if the TA1 and TA8 bind in the same manner as the Tip peptide, a competition experiment was devised. Compared to two control peptides (GMPTAPLAPRPANLGERQA and DYKDDDDKLTVYHSKVNLP), the Tip peptide reduced the binding of TA1 and TA8 to the Lyn SH3 domain (Figure 4.7B) in a concentration-dependent manner, implying that both monobodies bind to the surface on the SH3 domain as the Tip peptide. Upon activation of SFKs, this groove on SH3 domain becomes available for binding to proteins or sensor in the cells (*36, 76, 77*), suggesting that TA1 and TA8 monobodies can bind to this region and sense the activation of the Lyn kinase.

To build a biosensor that could be used to sense Lyn activation in cells, the TA1 monobody was fused to a GFP variant (mCerulean), which permitted ratiometric imaging (*36*). Next, alanine 24 in the monobody was mutated to cysteine, to permit alkylation with the solvatochromatic dye, merocyanine (*78*), as described elsewhere (*36*). To monitor the response of the TA1 biosensor *in vitro*, it was mixed with three different concentrations of purified Lyn SH3 domain,

which led to a 70-100% increase in fluorescence intensity (data not shown), demonstrating the potential of this sensor for live cell imaging of Lyn activation.

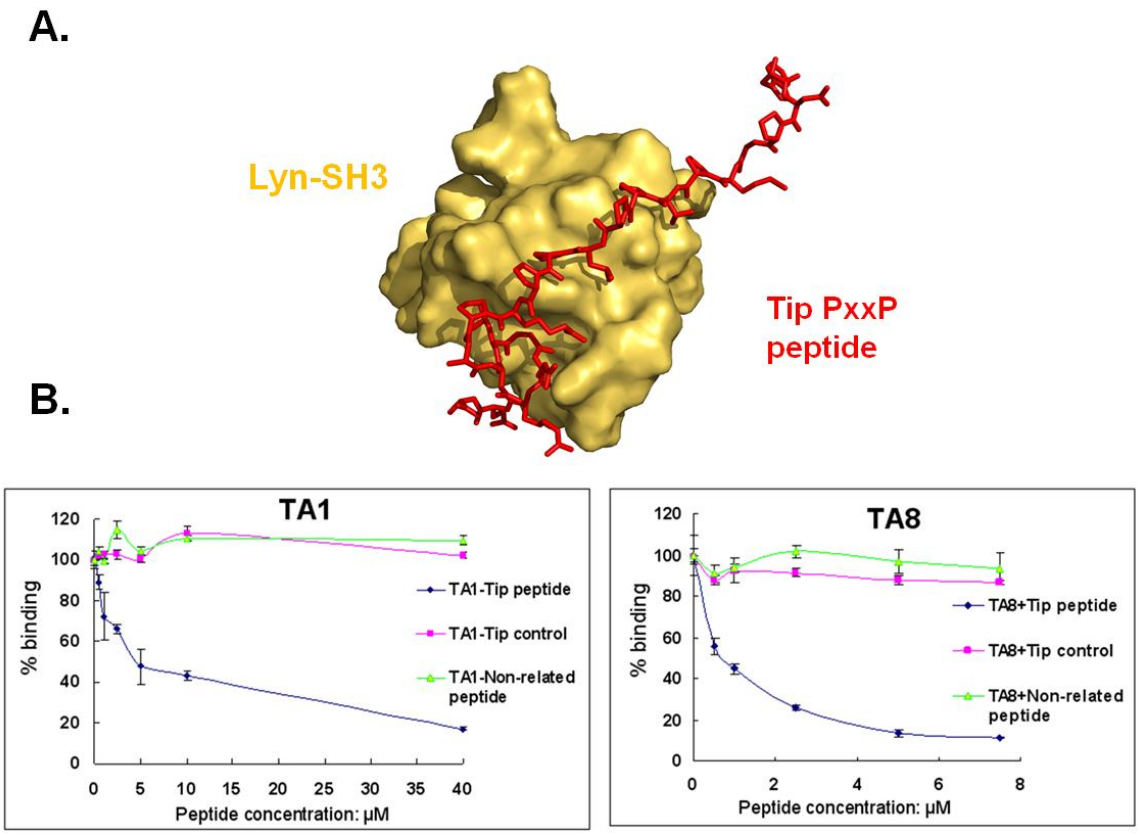

Figure 4.7. Competition binding assays for mapping the binding location of TA1 and TA8 monobodies. **A.** The NMR surface structure of the Lyn SH3 domain in complex with the structure of the Tip proline-rich peptide (GMPTPPLPPRPANL GERQA)(*53*), generated by PyMol program (*58*) with PDB file: 1WA7. **B.** Competition binding assays of TA1 and TA8 monobodies to the Lyn SH3 domain. Alkaline-phosphatase fusion proteins of TA1 and TA8 were added along with the Tip proline-rich peptide over a range of concentrations for binding to the Lyn SH3 domain. Two peptides served as negative controls: one is the Tip peptide, with two proline residues replaced by alanine (GMPTAPLAPRPANLGERQA), and the other one is an unrelated peptide (DYKDDDDKLTVYHSKVNLP) of the same length as Tip peptide.

4.5 Conclusions

Specificity and affinity are two of the most important criteria to evaluate an antibody or affinity reagent. While the conventional methods, such as hybridoma technology, continue to produce many high-quality antibodies for the scientific community, the *in vitro* display methods, such as phage display, provide fruitful alternative sources of affinity reagents with great specificity and affinity. With phage display, Pershad and her co-workers were able to isolate and affinity mature antibody fragments that are highly selective to a panel of 20 human SH2 domains (*3, 64*). Phage display permits recursive rounds of directed evolution of existing affinity reagents to improve the affinity (*67, 68*) or change the specificity (*8, 9*). With phage display, alternative scaffolds, such as the affibody (*14*), nanobody (*79*), or FN3 monobody (*80*), can be engineered into affinity reagents for applications for which antibodies are not suitable, such as living cell biosensors (*36*). Here in this study, I present work describing the isolation of two FN3 monobodies, TA1 and TA8, both of which bound primarily to the Lyn SH3 domain, out of 150 SH3 domains examined. Because of the weak affinity of TA8 for the Lyn SH3 domain, directed evolution experiments were performed to improve its binding by > 8-fold, while retaining its specificity. Competition-binding assays mapped the binding location of TA1 and TA8 to the same groove region on the Lyn SH3 domain where it binds PxxP cellular ligands. Thus, these two monobodies can potentially act as biosensors for Lyn activity, as supported by preliminary experiments.

4.6 References

1. Naidoo, N., Pawitan, Y., Soong, R., Cooper, D. N., and Ku, C. S. (2011) Human genetics and genomics a decade after the release of the draft sequence of the human genome, *Hum Genomics 5*, 577-622.

2. Ayriss, J., Woods, T., Bradbury, A., and Pavlik, P. (2007) High-throughput screening of single-chain antibodies using multiplexed flow cytometry, *J Proteome Res 6*, 1072-1082.

3. Pershad, K., Pavlovic, J. D., Graslund, S., Nilsson, P., Colwill, K., Karatt-Vellatt, A., Schofield, D. J., Dyson, M. R., Pawson, T., Kay, B. K., and McCafferty, J. (2010) Generating a panel of highly specific antibodies to 20 human SH2 domains by phage display, *Protein Eng Des Sel 23*, 279-288.

4. Yang, W. P., Green, K., Pinz-Sweeney, S., Briones, A. T., Burton, D. R., and Barbas, C. F., 3rd. (1995) CDR walking mutagenesis for the affinity maturation of a potent human anti-HIV-1 antibody into the picomolar range, *J Mol Biol 254*, 392-403.

5. Schier, R., McCall, A., Adams, G. P., Marshall, K. W., Merritt, H., Yim, M., Crawford, R. S., Weiner, L. M., Marks, C., and Marks, J. D. (1996) Isolation of picomolar affinity anti-c-erbB-2 single-chain Fv by molecular evolution of the complementarity determining regions in the center of the antibody binding site, *J Mol Biol 263*, 551-567.

6. Gao, J., Sidhu, S. S., and Wells, J. A. (2009) Two-state selection of conformation-specific antibodies, *Proc Natl Acad Sci U S A 106*, 3071-3076.

7. Huang, R., Fang, P., and Kay, B. K. (2012) Isolation of monobodies that bind specifically to the SH3 domain of the Fyn tyrosine protein kinase, *N Biotechnol 29*, 526-533.

8. Fagete, S., Ravn, U., Gueneau, F., Magistrelli, G., Kosco-Vilbois, M. H., and Fischer, N. (2009) Specificity tuning of antibody fragments to neutralize two human chemokines with a single agent, *MAbs 1*, 288-296.

9. Bostrom, J., Yu, S. F., Kan, D., Appleton, B. A., Lee, C. V., Billeci, K., Man, W., Peale, F., Ross, S., Wiesmann, C., and Fuh, G. (2009) Variants of the antibody herceptin that interact with HER2 and VEGF at the antigen binding site, *Science 323*, 1610-1614.

10. Gram, H., Marconi, L. A., Barbas, C. F., 3rd, Collet, T. A., Lerner, R. A., and Kang, A. S. (1992) In vitro selection and affinity maturation of antibodies from a naive combinatorial immunoglobulin library, *Proc Natl Acad Sci U S A 89*, 3576-3580.

11. Hackel, B. J., Kapila, A., and Wittrup, K. D. (2008) Picomolar affinity fibronectin domains engineered utilizing loop length diversity, recursive mutagenesis, and loop shuffling, *J Mol Biol 381*, 1238-1252.

12. Hackel, B. J., Ackerman, M. E., Howland, S. W., and Wittrup, K. D. (2010) Stability and CDR composition biases enrich binder functionality landscapes, *J Mol Biol 401*, 84-96.

13. Wojcik, J., Hantschel, O., Grebien, F., Kaupe, I., Bennett, K. L., Barkinge, J., Jones, R. B., Koide, A., Superti-Furga, G., and Koide, S. (2010) A potent and highly specific FN3 monobody inhibitor of the Abl SH2 domain, *Nat Struct Mol Biol 17*, 519-527.

14. Nilsson, F. Y., and Tolmachev, V. (2007) Affibody molecules: new protein domains for molecular imaging and targeted tumor therapy, *Curr Opin Drug Discov Devel 10*, 167-175.

15. Silverman, J., Liu, Q., Bakker, A., To, W., Duguay, A., Alba, B. M., Smith, R., Rivas, A., Li, P., Le, H., Whitehorn, E., Moore, K. W., Swimmer, C., Perlroth, V., Vogt, M., Kolkman, J., and Stemmer, W. P. (2005) Multivalent avimer proteins evolved by exon shuffling of a family of human receptor domains, *Nat Biotechnol 23*, 1556-1561.

16. Skerra, A. (2008) Alternative binding proteins: anticalins - harnessing the structural plasticity of the lipocalin ligand pocket to engineer novel binding activities, *FEBS J 275*, 2677-2683.

17. Boersma, Y. L., and Pluckthun, A. (2011) DARPins and other repeat protein scaffolds: advances in engineering and applications, *Curr Opin Biotechnol 22*, 849-857.

18. Grabulovski, D., Kaspar, M., and Neri, D. (2007) A novel, non-immunogenic Fyn SH3-derived binding protein with tumor vascular targeting properties, *J Biol Chem 282*, 3196-3204.

19. Kaneko, T., Huang, H., Cao, X., Li, X., Li, C., Voss, C., Sidhu, S. S., and Li, S. S. (2012) Superbinder SH2 Domains Act as Antagonists of Cell Signaling, *Sci Signal 5*, ra68.

20. Koide, A., Bailey, C. W., Huang, X., and Koide, S. (1998) The fibronectin type III domain as a scaffold for novel binding proteins, *J Mol Biol 284*, 1141-1151.

21. Xu, L., Aha, P., Gu, K., Kuimelis, R. G., Kurz, M., Lam, T., Lim, A. C., Liu, H., Lohse, P. A., Sun, L., Weng, S., Wagner, R. W., and Lipovsek, D. (2002) Directed evolution of high-affinity antibody mimics using mRNA display, *Chem Biol 9*, 933-942.

22. Olson, C. A., Liao, H. I., Sun, R., and Roberts, R. W. (2008) mRNA display selection of a high-affinity, modification-specific phospho-IkappaBalpha-binding fibronectin, *ACS Chem Biol 3*, 480-485.

23. Lipovsek, D., Lippow, S. M., Hackel, B. J., Gregson, M. W., Cheng, P., Kapila, A., and Wittrup, K. D. (2007) Evolution of an interloop disulfide bond in high-affinity antibody mimics based on fibronectin type III domain and selected by yeast surface display: molecular convergence with single-domain camelid and shark antibodies, *J Mol Biol 368*, 1024-1041.

24. Koide, A., Tereshko, V., Uysal, S., Margalef, K., Kossiakoff, A. A., and Koide, S. (2007) Exploring the capacity of minimalist protein interfaces: interface energetics and affinity maturation to picomolar KD of a single-domain antibody with a flat paratope, *J Mol Biol 373*, 941-953.

25. Koide, A., Abbatiello, S., Rothgery, L., and Koide, S. (2002) Probing protein conformational changes in living cells by using designer binding proteins: application to the estrogen receptor, *Proc Natl Acad Sci U S A 99*, 1253-1258.

26. Karatan, E., Merguerian, M., Han, Z., Scholle, M. D., Koide, S., and Kay, B. K. (2004) Molecular recognition properties of FN3 monobodies that bind the Src SH3 domain, *Chem Biol 11*, 835-844.

27. Koide, A., Gilbreth, R. N., Esaki, K., Tereshko, V., and Koide, S. (2007) High-affinity single-domain binding proteins with a binary-code interface, *Proc Natl Acad Sci U S A 104*, 6632-6637.

28. Miller, K. R., Koide, A., Leung, B., Fitzsimmons, J., Yoder, B., Yuan, H., Jay, M., Sidhu, S. S., Koide, S., and Collins, E. J. (2012) T cell receptor-like recognition of tumor in vivo by synthetic antibody fragment, *PLoS One 7*, e43746.

29. Karkkainen, S., Hiipakka, M., Wang, J. H., Kleino, I., Vaha-Jaakkola, M., Renkema, G. H., Liss, M., Wagner, R., and Saksela, K. (2006) Identification of preferred protein interactions by phage-display of the human Src homology-3 proteome, *EMBO Rep 7*, 186-191.

30. Li, S. S. (2005) Specificity and versatility of SH3 and other proline-recognition domains: structural basis and implications for cellular signal transduction, *Biochem J 390*, 641-653.

31. Buday, L., Wunderlich, L., and Tamas, P. (2002) The Nck family of adapter proteins: regulators of actin cytoskeleton, *Cell Signal 14*, 723-731.

32. McPherson, P. S. (1999) Regulatory role of SH3 domain-mediated protein-protein interactions in synaptic vesicle endocytosis, *Cell Signal 11*, 229-238.

33. Xu, W., Harrison, S. C., and Eck, M. J. (1997) Three-dimensional structure of the tyrosine kinase c-Src, *Nature 385*, 595-602.

34. Sicheri, F., Moarefi, I., and Kuriyan, J. (1997) Crystal structure of the Src family tyrosine kinase Hck, *Nature 385*, 602-609.

35. Young, M. A., Gonfloni, S., Superti-Furga, G., Roux, B., and Kuriyan, J. (2001) Dynamic coupling between the SH2 and SH3 domains of c-Src and Hck underlies their inactivation by C-terminal tyrosine phosphorylation, *Cell 105*, 115-126.

36. Gulyani, A., Vitriol, E., Allen, R., Wu, J., Gremyachinskiy, D., Lewis, S., Dewar, B., Graves, L. M., Kay, B. K., Kuhlman, B., Elston, T., and Hahn, K. M. (2011) A biosensor generated via high-throughput screening quantifies cell edge Src dynamics, *Nat Chem Biol 7*, 437-444.

37. Sun, G., Sharma, A. K., and Budde, R. J. (1998) Autophosphorylation of Src and Yes blocks their inactivation by Csk phosphorylation, *Oncogene 17*, 1587-1595.

38. Bolen, J. B., and Brugge, J. S. (1997) Leukocyte protein tyrosine kinases: potential targets for drug discovery, *Annu Rev Immunol 15*, 371-404.

39. Xiao, W., Nishimoto, H., Hong, H., Kitaura, J., Nunomura, S., Maeda-Yamamoto, M., Kawakami, Y., Lowell, C. A., Ra, C., and Kawakami, T. (2005) Positive and negative regulation of mast cell activation by Lyn via the FcepsilonRI, *J Immunol 175*, 6885-6892.

40. Barua, D., Hlavacek, W. S., and Lipniacki, T. (2012) A computational model for early events in B cell antigen receptor signaling: analysis of the roles of Lyn and Fyn, *J Immunol 189*, 646-658.

41. Katagiri, K., Yokoyama, K. K., Yamamoto, T., Omura, S., Irie, S., and Katagiri, T. (1996) Lyn and Fgr protein-tyrosine kinases prevent apoptosis during retinoic acid-induced granulocytic differentiation of HL-60 cells, *J Biol Chem 271*, 11557-11562.

42. Yoo, S. K., Freisinger, C. M., Lebert, D. C., and Huttenlocher, A. (2012) Early redox, Src family kinase, and calcium signaling integrate wound responses and tissue regeneration in zebrafish, *J Cell Biol 199*, 225-234.

43. Wang, Y. H., Fan, L., Wang, L., Zhang, R., Zou, Z. J., Fang, C., Zhang, L. N., Li, J. Y., and Xu, W. (2012) The expression levels of Lyn, Syk, PLCgamma2 and ERK in patients with chronic lymphocytic leukemia, and higher levels of Lyn associate with a shorter treatment free survival, *Leuk Lymphoma*.

44. Ingley, E. (2012) Functions of the Lyn tyrosine kinase in health and disease, *Cell Commun Signal 10*, 21.

45. Tabe, Y., Jin, L., Iwabuchi, K., Wang, R. Y., Ichikawa, N., Miida, T., Cortes, J., Andreeff, M., and Konopleva, M. (2012) Role of stromal microenvironment in nonpharmacological resistance of CML to imatinib through Lyn/CXCR4 interactions in lipid rafts, *Leukemia 26*, 883-892.

46. Tsantikos, E., Maxwell, M. J., Kountouri, N., Harder, K. W., Tarlinton, D. M., and Hibbs, M. L. (2012) Genetic interdependence of Lyn and negative regulators of B cell receptor signaling in autoimmune disease development, *J Immunol 189*, 1726-1736.

47. Kunkel, T. A. (1985) Rapid and efficient site-specific mutagenesis without phenotypic selection, *Proc Natl Acad Sci U S A 82*, 488-492.

48. Pershad, K., Sullivan, M. A., and Kay, B. K. (2011) Drop-out phagemid vector for switching from phage displayed affinity reagents to expression formats, *Anal Biochem 412*, 210-216.

49. Arbabi Ghahroudi, M., Desmyter, A., Wyns, L., Hamers, R., and Muyldermans, S. (1997) Selection and identification of single domain antibody fragments from camel heavy-chain antibodies, *FEBS Lett 414*, 521-526.

50. Pershad, K., Sullivan, M. A., and Kay, B. K. (2011) Drop-out phagemid vector for switching from phage displayed affinity reagents to expression formats, *Analytical Biochemistry 412*, 210-216.

51. Sparks, A. B., Quilliam, L. A., Thorn, J. M., Der, C. J., and Kay, B. K. (1994) Identification and characterization of Src SH3 ligands from phage-displayed random peptide libraries, *J Biol Chem 269*, 23853-23856.

52. Huang, R., Fang, P., and Kay, B. K. (2012) Improvements to the Kunkel mutagenesis protocol for constructing primary and secondary phage-display libraries, *Methods*.

53. Bauer, F., Schweimer, K., Meiselbach, H., Hoffmann, S., Rosch, P., and Sticht, H. (2005) Structural characterization of Lyn-SH3 domain in complex with a herpesviral protein reveals an extended recognition motif that enhances binding affinity, *Protein Sci 14*, 2487-2498.

54. Bass, S. H., Mulkerrin, M. G., and Wells, J. A. (1991) A systematic mutational analysis of hormone-binding determinants in the human growth hormone receptor, *Proc Natl Acad Sci U S A 88*, 4498-4502.

55. Bradford, M. M. (1976) A rapid and sensitive method for the quantitation of microgram quantities of protein utilizing the principle of protein-dye binding, *Anal Biochem 72*, 248-254.

56. Thomas, S. M., and Brugge, J. S. (1997) Cellular functions regulated by Src family kinases, *Annu Rev Cell Dev Biol 13*, 513-609.

57. Manning, G., Whyte, D. B., Martinez, R., Hunter, T., and Sudarsanam, S. (2002) The protein kinase complement of the human genome, *Science 298*, 1912-1934.

58. DeLano, W. (2002) The PYMOL molecular graphics system.

59. Main, A. L., Harvey, T. S., Baron, M., Boyd, J., and Campbell, I. D. (1992) The three-dimensional structure of the tenth type III module of fibronectin: an insight into RGD-mediated interactions, *Cell 71*, 671-678.

60. Schlesinger, M. J., and Andersen, L. (1968) Multiple molecular forms of the alkaline phosphatase of Escherichia coli, *Ann N Y Acad Sci 151*, 159-170.

61. Zhou, X., Sun, Q., Kini, R. M., and Sivaraman, J. (2008) A universal method for fishing target proteins from mixtures of biomolecules using isothermal titration calorimetry, *Protein Sci 17*, 1798-1804.

62. Viguera, A. R., Arrondo, J. L., Musacchio, A., Saraste, M., and Serrano, L. (1994) Characterization of the interaction of natural proline-rich peptides with five different SH3 domains, *Biochemistry 33*, 10925-10933.

63. Rich, R. L., and Myszka, D. G. (2007) Higher-throughput, label-free, real-time molecular interaction analysis, *Anal Biochem 361*, 1-6.

64. Dyson, M. R., Zheng, Y., Zhang, C., Colwill, K., Pershad, K., Kay, B. K., Pawson, T., and McCafferty, J. (2011) Mapping protein interactions by combining antibody affinity maturation and mass spectrometry, *Anal Biochem 417*, 25-35.

65. Colwill, K., and Graslund, S. (2011) A roadmap to generate renewable protein binders to the human proteome, *Nat Methods 8*, 551-558.

66. Nilvebrant, J., Alm, T., Hober, S., and Lofblom, J. (2011) Engineering bispecificity into a single albumin-binding domain, *PLoS One 6*, e25791.

67. Scalley-Kim, M. L., Hess, B. W., Kelly, R. L., Krostag, A. R., Lustig, K. H., Marken, J. S., Ovendale, P. J., Posey, A. R., Smolak, P. J., Taylor, J. D., Wood, C. L., Bienvenue, D. L., Probst, P., Salmon, R. A., Allison, D. S., Foy, T. M., and Raport, C. J. (2012) A novel highly potent therapeutic antibody neutralizes multiple human chemokines and mimics viral immune modulation, *PLoS One 7*, e43332.

68. Muller, B. H., Savatier, A., L'Hostis, G., Costa, N., Bossus, M., Michel, S., Ott, C., Becquart, L., Ruffion, A., Stura, E. A., and Ducancel, F. (2011) In vitro affinity maturation of an anti-PSA antibody for prostate cancer diagnostic assay, *J Mol Biol 414*, 545-562.

69. Karanicolas, J., Corn, J. E., Chen, I., Joachimiak, L. A., Dym, O., Peck, S. H., Albeck, S., Unger, T., Hu, W., Liu, G., Delbecq, S., Montelione, G. T., Spiegel, C. P., Liu, D. R., and Baker, D. (2011) A de novo protein binding pair by computational design and directed evolution, *Mol Cell 42*, 250-260.

70. Sparks, A. B., Rider, J. E., Hoffman, N. G., Fowlkes, D. M., Quillam, L. A., and Kay, B. K. (1996) Distinct ligand preferences of Src homology 3 domains from Src, Yes, Abl, Cortactin, p53bp2, PLCgamma, Crk, and Grb2, *Proc Natl Acad Sci U S A 93*, 1540-1544.

71. Sparks, A. B., Hoffman, N. G., McConnell, S. J., Fowlkes, D. M., and Kay, B. K. (1996) Cloning of ligand targets: systematic isolation of SH3 domain-containing proteins, *Nat Biotechnol 14*, 741-744.

72. Mayer, B. J. (2001) SH3 domains: complexity in moderation, *J Cell Sci 114*, 1253-1263.

73. Feng, S., Chen, J. K., Yu, H., Simon, J. A., and Schreiber, S. L. (1994) Two binding orientations for peptides to the Src SH3 domain: development of a general model for SH3-ligand interactions, *Science 266*, 1241-1247.

74. Yu, H., Chen, J. K., Feng, S., Dalgarno, D. C., Brauer, A. W., and Schreiber, S. L. (1994) Structural basis for the binding of proline-rich peptides to SH3 domains, *Cell 76*, 933-945.

75. Schweimer, K., Hoffmann, S., Bauer, F., Friedrich, U., Kardinal, C., Feller, S. M., Biesinger, B., and Sticht, H. (2002) Structural Investigation of the Binding of a Herpesviral Protein to the SH3 Domain of Tyrosine Kinase Lck, *Biochemistry 41*, 5120-5130.

76. Cowan-Jacob, S. W., Fendrich, G., Manley, P. W., Jahnke, W., Fabbro, D., Liebetanz, J., and Meyer, T. (2005) The crystal structure of a c-Src complex in an active conformation suggests possible steps in c-Src activation, *Structure 13*, 861-871.

77. Yadav, S. S., and Miller, W. T. (2007) Cooperative activation of Src family kinases by SH3 and SH2 ligands, *Cancer Lett 257*, 116-123.

78. Toutchkine, A., Nguyen, D. V., and Hahn, K. M. (2007) Merocyanine dyes with improved photostability, *Org Lett 9*, 2775-2777.

79. Rahbarizadeh, F., Ahmadvand, D., and Sharifzadeh, Z. (2011) Nanobody; an old concept and new vehicle for immunotargeting, *Immunol Invest 40*, 299-338.

80. Koide, S., Koide, A., and Lipovsek, D. (2012) Target-binding proteins based on the 10th human fibronectin type III domain (^{10}Fn3), *Methods Enzymol 503*, 135-156.

CHAPTER 5

CONCLUSIONS

5.1 Introduction

Protein kinases, known for phosphorylating their protein substrates to relay signaling events, contain 518 members and encompass ~2% of human genes. One kinase subgroup is the Src family kinases (SFKs), which respond to environmental stimuli and regulate signaling pathways involved in cell proliferation, migration, differentiation, and survival. To generate affinity reagents that can be used to detect SFK activation, I use phage display for directed evolution of a protein scaffold, the FN3 monobody. In the subsections below, I review what has been accomplished in my Ph.D. thesis and then provide some directions for future experiments.

5.2 Efficient generation of affinity reagents with high affinity and specificity via phage display

In the last two decades, phage display, one of several *in vitro* display methods, has been extensively used for biomedical research, such as mapping protein-protein interactions (*1, 2*), improving properties of existing proteins (*3-5*), identifying protein substrate (*6, 7*), designing enzyme antibodies (*8, 9*), and generating reagents for detecting biological samples (*10*), developing drug-delivery reagents (*11, 12*), building nanodevice (*13*), and treating human diseases (*14*). Compared to other conventional approaches for generating monoclonal antibodies, such as hybridoma technology (*15*), the power of phage display mostly relies on its capacity to isolate binders from a vast pool of variants (e.g., 1-10 billions). Since phage-display was invented in 1985, the size of

libraries has increased from 10^6-10^8 (*16*) to 10^{11} (*17*) at the current time. The selection outcome and the affinity of isolated clones are closely correlated with the size (i.e., diversity) of the library (*18*).

To build a phage display library consisting of >10^{10} members, one needs a large amount of template DNA. In Kunkel mutagenesis (*19*), mutant or variant proteins are generated by annealing oligonucleotides to a single-stranded DNA (ssDNA) template for *in vitro* synthesis of double-stranded DNA. As oligonucleotides are readily obtained from commercial vendors, the bottleneck to building large libraries rests with the amount of ssDNA template. Previously, CJ236 *E. coli* cells produced low yields of ssDNA of poor quality for Kunkel mutagenesis. By comparing many growth conditions, I identified that by incubating the culture at 25°C compared to 37°C, I could increase the yield of ssDNA as high as sevenfold. With this improvement, ssDNA recovered from a 180 mL culture is sufficient to construct a phage library of > 10 billion clones. This improvement significantly reduces the time and effort for making phage libraries.

The quality of the phage library (i.e., the percentage of the phage particles displaying the recombinant polypeptides out of the total phage pool) also significantly influences the outcome of affinity selection experiments (*20, 21*). This is because non-binding phage particles, including those displaying only the wild-type coat protein-III or the wild-type scaffold (Figure 5.1), likely reduce the possibility of a potential binder making contact with its target in an ocean of non-binding phage particles.

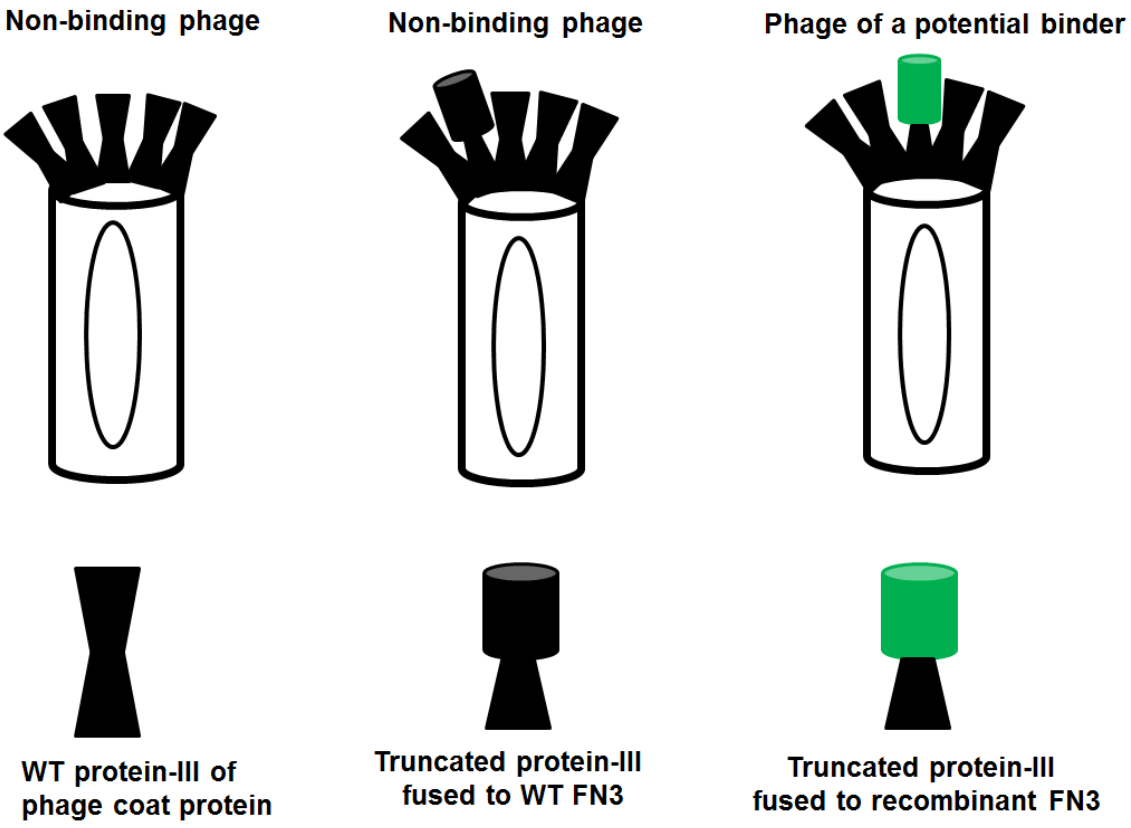

Figure 5.1. Three types of phage particles in a phage-display library of FN3 monobodies. The low mutation rate with the original Kunkel mutagenesis protocol and the prevalence of wild-type (WT) capsid protein-III from the helper virus generate a large fraction of non-binding phage particles in the phage library, which are in the way of potential binders to find their protein targets.

Kunkel mutagenesis usually generates libraries that are approximately 50% recombinant (*19, 22*). To increase the fraction of recombinants, endonuclease restriction sites were introduced into the FN3 coding region, so that the enzyme can preferentially cleave wild-type clones, thereby generating libraries that are 99ï 100% recombinant. However, the restriction digestion procedure only worked efficiently on DNA extracted from *E.coli*, not dsDNA synthesized *in vitro*. Thus, in *vitro* synthesized dsDNA was electroporated into *E.coli* cells, extracted from the transformed cells, cleaved with the restriction endonuclease, and then electroporated back into *E. coli* again. This method yielded libraries that were 99-100% recombinant.

While our method represents a major improvement over previous techniques, it requires two steps of electroporation, which brings up the cost of constructing a high-quality library, as the electrocompetent cells are costly. Recently, an alternative method to make a library of 99-100% recombinant was published (*23*). In the new method, *in vitro* synthesized dsDNA is digested with uracil-DNA glycosylase to cleave the non-recombinant strand due to its inserted uracil. The remaining recombinant strand is then used as template for performing órolling circleô amplification *in vitro* with phi29 DNA polymerase. The resulting DNA concatemer is then digested and re-ligated (by self-ligation) to make double-stranded plasmid DNA for electroporation of *E. coli* cells. The main advantage of this method is that it eliminates the step of second electroporation, thereby lowering the cost of library construction.

Even with a large phage library containing a high proportion of phage particles displaying the recombinant polypeptides, affinity maturation experiments are usually necessary to fine-tune binders for improved specificity (*24, 25*), affinity (*24, 26, 27*), or both (*24*). In some case, even with a small primary library, recursive rounds of affinity maturation have yielded binder with affinity as high as 1 pM (*28*). To save time and effort for performing affinity maturation experiments, I modified the Kunkel mutagenesis protocol for conveniently building secondary libraries out of existing binders. By error-prone and/or asymmetric PCR, double-stranded or single-stranded DNA fragments carrying random mutations can be generated and used as ómegaprimersôfor priming DNA synthesis *in vitro*. This modified method eliminates the time-consuming steps of digestion and ligation, necessary steps in the conventional approach for constructing mutagenic libraries. With my modified protocol, I can construct a secondary library and screen it to yield enhanced binders in less than one week. To demonstrate the application of this method, I constructed two mutagenic phage libraries and screened to identify three variants that bound two- to four-fold tighter to the Pak1 kinase than the original clone.

I plan to use the modified method to create secondary libraries by shuffling the mutagenized loops of a phage pool enriched by affinity selection of the primary library. First, in such experiments, a pool of clones after affinity selections will be used directly as a template for mutagenic PCR. Second, instead of amplifying the complete FN3 coding region, I will amplify the BC loop and the FG loop separately by error-prone PCR, and then anneal these two

segments of DNA to the ssDNA template to create a secondary library. This method should not only add mutations to the DNA, via error-prone PCR, but also create FN3 variants that contain the best BC and FG loop sequences present in the enriched binder pool.

5.3 Evaluation of the FN3 monobodies in biological contexts

SFKs are a group of protein tyrosine kinases with highly conserved domains and sequences. SFKs, which contain a unique domain, a Src-homology 3 (SH3) domain, a Src-homology 2 (SH2) domain, a proline-rich (PxxP) linker and a kinase domain, followed by a C-terminal regulatory tail. As this unique domain differs significantly among SFKs, it has been used as the main antigen to develop antibodies that can distinguish one member from the other SFKs. But antibodies that have been developed against the kinase domain for recognizing the active form of the SFKs cross-react with multiple members of the SFKs, making the research results inconclusive (*29*). Currently available sensors for SFKs have the same specificity issue as their substrate motifs can be recognized and phosphorylated by multiple kinases (*30-32*). In my thesis study, I was able to isolate, characterize and affinity-mature multiple FN3 monobodies that could selectively recognize the Fyn and Lyn tyrosine kinases.

For Fyn tyrosine kinase, one isolated monobody bound to the Fyn SH3 domain, with a K_D of 166 ± 6 nM, and not any of the other 149 human SH3 domains examined. Interestingly, this monobody competed with proline-rich

ligands for binding at a site on the Fyn SH3 domain. I was able to use G9-monobody to immunoprecipitate active recombinant Fyn kinase, demonstrating its potential for developing into a sensor of detecting active cellular Fyn kinase.

For Lyn kinase, two monobodies, TA1 and TA8, were isolated that selectively bound to the Lyn SH3 domain out of 150 SH3 domains examined. While the affinity of TA8 was weak (~5 μM), affinity maturation identified TA8 variants that bound more than 8-fold tighter to Lyn SH3 domain. The successful experiment of evaluating the TA1 biosensor in solution implicates its potential as a living-cell biosensor of Lyn activation.

However, before evaluating these monobodies as biosensors in living cells, I still need to conduct additional biological experiments to verify their functionality further. One experiment will be to confirm that they truly bind to the active kinase molecule. To do so, NIH3T3 cells can be cultured until 50-70% confluency, serum starved, and stimulated with PBS-resuspended platelet derived growth factor or epidermal growth factor (*33*). As a control, half of the cells can be treated with PBS only. The treated cells can be lysed with detergent, spun-down and mixed with biotinylated monobodies for pull-down experiments. A kinase assay can be performed to confirm the activities of kinase molecules pulled down from the stimulated cell lysate but not from the mock-treated one. Alternatively, monoclonal antibodies, which bind to the phosphotyrosine (Y416) in the kinase domain, can be used to determine the identity of immunoprecipitated kinase molecules. As a backup plan, serum starved cells can be harvested, lysed without stimulation, and treated with protein tyrosine phosphatase alpha (*34*) for

in vitro activation, followed by immunoprecipitation experiments or a kinase assay as described above. For Lyn kinase, due to its restricted expression in hematopoietic cells, different cells lines, such as mast cells or monocytes, can be used for the same set of experiments.

If the above experiments confirm the ability of the isolated monobodies for selectively recognizing the active kinase form of Fyn and/or Lyn, then in theory, they all can be converted into sensors for living-cell studies. The reason is that the tested TA1 sensor was constructed by inserting the reporter dye in the same amino acid residue as the one for Src sensor (*32*). Thus, this same residue may be used repeatedly in the future for conjugating the dye molecule to other monobodies.

5.4 Verifying the specificity of FN3 monobodies

While the isolated monobodies exhibited remarkable specificity among the 150 SH3 domains examined, there are still several types of experiments that can be done to further verify their specificity. First, there are more than 300 SH3 domains encoded by the human genome (*35*), and I only tested half of them with the array. Thus, there is the possibility that the SH3 domain-binding monobodies will bind to another human SH3 domain (s) that I have yet to test. With a nucleic acid programmable protein array (NAPPA) (*36, 37*), one can simultaneously express tens of hundreds of proteins on slides and probe them with a monobody. I may be able to do the same with all 300 human SH3 domains.

A second approach to verify the specificity of the monobodies will be to perform a pull-down assay with lysates prepared from a Fyn knockout cell line (*38*) or blood sample from the Lyn knockout mouse (*39*), and compare it with similar samples of normal cell line or animal. Two caveats with this approach are that the SFK molecules need to be activated for this experiment to work and the small sample size may not contain enough kinase to be detected. An alternative experiment will be to perform western blotting with the samples from knockout cell lines or mouse, as SH3 domains of SFKs are thermally stable (*40*) and may re-fold on the blot and permit binding of a monobody probe.

A third approach is to use RNAi technology (*41*) to establish stable knock-down of the expression level of the targeted kinases. In this case, cell lines with its mRNA of Fyn or Lyn knocked down will be used to compare with the cells that are treated with control DNA in the pull-down or western blot experiments as described above. If monobodies are specific to their intended targets, significantly lower amount of kinase will be detected in the resting cells compared with the cells treated with control DNA.

A last approach is to use the monobodies to perform pull-down experiments with lysate of stimulated cells, elute proteins that are pulled out by monobodies and send the eluted sample out for liquid chromatographyï mass spectrometry (LS-MS) (*42*) analysis to determine the identity of the pulled out protein(s). If besides Fyn or Lyn, there are no other SH3-containing proteins identified by LS-MS or there are such proteins but found at much lower frequency, it indicates that the monobodies are specific. For this experiment to work, a large amount of

cell lysate is needed to be able to generate enough samples to obtain good signal in LS-MS analysis. A caveat with the LS-MS analysis is that upon activation, both Fyn and Lyn interact with their protein substrate for phosphorylation and some of their substrate proteins contain SH3 domains (*43*), which makes it more complicated to interpret the results. But if such proteins are observed, some additional binding experiments can help confirm the LS-MS data. To be able to pull down enough proteins for LS-MS analysis, the monobodies need to possess a K_D of 50 nM (*44*) or even lower, making an affinity maturation experiment a necessity.

5.5 Strategies for improving and expanding the current work

In this thesis research, I generated several highly specific FN3 monobodies for building biosensors to monitor the activation of Fyn and Lyn kinases. This method can be applied to other kinases or other targets as well. Out of the 11 targets (SH3 domains of Abl, Fyn, Lyn, Lck, human lactoferrin, kinase domain and P21-binding domain of human Pak1 and four transcription factors) that have been selected for, we have isolated binders to ten of them. Besides biosensors, these monobodies can also be used as activators or inhibitors inside cells, depending on their targeted motifs and their binding affinity.

While our monobody library works for many targets so far, the affinity of the isolated FN3 monobodies is not as high as desired. Studies with antibodies suggest that varying the length of complementarity determining region may increase the affinity and specificity of antibodies (*45, 46*). In some recent studies,

FN3 monobodies with varied loop length are selected and affinity matured to achieve K_D of 1 pM (*47*) and 7 nM (*48*) with high specificity. So based on the above evidence, I plan to construct a new phage library of FN3 monobodies by varying the length of BC and FG loops. Then after two rounds of affinity selections, to expedite the affinity maturation process, the resulting phage pool will be used directly as the template for error-prone PCR and loop shuffling to create a secondary library that will be screened for tighter binders. This affinity maturation procedure will be repeated until binders with $K_D < 50$ nM are isolated. Phage ELISA will be the first assay to roughly estimate the K_D (*49*) and the specificity of the isolates, followed by more complex assays like isothermal titration calorimetry for the measurement of K_D or NAPPA array for further evaluating specificity. After all these evaluations and measurements, the monobodies will be finally applied to a real-life setting, to do experiments with biological samples and to study living cells as biosensors/activators/inhibitors . The plans for improving and expanding the current work are depicted in the figure 5.2.

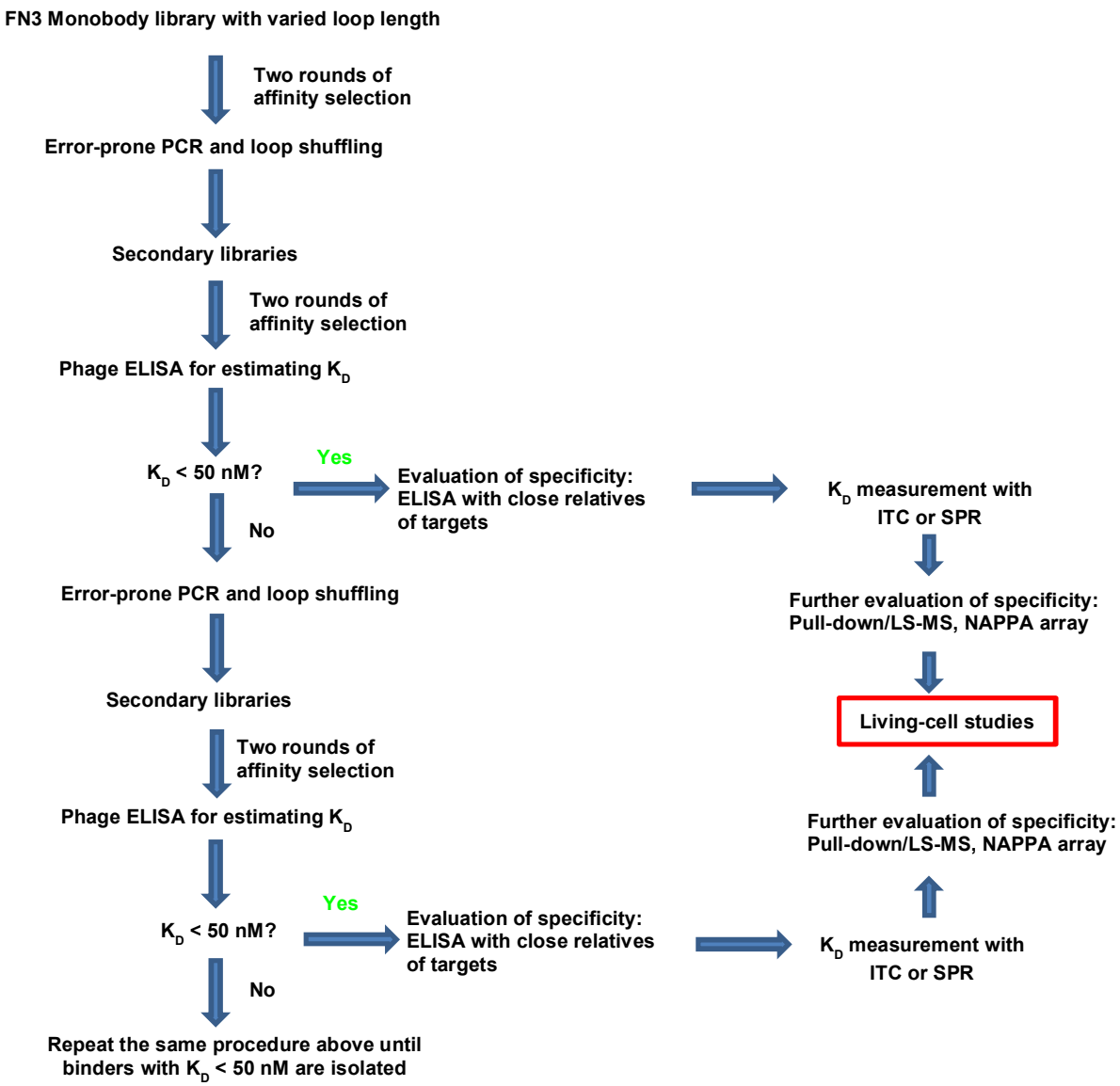

Figure 5.2. Strategies for improving and expanding the current work. To shorten the time of performing affinity maturation on single clone, a pool of phage clones enriched by affinity selection will be used directly for creating a secondary library. To simultaneously create mutations and recombination among existing clones, error-prone PCR will be performed to amplify the two mutagenized loops of monobodies separately for allowing loop shuffling in the following Kunkel mutagenesis. To save effort, phage ELISA will be used extensively to roughly characterize the isolated binders before using more complex assays for further characterization.

5.6 References

1. Gao, B., and Esnouf, M. P. (1996) Elucidation of the core residues of an epitope using membrane-based combinatorial peptide libraries, *J Biol Chem 271*, 24634-24638.

2. Sospedra, M., Pinilla, C., and Martin, R. (2003) Use of combinatorial peptide libraries for T-cell epitope mapping, *Methods 29*, 236-247.

3. Pershad, K., Wypisniak, K., and Kay, B. K. (2012) Directed evolution of the forkhead-associated domain to generate anti-phosphospecific reagents by phage-display, *J Mol Biol*.

4. Chu, R., Takei, J., Knowlton, J. R., Andrykovitch, M., Pei, W., Kajava, A. V., Steinbach, P. J., Ji, X., and Bai, Y. (2002) Redesign of a four-helix bundle protein by phage display coupled with proteolysis and structural characterization by NMR and X-ray crystallography, *J Mol Biol 323*, 253-262.

5. Grebien, F., Hantschel, O., Wojcik, J., Kaupe, I., Kovacic, B., Wyrzucki, A. M., Gish, G. D., Cerny-Reiterer, S., Koide, A., Beug, H., Pawson, T., Valent, P., Koide, S., and Superti-Furga, G. (2011) Targeting the SH2-kinase interface in Bcr-Abl inhibits leukemogenesis, *Cell 147*, 306-319.

6. Kridel, S. J., Chen, E., and Smith, J. W. (2001) A substrate phage enzyme-linked immunosorbent assay to profile panels of proteases, *Anal Biochem 294*, 176-184.

7. McCarter, J. D., Stephens, D., Shoemaker, K., Rosenberg, S., Kirsch, J. F., and Georgiou, G. (2004) Substrate specificity of the Escherichia coli outer membrane protease OmpT, *J Bacteriol 186*, 5919-5925.

8. Takahashi-Ando, N., Kakinuma, H., Fujii, I., and Nishi, Y. (2004) Directed evolution governed by controlling the molecular recognition between an abzyme and its haptenic transition-state analog, *J Immunol Methods 294*, 1-14.

9. Fernandez-Gacio, A., Uguen, M., and Fastrez, J. (2003) Phage display as a tool for the directed evolution of enzymes, *Trends Biotechnol 21*, 408-414.

10. Bradbury, A. R., Sidhu, S., Dubel, S., and McCafferty, J. (2011) Beyond natural antibodies: the power of in vitro display technologies, *Nat Biotechnol 29*, 245-254.

11. Kamada, H., Okamoto, T., Kawamura, M., Shibata, H., Abe, Y., Ohkawa, A., Nomura, T., Sato, M., Mukai, Y., Sugita, T., Imai, S., Nagano, K., Tsutsumi, Y., Nakagawa, S., Mayumi, T., and Tsunoda, S. (2007) Creation of novel cell-penetrating peptides for intracellular drug delivery using systematic phage display technology originated from Tat transduction domain, *Biol Pharm Bull 30*, 218-223.

12. Gao, C., Mao, S., Ditzel, H. J., Farnaes, L., Wirsching, P., Lerner, R. A., and Janda, K. D. (2002) A cell-penetrating peptide from a novel pVII-pIX phage-displayed random peptide library, *Bioorg Med Chem 10*, 4057-4065.

13. Eteshola, E., Brillson, L. J., and Lee, S. C. (2005) Selection and characteristics of peptides that bind thermally grown silicon dioxide films, *Biomol Eng 22*, 201-204.

14. Neri, P., Zucchi, M., Allegri, P., Lettieri, M., Mariotti, C., and Giovannini, A. (2011) Adalimumab (Humira): a promising monoclonal anti-tumor necrosis factor alpha in ophthalmology, *Int Ophthalmol 31*, 165-173.

15. Tomita, M., and Tsumoto, K. (2011) Hybridoma technologies for antibody production, *Immunotherapy 3*, 371-380.

16. McCafferty, J., Griffiths, A. D., Winter, G., and Chiswell, D. J. (1990) Phage antibodies: filamentous phage displaying antibody variable domains, *Nature 348*, 552-554.

17. Scholle, M. D., Kehoe, J. W., and Kay, B. K. (2005) Efficient construction of a large collection of phage-displayed combinatorial peptide libraries, *Comb Chem High Throughput Screen 8*, 545-551.

18. Ling, M. M. (2003) Large antibody display libraries for isolation of high-affinity antibodies, *Comb Chem High Throughput Screen 6*, 421-432.

19. Kunkel, T. A. (1985) Rapid and efficient site-specific mutagenesis without phenotypic selection, *Proc Natl Acad Sci U S A 82*, 488-492.

20. Menendez, A., and Scott, J. K. (2005) The nature of target-unrelated peptides recovered in the screening of phage-displayed random peptide libraries with antibodies, *Anal Biochem 336*, 145-157.

21. Brammer, L. A., Bolduc, B., Kass, J. L., Felice, K. M., Noren, C. J., and Hall, M. F. (2008) A target-unrelated peptide in an M13 phage display library traced to an advantageous mutation in the gene II ribosome-binding site, *Anal Biochem 373*, 88-98.

22. Tonikian, R., Zhang, Y., Boone, C., and Sidhu, S. S. (2007) Identifying specificity profiles for peptide recognition modules from phage-displayed peptide libraries, *Nat Protoc 2*, 1368-1386.

23. Huovinen, T., Brockmann, E. C., Akter, S., Perez-Gamarra, S., Yla-Pelto, J., Liu, Y., and Lamminmaki, U. (2012) Primer extension mutagenesis powered by selective rolling circle amplification, *PLoS One 7*, e31817.

24. Huang, R., Fang, P., and Kay, B. K. (2012) Isolation of monobodies that bind specifically to the SH3 domain of the Fyn tyrosine protein kinase, *N Biotechnol 29*, 526-533.

25. Fagete, S., Ravn, U., Gueneau, F., Magistrelli, G., Kosco-Vilbois, M. H., and Fischer, N. (2009) Specificity tuning of antibody fragments to neutralize two human chemokines with a single agent, *MAbs 1*, 288-296.

26. Yang, W. P., Green, K., Pinz-Sweeney, S., Briones, A. T., Burton, D. R., and Barbas, C. F., 3rd. (1995) CDR walking mutagenesis for the affinity maturation of a potent human anti-HIV-1 antibody into the picomolar range, *J Mol Biol 254*, 392-403.

27. Groves, M., Lane, S., Douthwaite, J., Lowne, D., Rees, D. G., Edwards, B., and Jackson, R. H. (2006) Affinity maturation of phage display antibody populations using ribosome display, *J Immunol Methods 313*, 129-139.

28. Hackel, B. J., Kapila, A., and Wittrup, K. D. (2008) Picomolar affinity fibronectin domains engineered utilizing loop length diversity, recursive mutagenesis, and loop shuffling, *J Mol Biol 381*, 1238-1252.

29. Qayyum, T., McArdle, P. A., Lamb, G. W., Jordan, F., Orange, C., Seywright, M., Horgan, P. G., Jones, R. J., Oades, G., Aitchison, M. A., and Edwards, J. (2012) Expression and prognostic significance of Src family members in renal clear cell carcinoma, *Br J Cancer 107*, 856-863.

30. Wang, Y., Botvinick, E. L., Zhao, Y., Berns, M. W., Usami, S., Tsien, R. Y., and Chien, S. (2005) Visualizing the mechanical activation of Src, *Nature 434*, 1040-1045.

31. Ting, A. Y., Kain, K. H., Klemke, R. L., and Tsien, R. Y. (2001) Genetically encoded fluorescent reporters of protein tyrosine kinase activities in living cells, *Proc Natl Acad Sci U S A 98*, 15003-15008.

32. Gulyani, A., Vitriol, E., Allen, R., Wu, J., Gremyachinskiy, D., Lewis, S., Dewar, B., Graves, L. M., Kay, B. K., Kuhlman, B., Elston, T., and Hahn, K. M. (2011) A biosensor generated via high-throughput screening quantifies cell edge Src dynamics, *Nat Chem Biol 7*, 437-444.

33. Vacaresse, N., Moller, B., Danielsen, E. M., Okada, M., and Sap, J. (2008) Activation of c-Src and Fyn kinases by protein-tyrosine phosphatase RPTPalpha is substrate-specific and compatible with lipid raft localization, *J Biol Chem 283*, 35815-35824.

34. Samayawardhena, L. A., and Pallen, C. J. (2010) PTPalpha activates Lyn and Fyn and suppresses Hck to negatively regulate FcepsilonRI-dependent mast cell activation and allergic responses, *J Immunol 185*, 5993-6002.

35. Karkkainen, S., Hiipakka, M., Wang, J. H., Kleino, I., Vaha-Jaakkola, M., Renkema, G. H., Liss, M., Wagner, R., and Saksela, K. (2006) Identification of preferred protein interactions by phage-display of the human Src homology-3 proteome, *EMBO Rep 7*, 186-191.

36. He, M., Stoevesandt, O., Palmer, E. A., Khan, F., Ericsson, O., and Taussig, M. J. (2008) Printing protein arrays from DNA arrays, *Nat Methods 5*, 175-177.

37. Pearlberg, J., and LaBaer, J. (2004) Protein expression clone repositories for functional proteomics, *Curr Opin Chem Biol 8*, 98-102.

38. Klinghoffer, R. A., Sachsenmaier, C., Cooper, J. A., and Soriano, P. (1999) Src family kinases are required for integrin but not PDGFR signal transduction, *EMBO J 18*, 2459-2471.

39. Stafford, S., Lowell, C., Sur, S., and Alam, R. (2002) Lyn tyrosine kinase is important for IL-5-stimulated eosinophil differentiation, *J Immunol 168*, 1978-1983.

40. Chen, Y. J., Lin, S. C., Tzeng, S. R., Patel, H. V., Lyu, P. C., and Cheng, J. W. (1996) Stability and folding of the SH3 domain of Bruton's tyrosine kinase, *Proteins 26*, 465-471.

41. Miest, T., Saenz, D., Meehan, A., Llano, M., and Poeschla, E. M. (2009) Intensive RNAi with lentiviral vectors in mammalian cells, *Methods 47*, 298-303.

42. Hsieh, Y., and Korfmacher, W. A. (2006) Increasing speed and throughput when using HPLC-MS/MS systems for drug metabolism and pharmacokinetic screening, *Curr Drug Metab 7*, 479-489.

43. Mano, H., Yamashita, Y., Miyazato, A., Miura, Y., and Ozawa, K. (1996) Tec protein-tyrosine kinase is an effector molecule of Lyn protein-tyrosine kinase, *FASEB J 10*, 637-642.

44. Dyson, M. R., Zheng, Y., Zhang, C., Colwill, K., Pershad, K., Kay, B. K., Pawson, T., and McCafferty, J. (2011) Mapping protein interactions by combining antibody affinity maturation and mass spectrometry, *Anal Biochem 417*, 25-35.

45. Rock, E. P., Sibbald, P. R., Davis, M. M., and Chien, Y. H. (1994) CDR3 length in antigen-specific immune receptors, *J Exp Med 179*, 323-328.

46. Barrios, Y., Jirholt, P., and Ohlin, M. (2004) Length of the antibody heavy chain complementarity determining region 3 as a specificity-determining factor, *J Mol Recognit 17*, 332-338.

47. Hackel, B. J., Kapila, A., and Dane Wittrup, K. (2008) Picomolar Affinity Fibronectin Domains Engineered Utilizing Loop Length Diversity, Recursive Mutagenesis, and Loop Shuffling, *Journal of Molecular Biology 381*, 1238-1252.

48. Wojcik, J., Hantschel, O., Grebien, F., Kaupe, I., Bennett, K. L., Barkinge, J., Jones, R. B., Koide, A., Superti-Furga, G., and Koide, S. (2010) A potent and highly specific FN3 monobody inhibitor of the Abl SH2 domain, *Nat Struct Mol Biol 17*, 519-527.

49. Friguet, B., Chaffotte, A. F., Djavadi-Ohaniance, L., and Goldberg, M. E. (1985) Measurements of the true affinity constant in solution of antigen-antibody complexes by enzyme-linked immunosorbent assay, *J Immunol Methods 77*, 305-319.

APPENDIX

AFFINITY MATURATION OF A FN3 MONOBODY FOR IMPROVED SPECIFICITY AND AFFINITY

Introduction

In molecular evolution experiments, in order to improve the properties of an existing clone, further rounds of directed evolution are performed by creating a secondary library based on the existing clone. This procedure is also termed affinity maturation, a term borrowed from the similar process of the immune system, in which existing antibodies undergo somatic mutations and achieve tighter binding after selection (*1*).

Affinity selection of a primary phage library identified a FN3 monobody (Chapter 3), D10, that bound to the Fyn SH3 domain. Phage ELISA showed that D10 bound weakly to the Fyn SH3 domain (data not shown) while cross-reacted with SH3 domain of Yes (Figure 1), a close relative of Fyn kinase. To improve the binding affinity and specifity of D10, I decided to generate a secondary library for affinity maturation.

Materials and methods

Constructing of a secondary library of D10

D10 DNA was used as the template to perform error-prone PCR (*2*). An amplified DNA fragment was purified with QIAquick PCR purification kit (Qiagen) and digested for ligating into a phagemid vector (*3*). The ligation mix was purified with QIAquick PCR purification kit (Qiagen) and transformed into TG1 cells (Lucigen). After transformation, cells were recovered at 37 °C with 200 rpm shaking for 30 min, before serial dilutions of the recovered cells were plated (to determine transformation efficiency) on 2×YT agar plates with carbenicillin (50

µg/mL), and incubated overnight at 30 °C. The next day cells were scraped from the agar plate. To amplify phage particles for affinity selections, cells were used to inoculate 2×YT medium, containing carbenicillin (50 µg/mL), kanamycin (50 µg/mL), and helper virus, M13-K07 (New England BioLabs) for overnight incubation at 25 °C.

Phage particles, displaying monobody variants, were amplified, and resuspended in Tris-buffered saline (TBS; 50 mM Trisï HCl, 150 mM NaCl, pH 7.5) containing 0.5% Tween (volume/volume) + 0.5% bovine serum albumin (BSA; mass/volume). The suspension of phage particles was then mixed with the target, biotinylated Fyn SH3 domain (100 nM, final concentration) and non-biotinylated SH3 domain of Fgr and Yes (1 µM). After 2 h incubation, streptavidin-coated magnetic beads (Promega) were added to the phage solution. Beads were collected with a magnet after 15 min tumbling, followed by six washes with PBS-0.5% Tween, three washes with PBS-0.1% Tween, and three washes with PBS (All the solutions contained the non-biotinylated SH3 domain of Src, Fgr and Yes). Bound phage particles were eluted with 50 mM glycine (pH 2) for 10 min, which was neutralized with Trisï HCl (pH 10) and used to infect mid-log phase TG1 cells for 30 min at 37 °C with 100 rpm shaking. Infected cells were pelleted and spread on 2×YT agar plates with carbenicillin (50 µg/mL), and incubated overnight at 30 °C. The next day, bacterial colonies were scraped from the plate and used to inoculate cultures for amplifying viral particles, which would be used for the next round of affinity selection. To increase the stringency, the

second round of selection was performed with a reduced concentration of the target protein (10 nM) and with additional washes.

Phage ELISA and mapping of binding location

Phage ELISA assays were performed as described in a previous study(*4*). Briefly, the SH3 domain fusion proteins were directly immobilized on a Nunc microtiter plate (Thermo Fisher Scientific), by aliquoting 5 εg/mL solutions (in PBS) into triplicate wells, and incubating the plates overnight at 4ºC. The following day, non-specific binding sites in the wells were blocked with excess casein (in PBS) for 1 h. After washing the wells with PBST, culture supernatants, which contained the phage particles, were added to wells for 1 h incubation, followed by washes of the microtiter plate and incubation with an anti-phage antibody that is conjugated to horseradish peroxidase (GE Healthcare). After 1 h incubation, the wells were washed, and the chromogenic substrate, 2,2'-Azino-bis(3-Ethylbenzothiazoline-6-Sulfonic Acid (ABTS), in the presence of hydrogen peroxide, was added and the resulting absorbance was determined at 405 nm with a microtiter plate spectrophotometer (BMG Labtech, Germany).

Isothermal titration calorimetry

His_6-tagged SUMO-FN3 monobody fusions and His_6-tagged SUMO-SH3 domain fusions were purified to homogeneity of >95% and dialyzed in the same beaker against 25 mM Tris-HCl (pH 7.5), 150 mM NaCl, and 100 mM imidazole. After overnight dialysis, their concentrations were determined with a NanoDrop ND-1000 spectrophotometer. Degassed samples were added to the loading cell

(1.4 mL) and syringe (300 µL) of a VP-ITC (GE Healthcare). FN3 monobodies were loaded into the syringe at 200 µM and SH3 domains were loaded into the cell at 22 µM. The reference well was loaded with water. FN3 monobodies were injected into the cell with a volume of 10 µL per injection at 25ºC, with a reference power of 10 µcal/s. The heat change of each injection was recorded, and analyzed with Origin software (GE Healthcare).

Results and discussion

A secondary library with a diversity of 6×10^6 was created. After two rounds of affinity selections, 92 clones were picked for phage ELISA, which identified 15 clones with 3- to 5-fold tighter binding than the wild-type D10. One clone (D10ô), with the highest ratio of binding affinity to Fyn SH3 divided by binding affinity to Yes SH3 domain (Fyn/Yes), was selected for further testing. In the phage ELISA with the SH3 domains of all SFKs, compared to D10, D10ônot only bound tighter to the Fyn SH3 domain than the D10 but also lost its binding to the Yes SH3 domain.

To measure the binding affinity of the D10ôto the Fyn SH3 domain, Isothermal titration calorimetry was performed, which measured the K_D of D10ôto be 310 nM (Figure 2), a 25-fold increase from the wild type (7.6 µM) (Figure 2).

Figure 3 is the sequence alignment of D10 and D10ôand the locations of the mutations in the FN3 scaffold. As the DVŸ VD mutation occurred in the unstructured N-terminal tail, it is likely that the single point mutation of Lysine to

Arginine contributes to the 25-fold increase in binding and the change of the specificity. Changing the three mutated residues of D10ǫ one at a time, back to the wild type can provide some clue about how each individual mutation contributes to the change of binding properties.

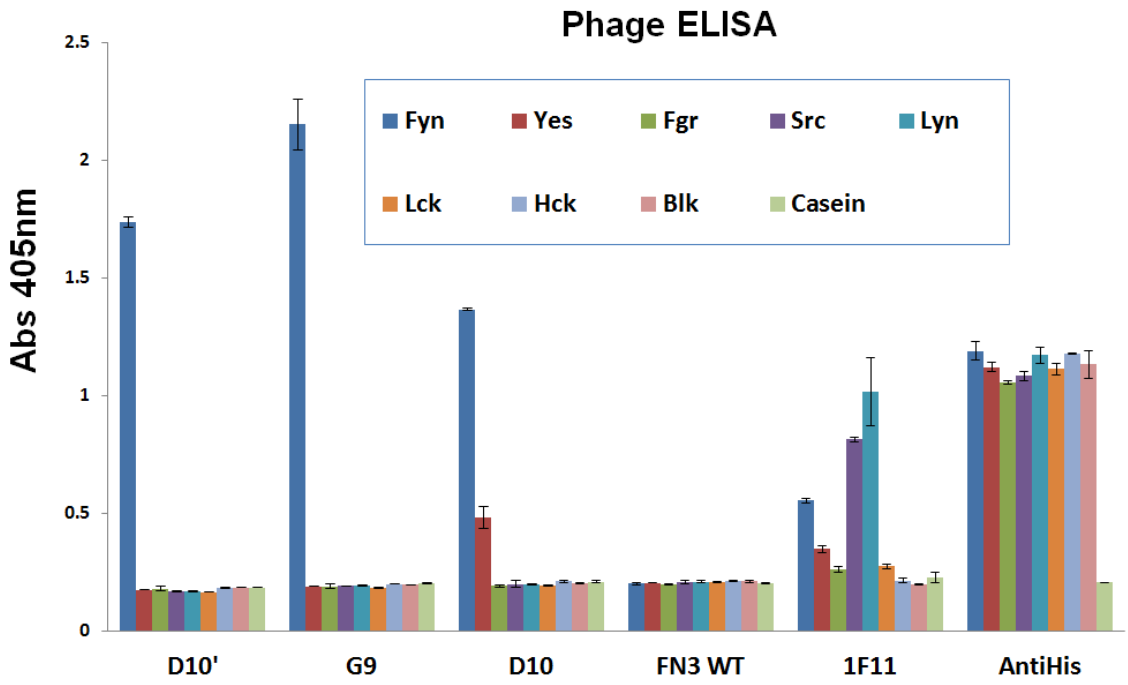

Figure 1. Phage ELISA of monobodies to the SH3 domains of all eight human SFKs. Microtiter plate wells were coated with equal amounts of target or casein (negative control), and probed with equivalent amounts of phage particles displaying the various binding monobodies. Phage particles displaying wild-type monobody (WT FN3) served as the non-binding negative control. 1F11 is a monobody that binds to several, but not all, SFKs SH3 domains. An anti-his_6 tag antibody, conjugated to horseradish peroxidase (HRP), was used to normalize the amount of SH3 domain protein immobilized in the microtiter plate wells. Error bars correspond to standard deviation of triplicate measurements.

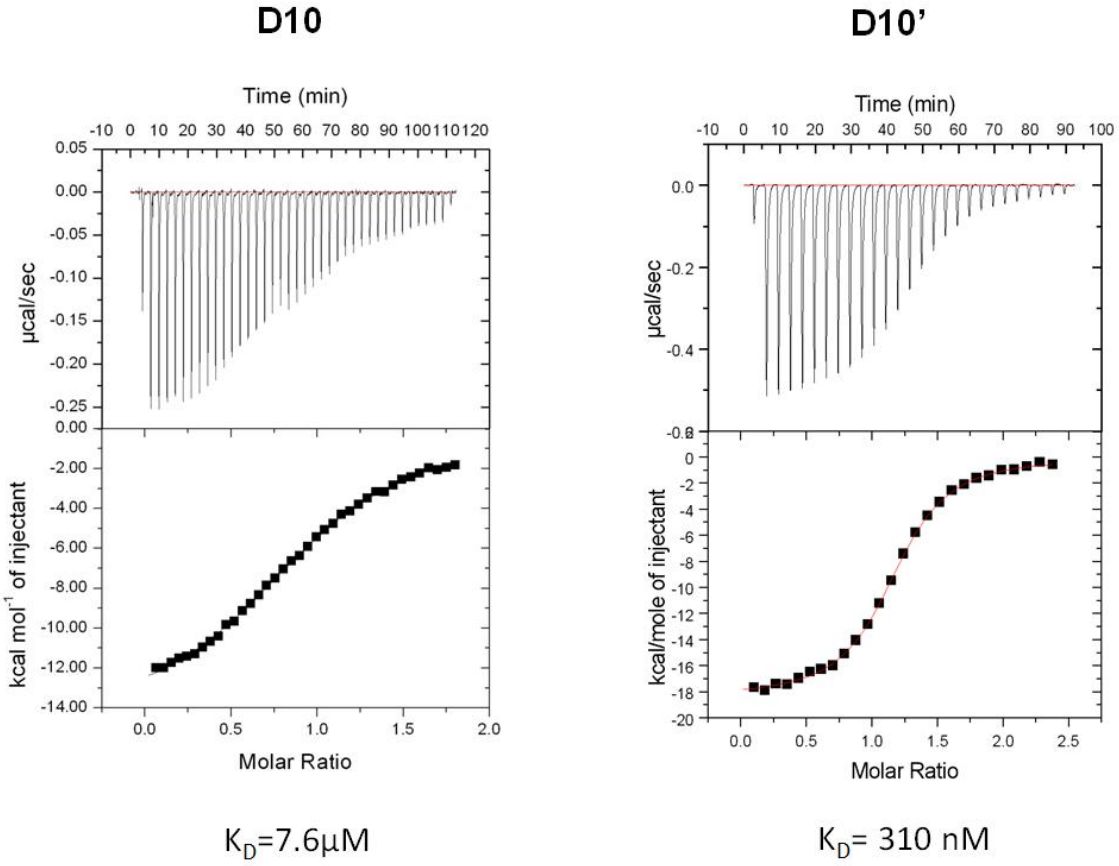

Figure 2. Isothermal titration calorimetry (ITC) measurements of the K_D of D10 and D10'. The thermogram (top panel) and the plotted titration curve (bottom panel) were obtained with a Microcal VP-ITC.

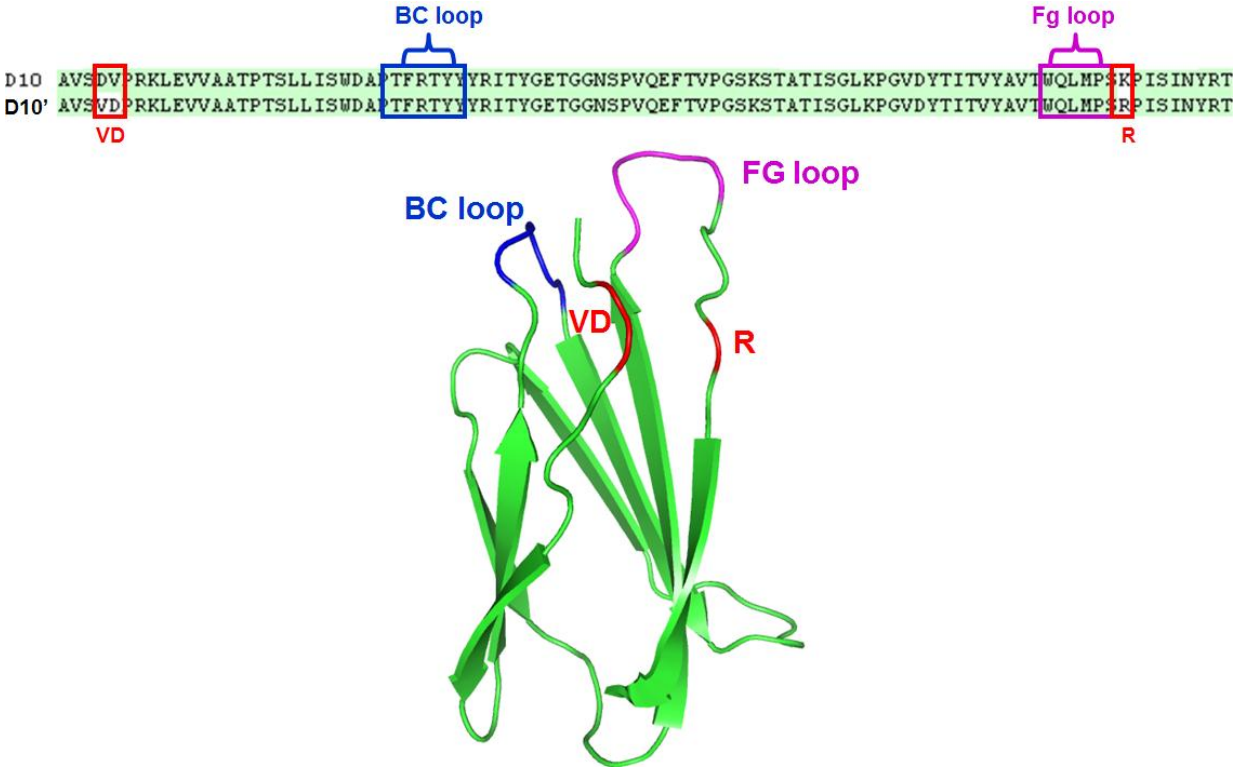

Figure 3. Sequence alignment of D10 and D10’ and the locations of the mutated residues on the D10’ FN3 scaffold.

References

1. Nossal, G. J. (1992) The molecular and cellular basis of affinity maturation in the antibody response, *Cell 68*, 1-2.

2. Cadwell, R. C., and Joyce, G. F. (1994) Mutagenic PCR, *Genome Res. 3*, S136-140.

3. Pershad, K., Sullivan, M. A., and Kay, B. K. (2011) Drop-out phagemid vector for switching from phage displayed affinity reagents to expression formats, *Anal Biochem 412*, 210-216.

4. Karatan, E., Merguerian, M., Han, Z., Scholle, M. D., Koide, S., and Kay, B. K. (2004) Molecular recognition properties of FN3 monobodies that bind the Src SH3 domain, *Chem Biol 11*, 835-844.

VITA

NAME: Renhua Huang

EDUCATION: Ph.D., Molecular biology, University of Illinois at Chicago, 2012

B.S., Biotechnology, Guangxi University, China, 2002

TEACHING: Department of Biological Sciences, University of Illinois at Chicago, Cell biology lab, 2006

Department of Biological Sciences, University of Illinois at Chicago, Cell biology, 2007

Department of Biological Sciences, University of Illinois at Chicago, Biochemistry, 208

MENTORING: Supervised five undergraduate students for research 2007-2012

ABSTRACTS: (POSTERS) Huang R, Fang P and Kay BK. Isolation of monobodies that monitor Fyn kinase activaton. Protein Modules and Networks in Health and Diseases, FEBS workshop, Seefeld, Austria, 2011

Huang R, Hao Z, Hahn K, Kuhlman B, and Kay BK. Biosensors for monitoring activation of Lyn kinases in living cells. Gordon conference for bioanalytical sensors. New London, NH, 2010

Huang R, Hao Z, Hahn KM, Kuhlman B, and Kay BK. Protein kinase biosensors built on FN3 monobodies. The 4th annual PEGS (The essential protein engineering summit), Boston, MA, 2008.

ABSTRACTS: (TALK) Huang R, Hao Z, Hahn KM, Kuhlman B, and Kay BK. Protein kinase biosensors built on FN3 monobodies. The 4th annual PEGS (The essential protein engineering summit), Boston, MA, 2008.

PUBLICATIONS:

Huang R, Pershad K, Kokoszka M and Kay BK. Phage-displayed Combinatorial Peptides. Amino Acids, Peptides and Proteins in Organic Chemistry, Volume 4, 2011.

Huang R, Fang P, and Kay BK. Improvements to the kunkel mutagenesis protocol for constructing primary and secondary phage-display libraries. Methods, (2012), http://dx.doi.org/10.1016/j.ymeth.2012.08.008

Huang R, Fang P, and Kay BK. Isolation of monobodies that bind specifically to the SH3 domain of the Fyn tyrosine protein kinase. New Biotechnology, (2012), 29(5):526-533

Kashyap MK, Kumar A, Emelianenko N, Kashyap A, Kaushik R, Huang R, et al. Biochemical and molecular markers in renal cell carcinoma: an update and future prospects. Biomarkers. 2005 Jul-Aug; 10(4):258-94.

HONORS:

Research achievement, University of Illinois at Chicago, Chicago, IL, 2011, 2012

Excellent student award, Guangxi University, Nanning, China, 1999, 2000, 2001, 2002